Alma Mater Studiorum-Università di Bologna

SCUOLA DI SCIENZE

Dipartimento di Chimica Industriale "Toso Montanari"

Corso di Laurea Magistrale in

Chimica Industriale

Classe LM-71 - Scienze e Tecnologie della Chimica Industriale

Synthesis of Metal-Binding Ligand-Containing Copolymers, Nanoparticles and Blends

Tesi di laurea sperimentale

CANDIDATO
Federico Ferrari

RELATORE
Prof.ssa Letizia Sambri

CORRELATORI
Dr.ssa Dafni Moatsou

Dr.ssa Claudia Bizzarri

Prof. Michael A.R. Meier

Anno Accademico 2018-2019

Table of contents

1 Introduction

1.1 Catalysis

1.1.1 Catalysts for photoredox transformations

The development of photoredox catalysis has recently enabled the design of powerful synthetic tools based on the generation of radical species under mild and environmentally friendly conditions.[1] In recent years, many applications for photoredox catalysis have been developed, such as disinfection[2] and CO_2 photoreduction.[3] Researchers have largely focussed on ruthenium and iridium complexes in association with π-deficient ligands. These transition metal complexes are useful photocatalysts because these types of ligands feature strong absorption in the visible region of the electromagnetic spectrum, high oxidation and reduction potentials, and long-lived excited states (typically in the μs range).[4] However, much less attention has been devoted to copper complexes, despite their potential activation of various types of reactions. Copper complexes have been scarcely used in photoredox transformations,[5-6] possibly because of their short-lived excited states. Based on the recent interest in copper-catalysed radical processes, a broadly applicable copper catalyst for photoredox transformations of organic halides was investigated by Bastien Michelet *et al.*[7] In their work, they used a copper (I) complex ([(DPEphos)(bcp)Cu]PF_6) to perform various reactions on non-activated halides, such as cyclisation, C-X bond cleavage, and aromatic coupling. Some general reactions and the structure of the catalyst are shown in scheme 1.

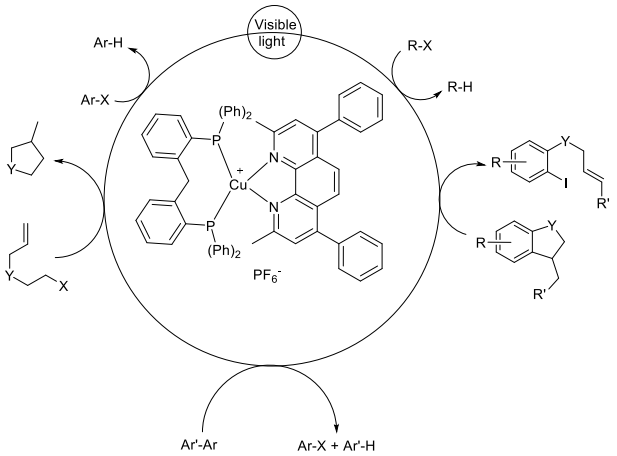

Scheme 1 Chemical structure of the copper catalyst employed by Bastien Michelet et al. and its photocatalytic catalysis in cyclization reactions (right and left), coupling reactions (bottom), and C-X bond cleavage reactions (top). [1]

1.1.2 Copper as heterogeneous catalyst

Copper is also as an important heterogeneous catalyst, used for example in "click" reactions[8] and in CO_2 reduction.[9] Heterogeneous catalysis is an alternative to homogeneous catalysis. In this type of catalysis, the starting materials may be liquids, gases, or dissolved and the catalyst is a solid or a liquid (but in this case the starting materials are not be miscible with the catalyst). Instead, in homogeneous catalysis, the catalyst and the starting materials are present the same phase. A typical example of heterogeneous catalysis is the alkylation of benzene. In this reaction, benzene (in the gas phase) enters into a reactor loaded with catalyst (in this case zeolites are used) and the alkylated products are formed.[10] No isolation of the catalyst from the final product was needed. Furthermore, owing to the shape selectivity of zeolites, only the monoalkylated product was obtained and by-products were prevented.[10] The use of heterogeneous catalysis has also been shown to prevent waste in industrial production.[11] The solid catalyst can be recovered and reused Nowadays, homogeneous copper-based complexes represent a new and cheaper alternative to ruthenium-based photocatalysts.[1] Copper photocatalysts are under the spotlight for their great ability to generate radicals under mild conditions. Copper is also used as heterogeneous catalyst for a wide range of reactions. Nowadays, researchers are focussing on copper nanoparticles as they exhibit greater activity compared to traditional heterogeneous catalysts (owing to the greater surface area of the nanoparticles).[12]

1.2 Nanoparticles

The word "nanotechnology" was introduced by Nobel laureate Richard P. Feynman during his 1959 lecture "There's Plenty of Room at the Bottom".[13] In the last years, there have been various revolutionary developments in the field. Nanotechnology focusses on the production of materials at the nanoscale. Nanoparticles (NPs) are a wide class of materials that include particulate substances that have at least one dimension smaller than 100 nm.[14] Depending on their shape, these materials can be classified as 1D, 2D, or 3D.[15] Nanoparticles represent a huge breakthrough in material science, their application open to incredible possibilities, thanks to their nanosize such as catalysis and drug delivery.

1.2.1 NP classification

NPs are separated into various categories depending on their morphology, size, and chemical properties. Their properties, in fact, are strongly based on their size and morphology. Some of the most studied nanoparticles are: fullerenes (carbon-based nanoparticles, made of globular hollow cages), carbon nanotubes (also carbon-based nanoparticles with tubular structures[16]), metal NPs (made of metal precursors), ceramic NPs (inorganic non-metallic solids, obtained through heat and successive cooling), and polymeric NPs. For what concerns non-polymeric nanoparticles, various methods can be employed for their synthesis, which are usually divided into two classes: bottom-up and top-down.[17]

In the top-down syntheses, destructive approaches are often employed. In fact, the synthesis starts from a larger molecule that decomposes into smaller units which in turn generate the NPs. Typical examples of this synthesis include chemical vapor deposition (CVD) and physical vapor deposition (PVD).[18]

In the bottom-up syntheses, NPs are formed from relatively simpler substances, hence this approach is also called building up approach. It includes sol-gel, green synthesis, spinning, and biochemical synthesis.[18]

1.2.2 Synthesis of polymeric nanoparticles

New materials that have the potential of revolutionising a large part of the polymer industry are beginning to appear. Possible applications range from novel surfactants, dispersants, coatings, and adhesives, to biomaterials, membranes, drug delivery media, and materials for microelectronics. Polymeric nanoparticles have been synthesised by several methods depending on the requirements of their application.[19] The choice of the most suitable method plays a vital role in order to obtain NPs with the desired properties for a particular application. Several preparation methods have been developed and these can be divided into two groups, namely, those based on the polymerisation of monomers and those taking advantage of preformed polymers (Table 1).[20] These methods can be further classified into two more categories: the two-step emulsification procedures, that involve the preparation of an emulsification system followed by formation of nanoparticles and one-step procedures that go directly to the nanoprecipitation. For what concerns the polymerisation methods, the monomers are polymerised to form the polymer nanoparticles. This process can be done in two ways, either using emulsion polymerisation techniques or interfacial polymerisation.

Polymerisation of monomers	**Preformed polymers**
Emulsion	Emulsification- solvent evaporation
Mini Emulsion	Emulsification- solvent evaporation
Micro Emulsion	Salting-out
Interfacial Polymerisation	Nanoprecipitation
Controlled/Living radical	Dialysis
	Supercritical fluid technology

Table 1 List of ways to obtain polymer nanoparticles from monomers and preformed polymers.[21]

One of the most used techniques to obtain nanoparticles from preformed polymers is the nanoprecipitation method, also called solvent displacement. The method was first developed by Fessi *et al.;*[22] the basic principle of this technique is based on the interfacial deposition of a polymer after displacement of the organic solvent from a lipophilic solution to the aqueous phase as shown in Figure 1. The polymer is dissolved in a water-miscible solvent and this solution is added into a stirred aqueous solution in one shot, stepwise, dropwise, or by controlled addition rate, with the velocity and the method of addition influencing the morphology and size

of the NPs.[23] Due to the fast spontaneous diffusion of the polymer solution into the aqueous phase, the nanoparticles form instantaneously in an attempt to avoid the water molecules. This process is governed by the Marangoni effect, wherein a decrease in the interfacial tension between the two phases increases the surface area due to the rapid diffusion and leads to the formation of small droplets of organic solvent.[24] As the solvent diffuses out from the nanodroplets, the polymer precipitates in the form of nanocapsules or nanospheres. In general, the organic phase is added to the aqueous phase, but the protocol could also be reversed without compromising the nanoparticle formation. The most commonly used organic solvent is acetone because it is miscible with water and easy to remove by evaporation. It is also possible to use either two organic phases or two aqueous phases as long as solubility, insolubility, and miscibility conditions are satisfied.[23] Usually, surfactants could be included in the process to guarantee the stability of the colloidal suspension, but their presence is not required to ensure the formation of nanoparticles.[21] The obtained nanoparticles are typically characterised by well-defined sizes and narrow size distributions, often contrary to those produced by the emulsification solvent evaporation procedure.[21]

By carefully adjusting the nature and concentration of the components, organic phase/aqueous phase ratio, organic phase injection rate, fluid dynamics, and mixing speed, it is possible to control the NP physicochemical properties.

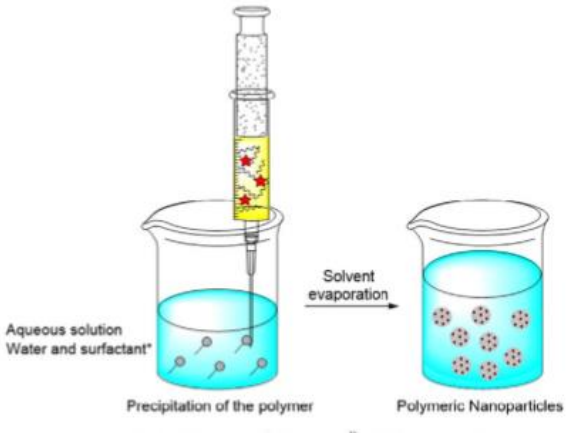

Figure 1 Nanoprecipitation of polymer[21]

1.2.3 Characterisation of NPs

Various characterisation techniques have been used for the analysis of the properties of NPs, such as X-ray diffraction (XRD), X-ray photoelectron spectroscopy (XPS), infrared (IR) spectroscopy, scanning electron microscopy (SEM), transmission electron microscopy (TEM), Brunauer–Emmett–Teller (BET), and dynamic light scattering (DLS). DLS is a powerful tool

to investigate the diffusion behaviour of molecules and particles in solution, by which the size of particles can be determined. The morphological analysis of NPs is important since morphology can influence the properties of the NPs such as colours, catalyst properties etc. There are several characterisation techniques for morphology, but microscopy techniques, such as polarised optical microscopy (POM), SEM, and TEM are the most important.

Optical properties are fundamental in photocatalytic applications and there are several characterisation techniques that allow the evaluation of these properties. Most such characterisation techniques are based on the Beer-Lambert law, whereby the absorbance (A) of a molecule is proportional to the optical path length l and the concentration of the attenuating species c, $A = \varepsilon lc$, where ε is the molar extinction coefficient.[25] These techniques give information about the absorption, reflectance, fluorescence and phosphorescence properties of NPs. Phosphorescence and fluorescence are two types of luminescence, the difference between which is that fluorescence is an emission produced by the transition S1→ S0 (first electronic singlet state to ground singlet state) ($h\nu = \lambda 3$, in Figure 1). On the other hand, phosphorescence is the result of an intersystem crossing between the S1 state and triplet state (T1) and then a transition from T1 to the ground state as showed in Figure 2.

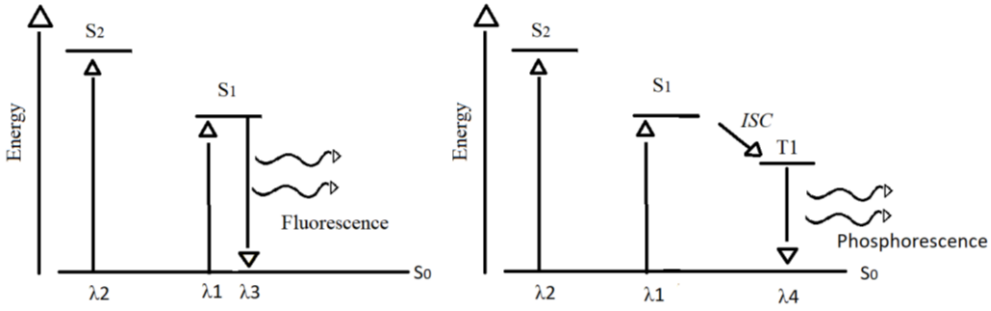

Figure 2 Fluorescence and phosphorescence emission diagram.

1.2.4 Microencapsulation

Microencapsulation is a process in which particles are surrounded by a coating or embedded into a homogeneous or heterogeneous matrix that provides a physical barrier that protects the active ingredient or the molecules.[26] The main applications for microencapsulation are to facilitate the manipulation of a substance and control its release in an adequate time and space, retarding evaporation of a volatile core, improving the handling properties of a sticky material, isolating a reactive core from chemical attack, sustained or prolonged drug release, protection

of the core against oxygen, light, heat, and moisture, decrease hygroscopic properties for a longer storage, or decrease potential danger of handling of toxic substances.

1.3 Radical polymerisation

Radical polymerisation is one of the most widely used polymerisation processes for commercial production of a variety of polymers. A large variety of monomers can undergo radical polymerisation including (meth)acrylates, styrene, (meth)acrylamides, butadiene, and vinyl acetate.[27] It is tolerant to a wide range of functional groups (e.g. hydroxyl group, carboxylic group, and amide group) and a variety of reaction conditions can be employed (bulk, solution, emulsion, miniemulsion, suspension).[27] However, the conventional process has some limitations with respect to the degree of control that can be asserted over the macromolecular structure, in particular, the molecular weight distribution, composition, and architecture.[27] To overcome the limitations of the classical radical polymerisation, living polymerisations may instead be used. In polymer chemistry, a living polymerisation is a form of chain-growth polymerisation where the ability of a growing polymer chain to terminate is virtually inexistent.[28] The recent emergence of techniques for implementing living radical polymerisation has provided a new set of tools for polymer chemists that allow very precise control over the polymerisation process while retaining much of the versatility of conventional radical polymerisation.

1.3.1 Molecular weight distribution

In polymer chemistry, it is unavoidable to obtain not just one molecular weight, but several. During the polymerisation, not all the chains grow at the same time therefore at the end of the process different length chains, thus different molecular weights will be obtained. While several means to describe molecular weight exist, three are commonly used, namely the number average molecular weight (M_n), the weight average molecular weight (M_w) and z average molecular weight (M_z). The mathematical definition is shown in Figure 2, where M_i is the molecular weight of each chain and N_i is the number of chains with that molecular weight.

$$M_n = \frac{\sum M_i N_i}{\sum N_i}, \quad M_w = \frac{\sum M_i^2 N_i}{\sum M_i N_i}, \quad M_z = \frac{\sum M_i^3 N_i}{\sum M_i^2 N_i}$$

Figure 3 Three common average molecular weights used to describe polymers

Since during the polymerisation not all the chains grow simultaneously, at the end of the process several chains with different lengths (and thus different molecular weight) will be obtained. The dispersity ($Đ_M$) indicates the breadth of the molecular weight distribution of the polymer and it is given by the ratio of M_w and M_n. The $Đ_M$ is always more or equal to one.

$$Đ_M = \frac{Mw}{Mn}$$

Figure 4 Mathematical definition of dispersity.

1.3.2 Mechanism

There are different polymerisation techniques that can be classified as chain-growth polymerisations, such as ionic polymerisations (anionic and cationic), ring-opening metathesis polymerisation (ROMP), coordination polymerisation, atom transfer radical polymerisation (ATRP) and reversible addition-fragmentation chain transfer (RAFT) polymerisation. The chain growth polymerisation mechanism can be divided into four processes: chain initiation, chain propagation, chain transfer, chain termination. The chain propagation and initiation steps are present in every chain-growth type polymerisation, but in some cases chain termination could be virtually absent (such as in anionic polymerisation).

The process begins with the generation of radicals (usually by the homolytic splitting of an initiator) and then the addition to monomer, which represents the chain initiation step. This is followed by the chain propagation step which involves the sequential addition of monomer units to the growing radical formed (indicated as $P_n^{\bullet}$ in the Scheme 2 below). Chain transfer entails the radical reacting with another molecule, usually solvent or the formed polymer chains, and transferring the radical which cannot sustain the polymerisation. At the end, chain termination occurs when the propagating radicals react *via* combination or disproportionation (the two radical species react to generate two non-radical species, by elimination or hydrogen transfer, for example).

Initiation

$$A_2 \xrightarrow{K_d} 2A\bullet$$

$$A\bullet + M \xrightarrow{K_i} P_1\bullet$$

Propagation

$$P_n\bullet + M \xrightarrow{K_p} P_{n+1}\bullet$$

Chain transfer

$$P_n\bullet + T_a \xrightarrow{K_{td}} P_n + T_a\bullet$$

Termination by disproportionation

$$P_n\bullet + P_m\bullet \xrightarrow{K_{td}} P_n^{H} + P_m^{-}$$

Termination by combination

$$P_n\bullet + P_m\bullet \xrightarrow{K_{tc}} P_{n+m}$$

Scheme 2 Reaction scheme of radical polymerisation.[29]

The molecular weight of chains during chain growth polymerisations increases rapidly at low monomer conversion. In fact, in living polymerisations, there is a linear correlation between the molecular weight and the monomer conversion as shown in Figure 5 while in step-growth polymerisation (another type of polymerisation mechanism, typical e.g. for the preparation of Nylon) the molecular weight is low until high monomer conversion and then increases rapidly (as only oligomers are formed at low conversions).

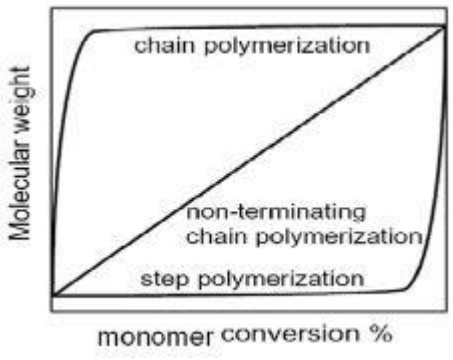

Figure 5 Conversion vs. MW in chain growth, step-growth and living polymerisation.[30]

The width of the molecular weight distribution in radical polymerisation, which is described by the dispersity (the ratio between M_w and M_n), is governed by statistical factors. The ratio of weight to number average molecular weights is usually broad ($M_w/M_n > 1.5$), but some factors can be optimised to try to reduce the ratio (such as solvent, monomer and initiator concentration).

1.3.3 Reversible-deactivation radical polymerisation

In an ideal living polymerisation, all chains are initiated, grow at the same rate, and survive the polymerisation (there is no termination). To confer living character on a radical polymerisation, it is necessary to suppress all processes that terminate chains in an irreversible way. Reversible-deactivation radical polymerisation (RDRP) is possible in the presence of reagents that react with the propagating radicals by reversible deactivation or reversible chain transfer so that the majority of chains are maintained in a dormant form. The concentration of the active propagating species in an RDRP may be similar to that for the conventional process although the cumulative lifetime of an individual chain as an active species will be lower. Rapid equilibration between the active and dormant forms ensures that all chains possess an equal chance for growth and that all chains will grow, albeit intermittently. Under these conditions, the molecular weight increases linearly with conversion and the molecular weight distribution can be very narrow (e.g. M_w/M_n *ca.* 1.1).

The RDRP techniques that have recently received greatest attention are nitroxide-mediated polymerisation (NMP), atom transfer radical polymerisation (ATRP), and reversible addition-fragmentation chain transfer (RAFT) polymerisation.

NMP was discovered in the early 1980s and in recent years has been exploited extensively for the synthesis of narrow molecular-weight distribution homopolymers and block copolymers of styrene and acrylates.[31] Recent developments have made NMP applicable to a wider, though still restricted, range of monomers. The low versatility of NMP is caused by the high activation/deactivation constant presented by several nitroxide/monomer systems (such as methacrylic acid and (2,2,6,6-tetramethylpiperidin-1-yl)oxyl, TEMPO), which renders the process not always controllable.[32]

Another example of RDRP is reversible addition-fragmentation chain-transfer (RAFT). The RAFT process involves free-radical polymerisation in the presence of chain transfer agents, also called RAFT agents. These are usually thiocarbonylthio compounds that react with the radicals generated and help to afford control over the polymerisation. The experimental conditions employed are those used for conventional free-radical polymerisation. The living character of the RAFT process is indicated by the narrow dispersity of the product and the linear molecular weight *vs.* conversion profile. The predictability of the molecular weight from the ratio of monomer consumed to transfer agent[33] and the ability to produce blocks or higher

molecular weight polymers by further monomer addition are the reasons why this polymerisation technique is so popular. Another advantage of the RAFT process is that it is compatible with a wide range of monomers and is tolerant to a variety of functional groups. This gives the ability to obtain a wide range of polymers without any need for protection or deprotection.

1.3.4 ATRP

Atom transfer radical polymerisation (ATRP) is an example of RDPR. ATRP was independently discovered by Mitsuo Sawamoto[34] and by Krzysztof Matyjaszewski in 1995.[35] In this particular type of polymerisation, a transition metal, often copper, is used to generate radicals from a dormant species (usually halides) and in this way start the polymerisation. What makes ATRP a controlled radical polymerisation is the equilibrium between the dormant species (indicated as P_n-X in Figure 6) and the propagating species (indicated as $P^{\cdot}_n$ in Figure 6). As a result, the polymerisation can be controlled leading to polymers with desired molecular weights and narrow dispersities. ATRP is a versatile technique: it can be used in a wide range of temperatures, with a wide range of monomers and solvents As the name implies, the atom transfer step is crucial in the reaction responsible for uniform polymer chain growth, making it easy to provide materials with highly specific, uniform characteristics. It is an inner sphere electron transfer process,[36] which involves a reversible homolytic halogen transfer between a dormant species, an initiator or a dormant propagating chain-end and a transition metal complex in the lower oxidation state. The transfer leads to the formation of propagating radicals.

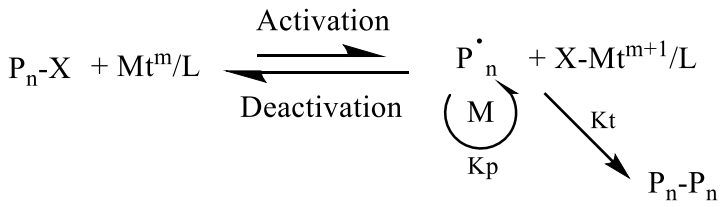

Figure 6 Activation and Deactivation equilibrium in ATRP.

1.3.5 ATRP process

The ATRP polymerisation process includes one or more (co)monomers, a transition metal complex in two or more oxidation states,[37] which can comprise various counterions and ligands, an initiator with one or more radically transferable atoms or groups, and an optional solvent. In fact, all of the components present in the reaction medium can, and often do, affect the interactions between the reagents that constitute the ATRP equilibrium (also shows in Figure 6 Activation and Deactivation equilibrium in ATRP.).[38]

However, even if all of the components can influence the reaction, there are four main variables that play an important role in the definition of K_{ATRP}: The temperature,[39] the pressure,[40] the media/solvent (which increases with polarity),[38] and the alkyl halide/ catalyst.[41]

The mechanism of ATRP starts with the reaction of the halide with a metal complex (in low oxidation state) to generate the radical. The radical then reacts with the monomer to generate the propagating species, that can be terminated by the reaction with a radical halide or can propagate reacting with more monomers. The termination reaction is an equilibrium thus justifying the living character of the polymerisation.

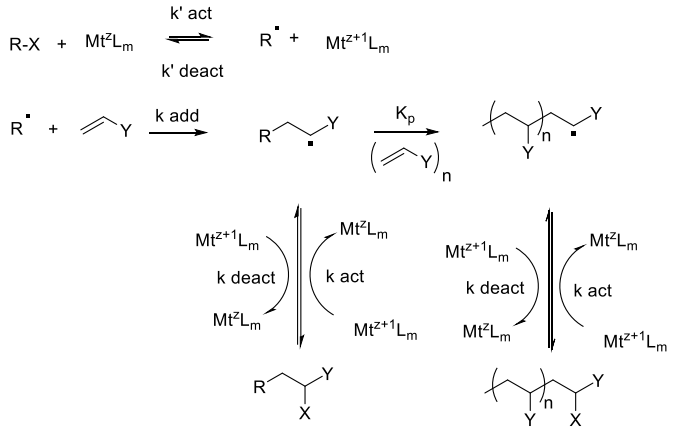

Scheme 3 Mechanism of metal complex-mediated ATRP with activation, addition, and termination.[42]

A wide range of metals can be employed in an ATRP including Ti,[43] Mo,[44] Re,[45] Fe,[46] Ru,[34] Os,[47] Rh,[48] although the most frequently one used is copper. The transition metal complex has to be at least partially soluble in the reaction medium, thus the reaction can proceed under homogeneous or heterogeneous conditions. Generally, homogeneous conditions are chosen because they provide better control since the concentration of activator and deactivator can be controlled.[49]

The reaction temperatures typically range from room temperature to around 150°C. ATRP can be conducted under vacuum or pressure, [37] and in the presence of water[50-51]. Oxygen should be removed from the reaction medium since it can oxidise the metal complex and shift the ATRP equilibrium, although a limited amount of oxygen can be tolerated, particularly in the presence of an added reducing agent such as Cu (0) or ascorbic acid.[52]

Owing to the variety of temperatures, monomers, initiator, complexes, and conditions that can be used for ATRP polymerisation, this technique shows promise for industrial synthesis of well-defined block copolymers and tailored polymers.

1.3.6 Photoinduced ATRP

Even if ATRP is really a versatile technique, nowadays not much research has been conducted on the possibility of photoinduced ATRP polymerisation, even if copper complexes (the most used metal in this technique) are well-known photocatalysts. A work from Yagci *et al.* [53] discussed the photochemical generation of the activator from adding $Cu^{II}X/L$ complex in the presence of methanol and subsequent reaction of the activator with the alkyl halide. In this work, high concentrations of catalyst were used. Furthermore, in the work from Mosnacek *et al.*, UV light was used to activate a reaction with lower concentrations of catalyst.[54] This demonstrates that is possible to photoinduce ATRP using copper complexes with low quantities of catalyst, similar to conventional ATRP.

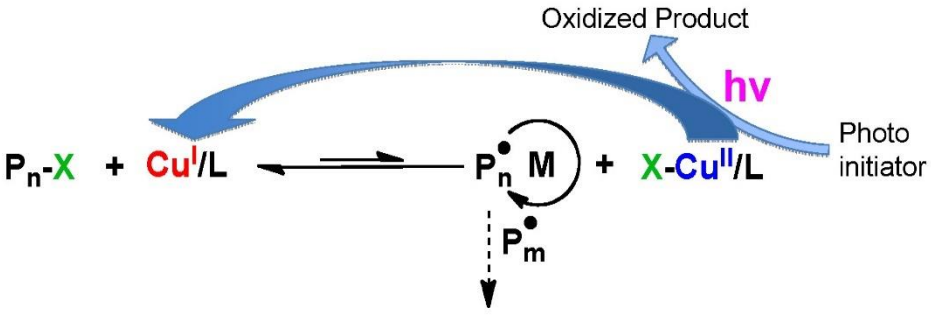

Figure 7 Copper cycle in photoinduced ATRP[55]

The main interest in photoinitiation of ATRP is due to the possibility of simple triggering the reaction by visible or UV light, which is an attractive feature for improving the versatility of the techniques and building useful materials with complex molecular architectures. Light-emitting diodes (LEDs) are commonly selected as the light source for photoinduced ATRP

since they are inexpensive, efficient, exhibit a long lifetime, and are available in various wavelengths with narrow emission range.

ATRP has also been reported utilising sunlight as the light source. Matyjaszewski *et al.*[54] demonstrated the photoinduced ATRP of methyl acrylate (MA) and methyl methacrylate (MMA) with good control of molecular weight and dispersity (M_W/M_n).

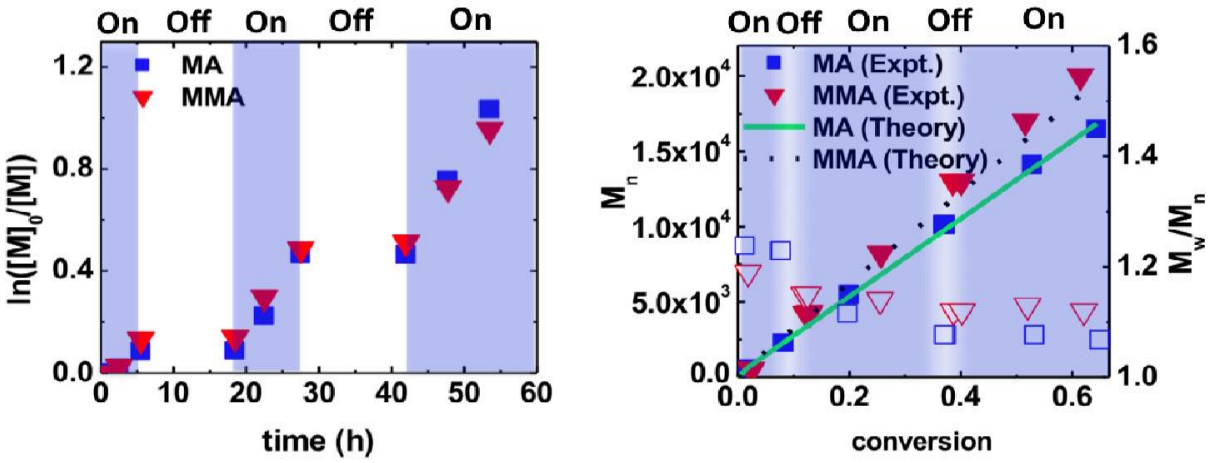

Figure 8 Correlation between time and ln([M]0/[M]) (left) and Mn and conversion (right) in ATRP Photoinduced of MA and MMA.[54]

In summary, ATRP is a strong and versatile example of RPRD. It requires a metal complex to catalyse the process (often copper is used) and allows to obtain polymers with a narrow molecular weight distribution and with tailored molecular weights. A photochemical version of ATRP is possible under mild reaction conditions.

1.4 Polymer blends

Polymer blends and composites became a central part of polymer science and engineering because they allow compositions with properties unreachable with homopolymers, and nowadays they represent 30% of the polymer market.[56] Polymer blends are a physical mixture of two or more polymers/molecules with no chemical bonding between them. Blends can have greater toughness and impact resistance, higher modulus, higher use temperature, a broader temperature range of sound and vibration damping, etc. at a lower cost compared to the pure polymer. The preparation of polymer blends dates back to nearly the beginning of the century. When two or more polymers are mixed, the phase structure obtained can be miscible or

immiscible. Based on that, polymer blends are classified as: a) completely miscible (the homogeneity is observed also at nanometric size and just one glass transition temperature (T_g) is observed), b) partially miscible (where one polymer is partially dissolved in the other one), c) completely immiscible (two T_g are observed and there is a defined separation between the two phases).

The blend of polycarbonate/polypropylene with carbon black as active compound is a typical example of polymer blends used to improve the material properties. Carbon black is a typical polymer filler, used mostly to increase the conductivity of the polymer matrix,[57] or, in the rubber industry where it gives the typical black colour to the tire.[58] Usually, to increase the conductivity of the polymer matrix, at least 30% w/w of carbon black is required.[59] However, owing to the phase separation in some polymers blends (such as polypropylene/polycarbonate), it is possible to reduce the quantity of carbon black required, down to 9% w/w, and consequentially preserve the mechanical properties of the blends, increase the conductivity and preserve the blends from photochemical ageing (carbon black is also a UV absorber).[59]

Another example of a polymer blend with an active compound is represented by the mixture of europium complex and poly[2-(6-cyano-6-methyl-heptyloxy)-(1,4-phenylene)] (CN-PPP). Mixing this rare-earth complex with a CN-PPP film resulted in the formation of an LED with strong red emission. The emission generated by the complex was enhanced by the energy transfer from the polymer to the complex.[60]

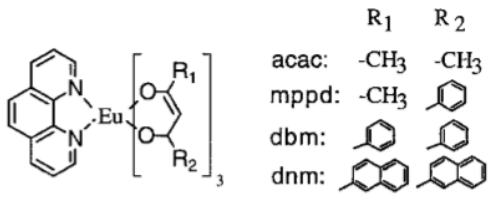

Figure 9 Europium complex structure and ligands used

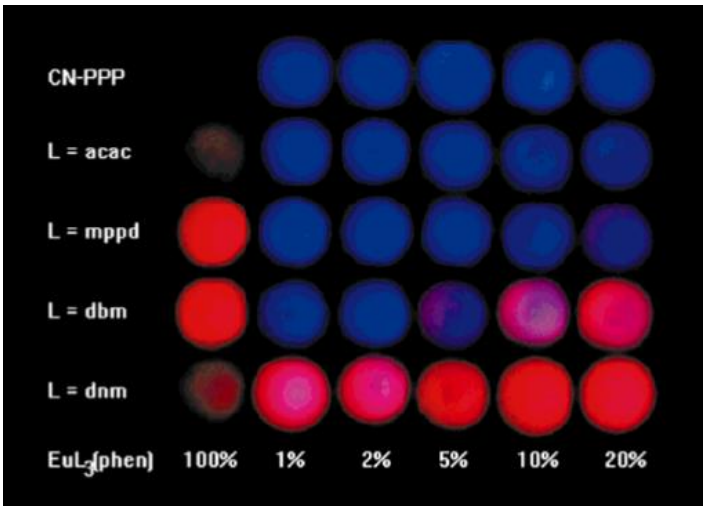

Figure 10 Photo of red emission of CN-PPP/Europium complex blends with different weight percentage and different ligands (L).[60]

As shown in Figure 10 Photo of red emission of CN-PPP/Europium complex blends with different weight percentage and different ligands (L) 1% w/w of the complex with the right ligand gives a brighter emission.

In summary, polymer blends could help to obtain a mixture of polymers with improved properties, often impossible to reach with a homopolymers.

1.5 Synthetic tools

During this work several organic reactions were employed. In this section of the introduction, the mechanisms behind the three key reactions of this work will be outlined.

1.5.1 Sonogashira coupling

In 1975 three independent work from Cassar,[61] Heck[62] and Sonogashira[63] reported three different ways to alkylate aryl halides using aromatic acetylenes. All three reactions use palladium as catalyst but the approach reported by Heck and Cassar required harsh conditions.[62] Instead, Sonogashira proposed a mild way to achieve the coupling.[63] The Sonogashira coupling reaction is one of the most widely used methods for the coupling of vinyl or aryl halides with terminal alkynes to form conjugated enynes or aryl. The reaction takes place between a vinyl or aryl halide and a terminal alkyne. The catalyst is based on palladium and it is fundamental for the conduction of the reaction. The exact mechanism of the reaction is still unknown since it is really difficult to isolate the organometallic intermediate.

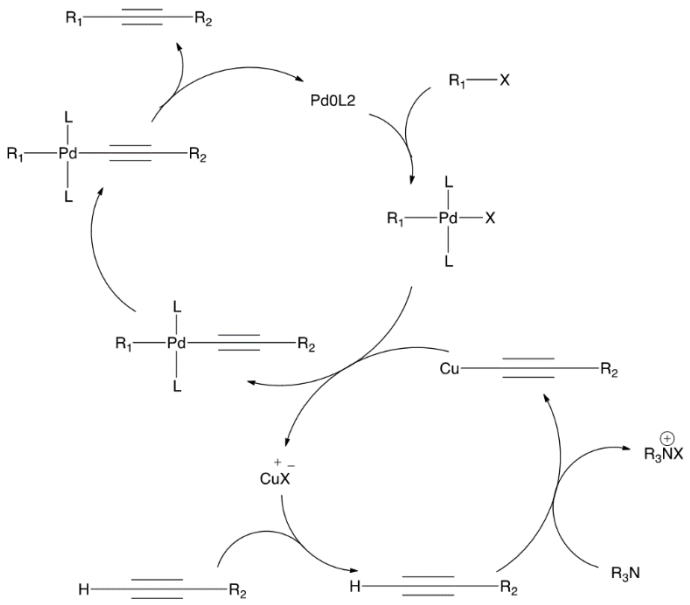

Scheme 4 Sonogashira mechanism

However, the mechanism is a combination between two catalyst cycles: the cycle of the palladium (the main catalyst) and the cycle of the copper (the co-catalyst). The mechanism starts with oxidative addition of the organic halide to the palladium complex. At the same time,

the copper reacts with the alkyne to generate the copper acetylide. Then, a transmetalation occurs between the palladium and the copper acetylide. The alkyne previously bonded to the copper is now bonded to the palladium. After that, an isomerisation and a reductive elimination occurs and leads to the final coupled product.

1.5.2 Huisgen cycloaddition

The Huisgen cycloaddition was discovered by Rudolf Huisgen in 1961.[64] This reaction is widely used for forming heterocycles from the reaction of an alkyne and an azide. Sharpless defined this reaction as "click" chemistry, which rendered it popular in the last few years.[65] For the formation of the triazoles designed for our project, we decided to use the Huisgen 1,3-dipolar cycloaddition reaction. In this reaction, an alkyne (terminal or internal) reacts with an azide to give the 1,4 and 1,5 adducts. The reaction can be catalysed using copper salts, usually copper (II) and a reducing agent to generate copper (I) in situ. The copper catalysed cycloaddition is called CuAAC. However, the copper catalyst works only with terminal alkynes because the copper (I) forms a π complex with the triple bond of the alkyne. Owing to the presence of a base, the terminal hydrogen, which is the most acidic, is deprotonated. This process leads to a copper acetylide intermediate. If the alkyne is internal, a ruthenium-mediated cycloaddition must be used (RuAAC).

The mechanism of the CuAAC starts with the formation of the copper acetylide. Then, the copper atom of the acetylide coordinates with the nitrogen of the azide. At this point, the copper-azide-acetylide complex is generated, and the cyclisation takes place. This is followed by the protonation of the cycle and the formation of the product by dissociation. The catalyst-ligand complex is regenerated for further reaction cycles.

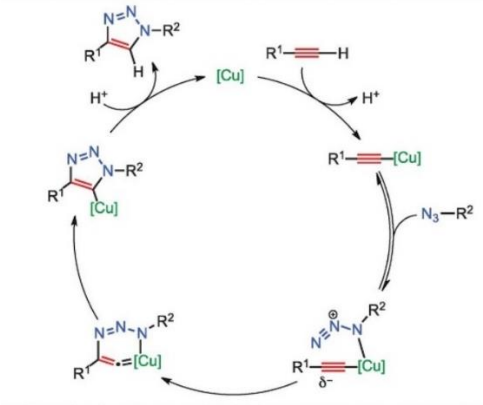

Scheme 5 CuAAC mechanism[66]

The RuAAC reaction works differently compared to the CuAAC, in the first step, the spectator ligands of the metal complex undergo displacement reaction to give an activated complex that is converted, with an oxidative coupling with the alkyne and the azide, to the ruthenium metallocycle (Ruthenacycle). A new C-N bond is formed between the more electronegative and less sterically demanding carbon of the alkyne and the terminal nitrogen of the azide. The metallacycle intermediate then undergoes reductive elimination releasing the aromatic triazole product and regenerating the catalyst for further reaction cycles.

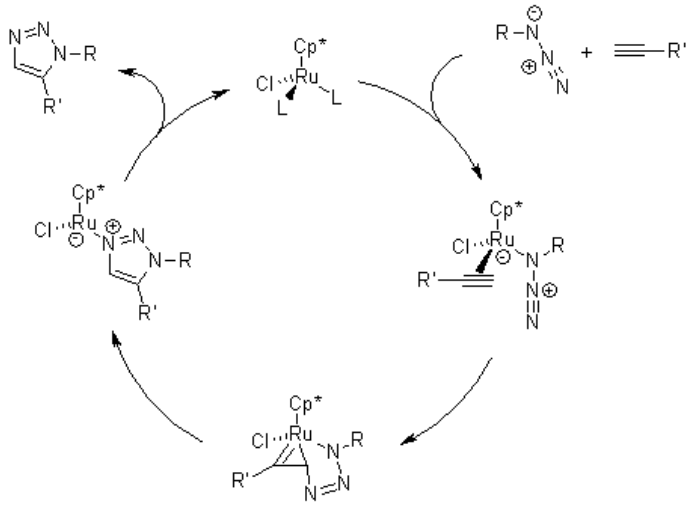

Scheme 6 RuAAC mechanism[67]

All these organic reactions are fundamental for reaching the molecules that we designed for this work: Sonogashira will be used to obtain the pyridine-alkyne and Huisgen cycloaddition to get to the triazoles. In the next chapter, the path for this work will be discussed.

2 Aim of the thesis

2.1 Polymer-copper complex nanoparticles

Copper shows intriguing abilities in photocatalysis, however, one of the major limitations of many copper complexes is that their photochemical properties might be quenched in solution, caused by Jahn-Teller distortion in the excited state.[68-69] As such, we herein seek to synthesise copper heteroleptic complexes that will subsequently be nanoprecipitated with a polymer. This will allow the polymer to encase the complex and prevent the solvent-induced quenching.

2.2 Polymer-copper complex blends

Subsequently, the preparation of blends of polymer with the aforementioned copper complexes, at different weight ratios is sought. The preparation of the blend is particularly interesting as the catalytic properties are anticipated to be inferior on account of the low surface area, however, owing to the polymer matrix better mechanical properties are anticipated. The blends, in fact, can combine the mechanical properties of the polymer and the luminescence of the complex, with the advantage that the polymer matrix can also prevent quenching from oxygen.

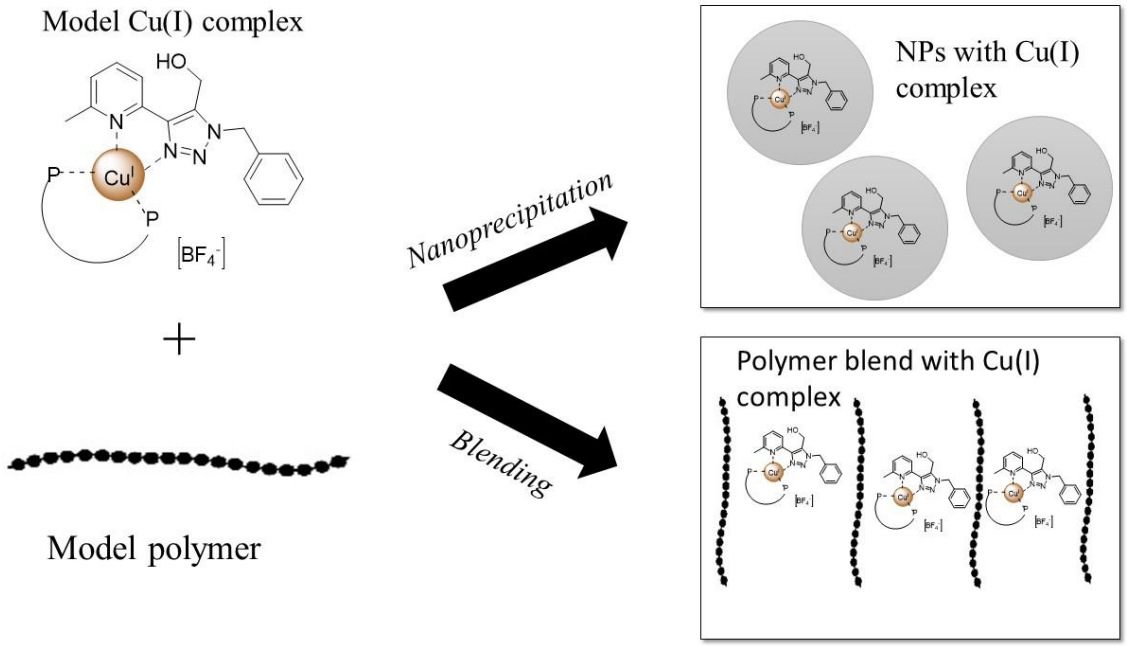

Figure 11 Blend and NPs synthesis overview.

2.3 Copper complex monomer

Particularly interesting is the synthesis of a monomer that contains copper and can be excited under ultraviolet (UV) light.

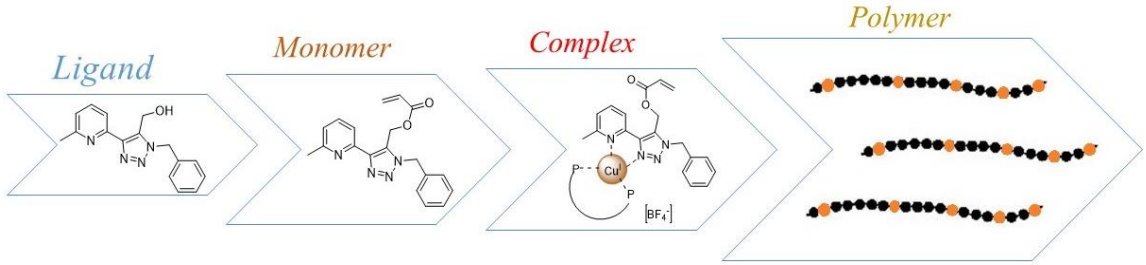

Figure 12 Monomer synthesis overview.

3 Results and discussion

3.1 Synthesis of pyridine derivatives

The aim of this part is to obtain derivatives of pyridine that could undergo further "click" reaction, thus they must contain an alkyne. Furthermore, in order to allow further functionalisation, they also must contain a functional handle such as a halide or a hydroxyl group. To reach this goal, we started from commercially available materials and employed a Sonogashira coupling reaction to bind the pyridine to the alkyne.

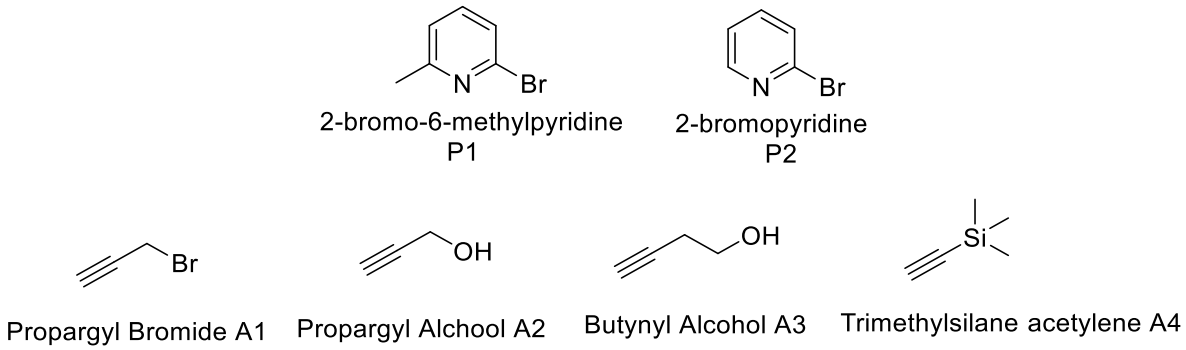

Scheme 7Materials used

In this chapter, we aimed to synthesise six pyridine-alkyne derivatives, one with bromide, two with a hydroxyl group, and two with a terminal alkyne.

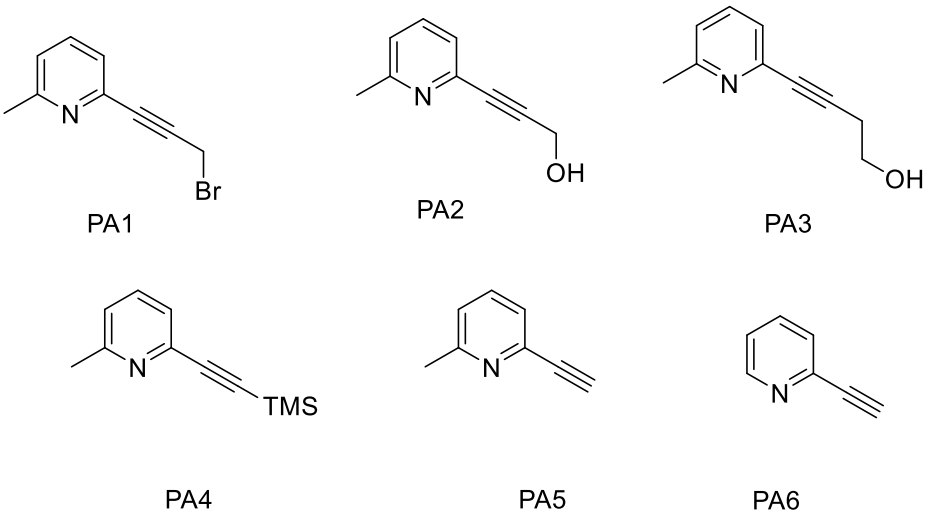

Scheme 8 Pyridine-Alkyne derivates

The last two carrying a terminal alkyne were chosen as they showed promise to undergo copper-mediated cycloaddition. This would allow introducing the functional group *via* a functional azide.

Unfortunately, only five of the six compounds were successfully synthesised, as in the case of PA1 no conversion was observed by thin layer chromatography (TLC) after 48 hours. This was attributed to the fact that the propargyl bromide was too old, which, as suggested by ^{1}H NMR spectra, resulted in degradation of the triple bond. The old bromide was disposed and propargyl alcohol (**A2**) was used instead for the next synthesis.

*3.1.1 Synthesis of 2-(2-propyn-1-ol)-6-methylpyridine (**PA2**)*

For the synthesis of PA2, the Sonogashira coupling reaction between the alcohol **A2** and the pyridine **P1** in stoichiometric ratio was employed. The pure product was isolated as a brown solid at a yield of 71.3%.

The ^{1}H NMR and the IR spectra were used to determine the presence of the pure product. The ^{1}H NMR spectrum showed the presence of a signal at 3.88 ppm which was attributed to the hydroxyl group and a shift of the signal from 4.22 ppm corresponding to the CH_2 group adjacent to the alcohol to 4.54 ppm was ascribed to the successful formation of the product.

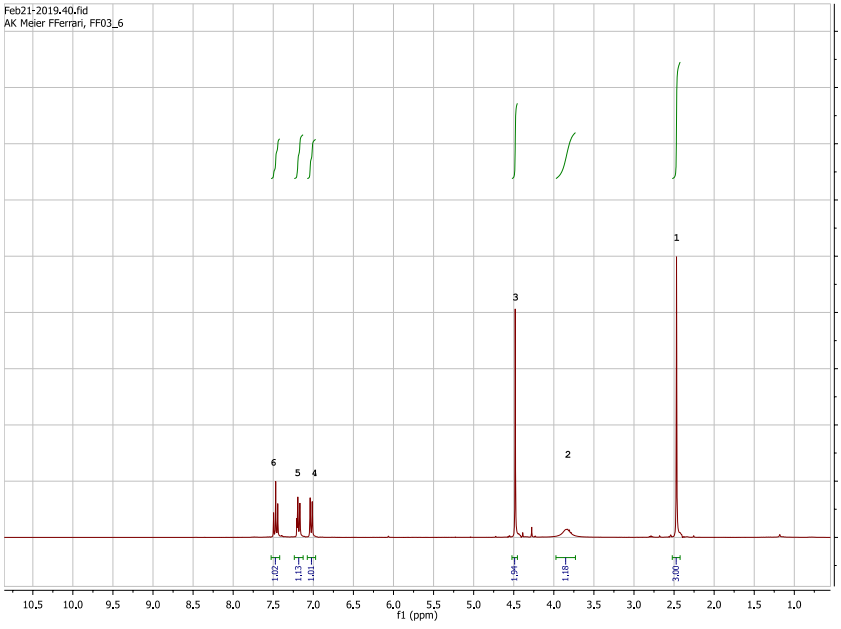

*Figure 13 1H NMR spectrum of the purified **PA2** in CDCl3 (300 MHz).*

^{1}H NMR ($CDCl_3$, 300 MHz) δ (ppm):), 7.47 (1H, d, ^{3}J = 1.0 Hz, -CH=CH-, *meta* pyridine), 7.12 (1H, t, ^{3}J = 1.0 Hz, -CH=CH-, *para* pyridine), 7.03 (1H, d, ^{3}J = 1.0 Hz, -CH=CH-, *meta* pyridine), 4.54 (2H, s, C-C**H**$_2$-OH), 3.88 (1H, s, -OH), 2.52 (3H, s, Ar-CH_3).
IR ν (cm^{-1}) 3202 (OH stretch), 1567 (C=C stretch).

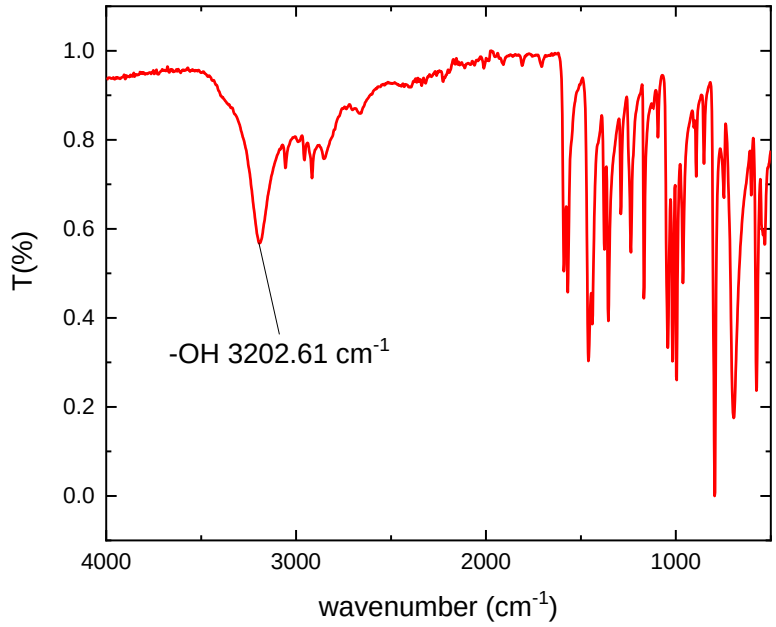

*Figure 14 IR spectrum of the purified **PA2***

*3.1.2 Synthesis of 2-(3-butynyl-1-ol)-6-methylpyridine (**PA3**)*

After the synthesis of the first PA with a hydroxyl group, we sought the synthesis of a similar compound, PA3, that bears one more -CH_2- unit between the alcohol and the alkyne. This was anticipated to prevent steric hindrance for further "click" and esterification reactions.

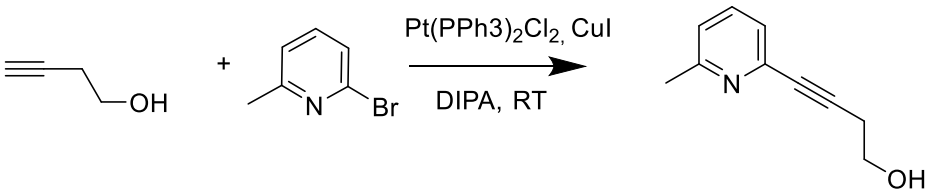

*Scheme 9 **PA3** reaction*

The product was isolated as a brown solid at a yield of 72.5%. ^{1}H NMR spectroscopy was used to determine the presence of the pure product. Compared to the spectra of the starting materials, the peaks corresponding to the methylene units of the butynyl alcohol (at 3.70 ppm and 2.22 ppm) were found to have shifted to 3.95 ppm and 2.78 ppm, respectively, which was attributed

to the deshielding of the respective protons due to the presence of the pyridine group. As such, the successful preparation of the title compound was concluded.

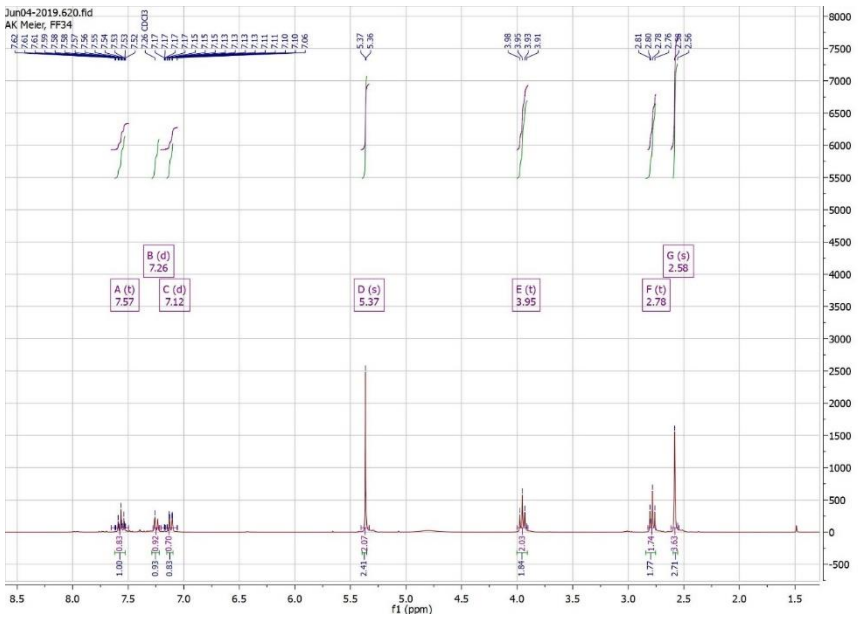

*Figure 15 ^{1}H NMR spectrum of the purified **PA3** in $CDCl_3$ (300 MHz).*

^{1}H NMR (300 MHz, Chloroform-*d*) δ 7.57 (1H, t, ^{3}J = 7.7 Hz, -CH=CH-, *para* pyridine), 7.28 (1H, d, ^{3}J = 7.7 Hz, -CH=CH-, *meta* pyridine), 7.12 (1H, d, ^{3}J = 7.7 Hz, -CH=CH-, *meta* pyridine), 3.95 (2H, t, ^{3}J = 6.6 Hz, -CH_2-C**H**$_2$-OH), 2.78 (2H, t, ^{3}J = 6.6 Hz, -C**H**$_2$-CH_2-OH), 2.58 (3H, s, Ar-CH_3).

*3.1.3 2-(Ethynyltrimethylsilane)-6-methylpyridine (**PA4**)*

Since it was not possible to utilise bromoacetylene directly, for the synthesis of PA5, we decided to use trimethylsilane acetylene instead to prepare PA4 and then remove the TMS group to obtain PA5.

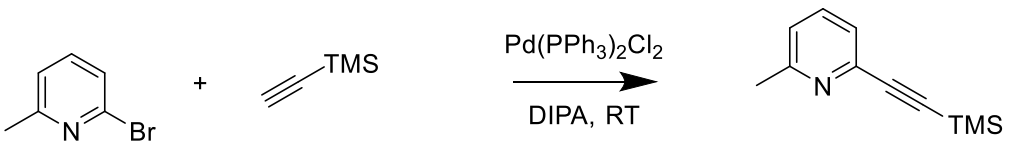

*Scheme 10 **PA4** reaction*

The product was isolated as a dark black solid at a yield of 81.3%. ^{1}H NMR spectroscopy was used to determine the presence of the pure product. Compared to the spectra of the starting materials, the peaks corresponding to the terminal hydrogen of the alkyne (at 2.22 ppm) disappeared in the spectra of the final product, which was attributed to the coupling between the pyridine and the alcohol. As such, the successful preparation of the title compound was concluded.

^{1}H NMR (300 MHz, Chloroform-*d*) δ 7.49 (1H, t, ^{3}J = 7.8 Hz, -CH=CH-, *para*), 7.26 (1H, d, ^{3}J = 7.8 Hz, -CH=CH-, *meta*), 7.05 (1H, d, ^{3}J = 7.8 Hz, -CH=CH-, *meta*), 2.52 (s, 3H, Ar-CH_3), 0.25 (9H, s, -CH_3).

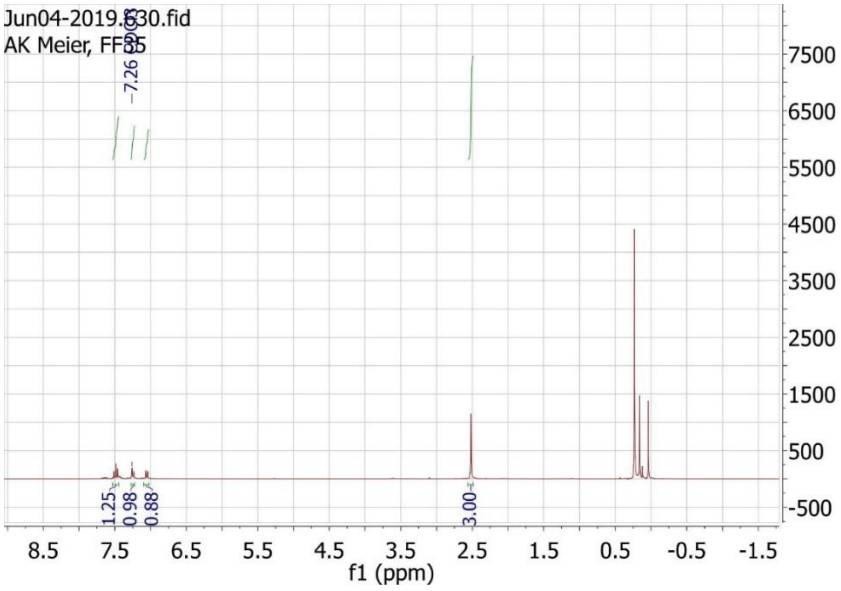

*Figure 16 ^{1}H NMR spectrum of the purified **PA4** in CDCl3 (300 MHz).*

*3.1.4 2-ethynyl-6-methylpyridine (**PA5**)*

The product **PA5** is obtained from the elimination of the trimethylsilane group in **PA4**. For the deprotection, a weak base was used. The reaction was monitored *via* TLC until complete conversion. The product was found to be air sensitive and so no further characterisation was possible.

3.2 Synthesis of triazoles

In order to obtain a ligand that can coordinate copper, it was necessary to transform the alkyne of the molecule into a triazole. This allows two nitrogens to be placed ideally to chelate the copper. For the formation of the triazole from the alkyne, we decided to use the Huisgen 1,3-dipolar cycloaddition reaction. Starting from the previously synthesised pyridine-alkynes we decided to design seven triazoles

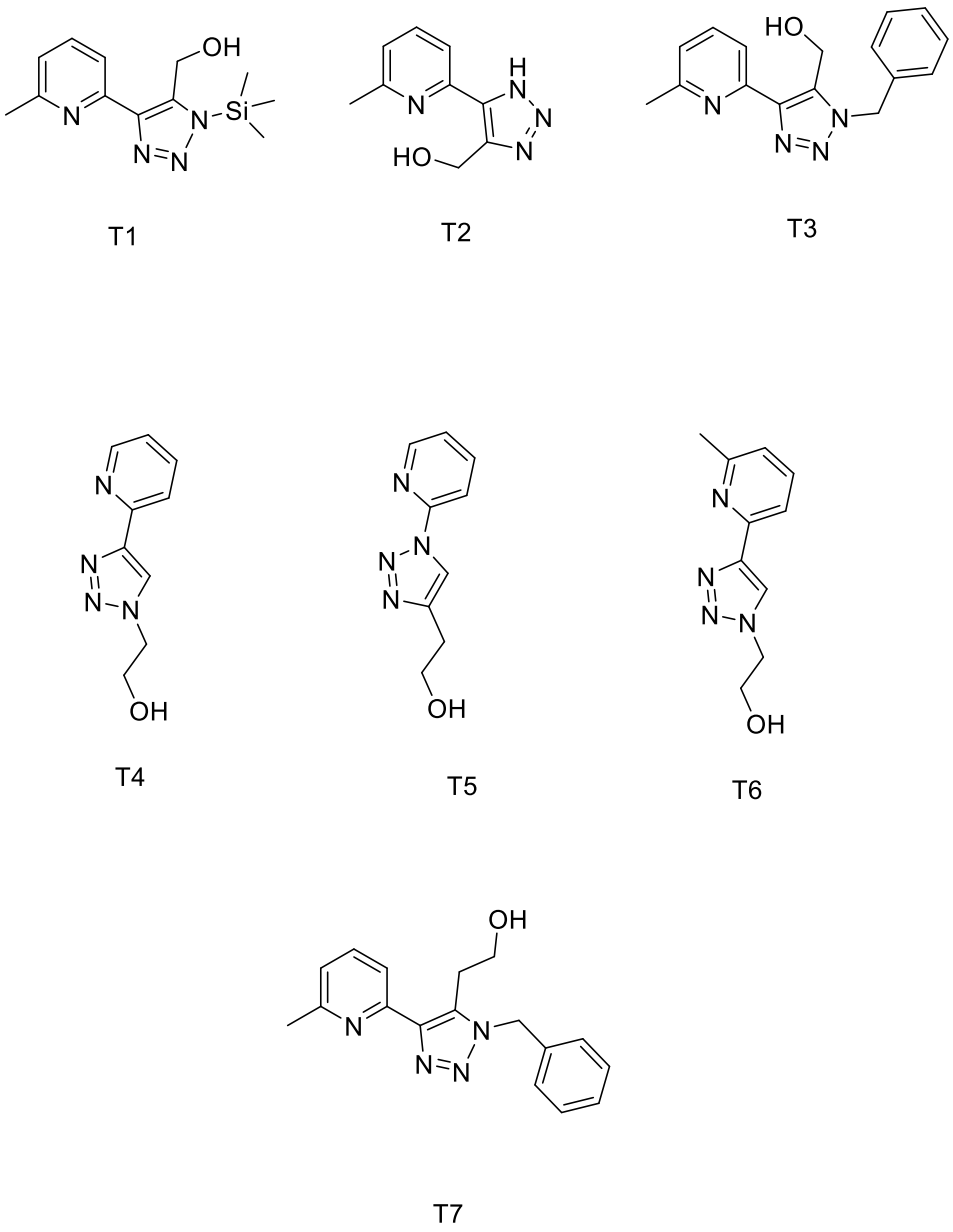

Scheme 11 Triazoles Designed

All the triazoles bear a hydroxyl group (for further functionalisation) separated by one (T1, T2, T3) or by two (T4, T5, T6, T7) -CH_2- units from the triazole. This design allows to understand how the steric hindrance impacts the ability of polymerisation and further functionalisation.

Furthermore, some triazoles bear a methyl group linked to the pyridine (T1, T2, T3, T6, T7) and two do not (T4, T5). The presence of the methyl group is anticipated to influence the rigidity of the system and thus the luminescence of the resulting complex. For the synthesis, the previously synthesised pyridine alkynes and the commercially available PA6 were employed.

*3.2.1 (5-(6-Methylpyridin-2-yl)-1-(trimethylsilyl)-1H-1,2,3-triazol-4-yl)methanol (**T1**) and (5-(6-methylpyridin-2-yl)-1H-1,2,3-triazol-4-yl)methanol (**T2**)*

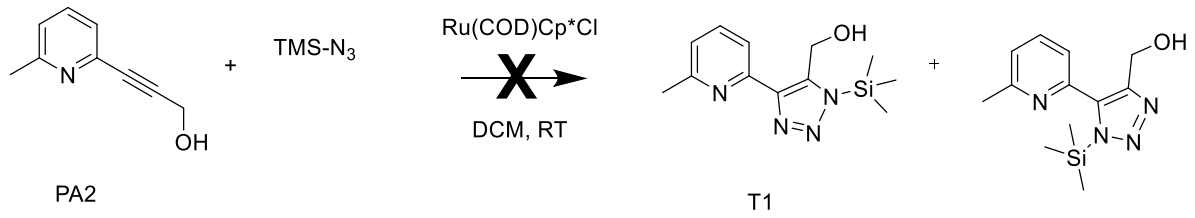

*Scheme 12 **T1** reaction*

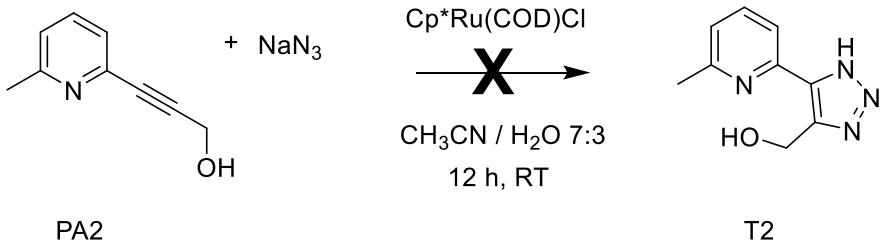

*Scheme 13 **T2** reaction*

We started from the pyridine-alkyne **PA2** previously synthesized employed RuAAC to obtain the desired product. Unfortunately, neither reaction took place, a ^{1}H NMR was collected and it showed no conversion (the chemical shift was exactly the same of the starting materials). The failure of the reaction was attributed to the incapacity of the catalyst to coordinate the azides in this solvent or due to the low solubility in dichloromethane (DCM) of the sodium azide. To probe the latter, we repeated the reaction with a DCM-soluble azide.

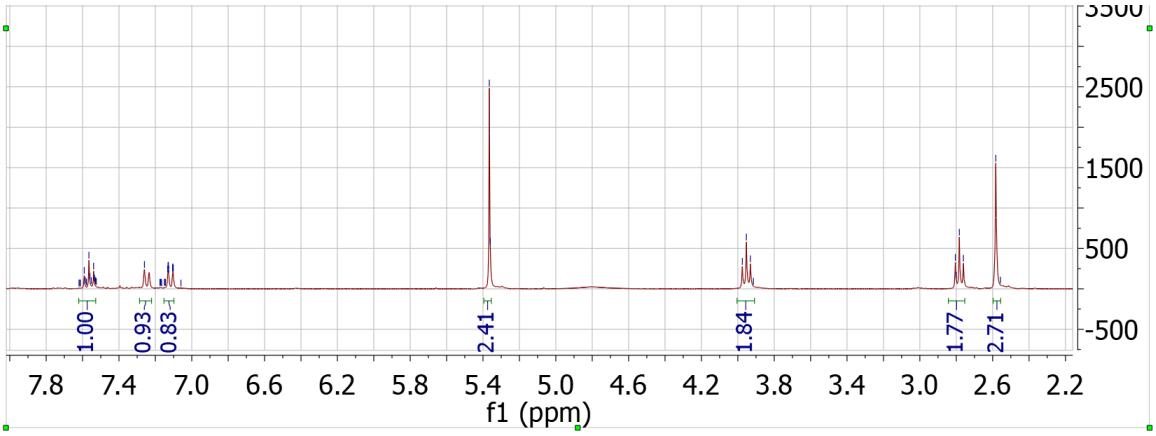

*Figure 17 ^{1}H NMR spectrum of **T1** in CDCl3 (300 MHz).*

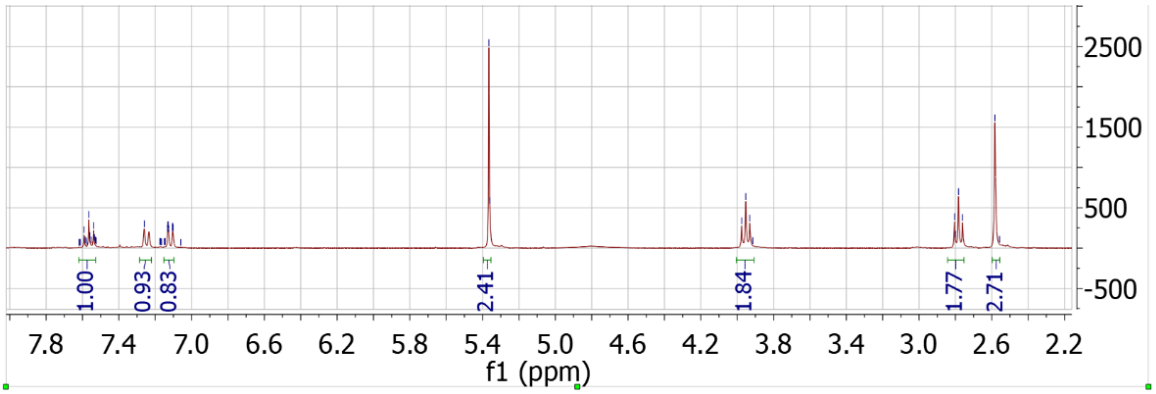

*Figure 18 ^{1}H NMR spectrum of **T2** in CDCl3 (300 MHz).*

*3.2.2 (1-benzyl-4-(6-methylpyridin-2-yl)-1H-1,2,3-triazol-5yl)methanol (**T3**)*

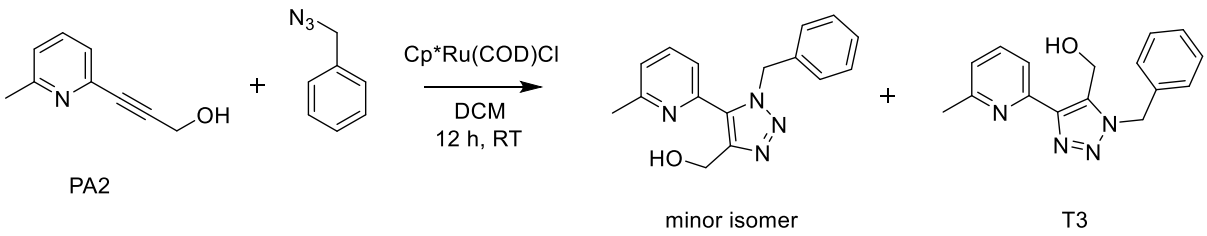

*Scheme 14 **T3** reaction*

When instead of trimethylsilane azide and sodium azide we used benzyl azide, that is well soluble in DCM, the reaction was found to progress.

Unfortunately, the ruthenium-mediated cycloaddition is not regioselective like the copper one, thus with this reaction, two isomers were obtained. It is noted that only one isomer is suitable

for the complexation, therefore the two isomers needed to be separated. The ratio between the isomers was found to be 7:3, with the minor isomer isolated as a brown solid at a yield of 22.3%.

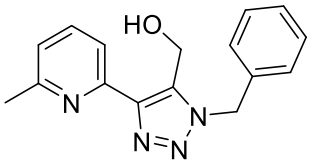

T3

Figure 19 ***T3*** *isomer suitable for complexation.*

The main isomer was isolated as a brown solid at a yield of 52.1%. ^{1}H NMR spectroscopy was used to determine the presence of the pure product. Compared to the spectra of the starting materials, the peak corresponding to the methylene units of the propargyl alcohol (at 4.54 ppm) were found to have shifted to 4.69 ppm, which was attributed to the deshielding of the respective protons due to the presence of the triazole group. Also, the peaks corresponding to the hydrogens of the pyridine (at 7.50, 7.25, 7.08 ppm) were found to have shifted to 8.15 ppm, 7.70 ppm, 7.12 ppm, respectively, which was attributed to the greater electron withdrawing effects of the triazole compared to the alkyne. As such, the successful preparation of the title compound was concluded.

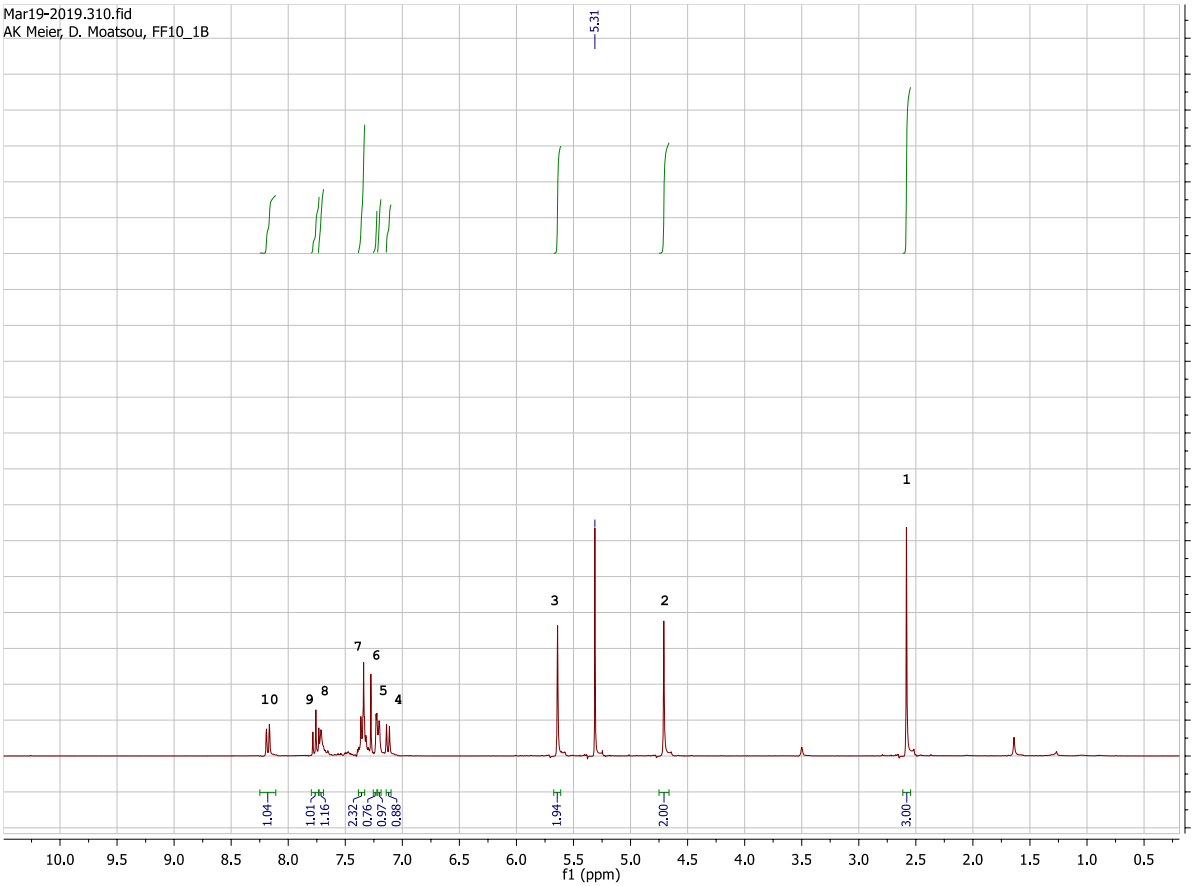

*Figure 20 [1]H NMR spectrum of the purified **T3** major isomer in CDCl3 (300 MHz).*

[1]H NMR ($CDCl_3$, 300 MHz) δ (ppm): 8.24 (1H, d, ^3J = 1.0Hz, -CH=CH-,*meta* pyridine), 7.74 (2H, d, ^3J = 1.0Hz, -CH=CH-, *meta* benzyl), 7.70 (1H, t, ^3J = 1.0 Hz, -CH=CH-, *para* pyridine), 7.35 (2H, t, ^3J = 1.0Hz, -CH=CH-,), 7.26 (2H, t, ^3J = 1.0 Hz, -CH=CH-), 7.12 (1H, d, ^3J = 1.0 Hz, -CH=CH-), 4.69 (2H, s, -CH_2-) 5.62 (2H, s, -CH_2-), 3.88 (1H, s, -OH), 2.52 (3H, s, CH_3).

*3.2.3 2-(4-(Pyridine-2-yl)-1H-1,2,3-triazol-1-yl)ethan-1-ol (**T4**)*

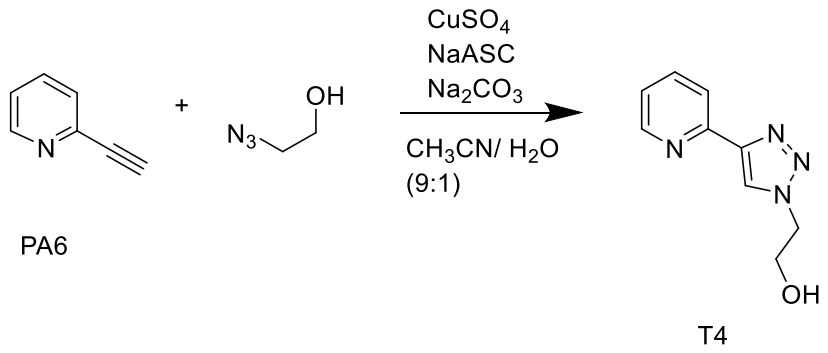

*Scheme 15 **T4** reaction*

After the successful ruthenium mediated cycloaddition (reaction T3), we decided to seek higher yields with a CuAAC. Since the previously starting materials were not suitable for that purpose (because it was an internal alkyne), we decided to use PA6 and 2-azidoethanol. Since this is a CuAAC, only the 1,5 adduct was obtained which led to higher yields.

The main isomer was isolated as a brown solid at a yield of 64.5%. ^{1}H NMR spectroscopy was used to determine the presence of the pure product. Compared to the spectra of the starting materials, the peak corresponding to the hydrogen of alkyne (at 4.08 ppm) were found to have shifted to 7.59 ppm, which was attributed to the deshielding of the respective protons due to the presence of the triazole group. As such, the successful preparation of the title compound was concluded.

^{1}H NMR (300 MHz, Chloroform-*d*) δ 8.04 (1H, d, ^{3}J = 7.7 Hz, -CH=CH-, *ortho*), 7.66 (1H, d, ^{3}J = 7.7 Hz, -CH=CH-, *meta*), 7.37 (1H, t, ^{3}J = 7.7 Hz, -CH=CH-, *para*), 7.12 (1H, d, ^{3}J = 7.7 Hz, -CH=CH-, *meta*), 7.59 (1H, s, =CH-), 3.92 (2H, t, ^{3}J = 6.6 Hz, -CH_2-), 3.66 (2H, t, ^{3}J = 6.6 Hz, -CH_2-).

*3.2.4 2-(1-(pyridine-2-yl)-1H-1,2,3-triazol-4-yl)ethan-1-ol (**T5**)*

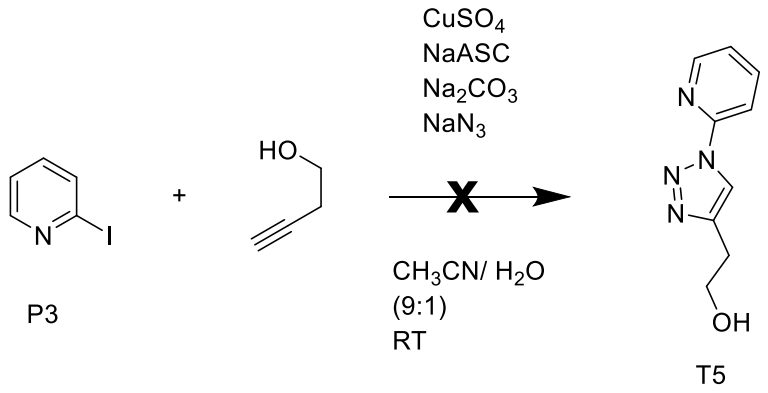

*Scheme 16 **T5** reaction*

Since CuAAC is known to result in high yields, we wanted to realise a one-pot click reaction with an *in situ* generation of pyridine azide. Unfortunately, the reaction did not work, as suggested by the mass spectrum collected from the product which showed no conversion of the 2-iodopiridine. The lack of reaction was attributed to the 2 position being unsuitable for this substitution.

*3.2.5 2-(4-(6-methylpyridin-2-yl)-1H-1,2,3-triazol-1-yl)ethan-1-ol (**T6**)*

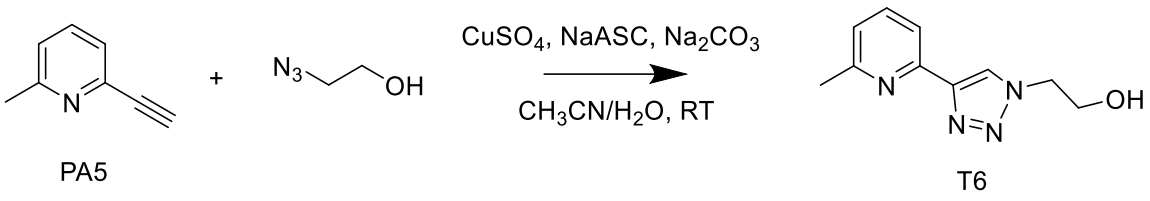

*Scheme 17 **T6** reaction*

Similar to the synthesis for the preparation of T4, we employed CuAAC utilising the pyridine alkyne PA5 while the 2-azidoethanol was synthesised *in situ*.

The product was isolated as a black solid at a yield of 64.3%. ^{1}H NMR spectroscopy was used to determine the presence of the pure product. Compared to the spectra of the starting materials, the peaks corresponding to the methylene groups of the azide (at 1.70 ppm and 4.17 ppm) were found to have shifted to 4.03 ppm and 4.51 ppm, respectively, which was attributed to the

deshielding of the respective protons due to the presence of the triazole group. Some impurities around 7.6 ppm and 3.6 ppm were detected, which were caused by a contamination of the NMR solvent. As such, the successful preparation of the title compound was concluded.

^{1}H NMR (300 MHz, Chloroform-*d*) δ 7.81 (1H, d, ^{3}J = 7.8 Hz, -CH=CH-, *meta*), 7.41 (1H, t, ^{3}J = 7.8 Hz, -CH=CH-, *para*), 7.00 (1H, d, ^{3}J = 7.8 Hz, -CH=CH-, *meta*), 4.51 (2H, t, ^{3}J = 5.0 Hz, -CH_2-), 4.03 (2H, t, ^{3}J = 5.0 Hz, -CH_2-), 2.47 (3H, s, -CH_3).

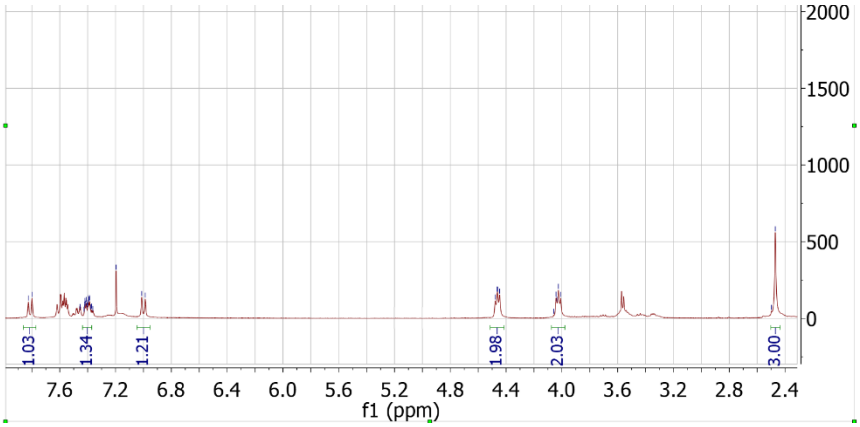

*Figure 21 ^{1}H NMR spectrum of the purified **T6** in CDCl3 (300 MHz)*

*3.2.6 2-(1-benzyl-5-(6-methylpyridin-2-yl)-1H-1,2,3-triazol-4-yl)ethan-1-ol (**T7**)*

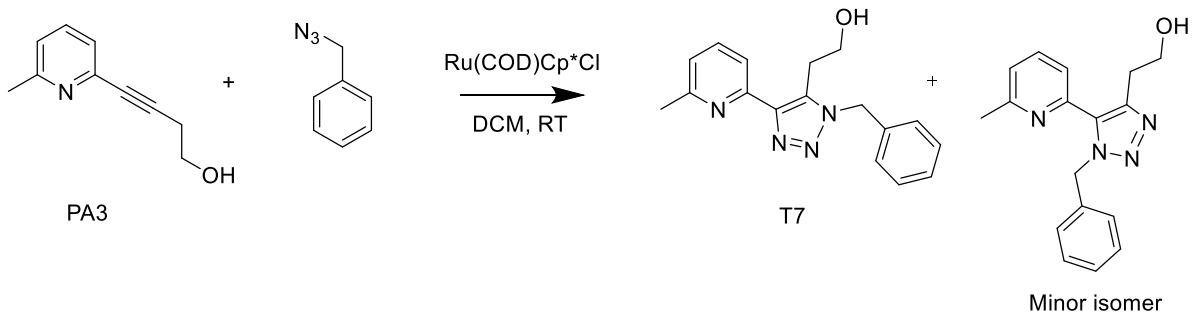

*Scheme 18 **T7** Reaction*

In this reaction we decided to use a pyridine derivative (PA3) that presents one more methylene unit compared to the previously used PA2 in reaction T3, which was hypothesised to prevent sterical effects in the subsequent esterification.

As ruthenium mediated cycloaddition was employed, two isomers were obtained (at a ratio of 7:3). As only one isomer is suitable for the complexation, they were separated by column chromatography. The minor isomer was isolated as a brown solid at a yield of 28.4%

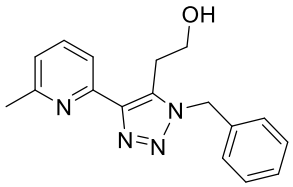

T7

Figure 22 ***T7*** *suitable isomer for complexation.*

The main isomer was isolated as a brown solid at a yield of 66.3%. ^{1}H NMR spectroscopy was used to determine the presence of the pure product. Compared to the spectra of the starting materials, the peak corresponding to the methylene unit of the butynyl alcohol (at 3.95 ppm) was found to have shifted to 3.16 ppm, which was attributed to the shielding caused by the presence of the triazole group. As such, the successful preparation of the title compound was concluded.

^{1}H NMR (300 MHz, Chloroform-*d*) δ 7.93 (1H, d, ^{3}J = 7.8 Hz, -CH=CH-, *meta pyridine*), 7.65 (1H, t, ^{3}J = 7.8 Hz, -CH=CH-, *para pyridine*), 7.26 (6H,m, -CH=CH-, benzyl), 7.06 (1H, d, ^{3}J = 7.8 Hz, -CH=CH-, *meta pyridine*), 5.53 (2H, s, -CH_2), 3.68 (2H, t, ^{3}J = 8.8 Hz, -CH_2-), 3.16 (2H, t, ^{3}J = 8.8 Hz, -CH_2-), 2.48 (3H, s, -CH_3).

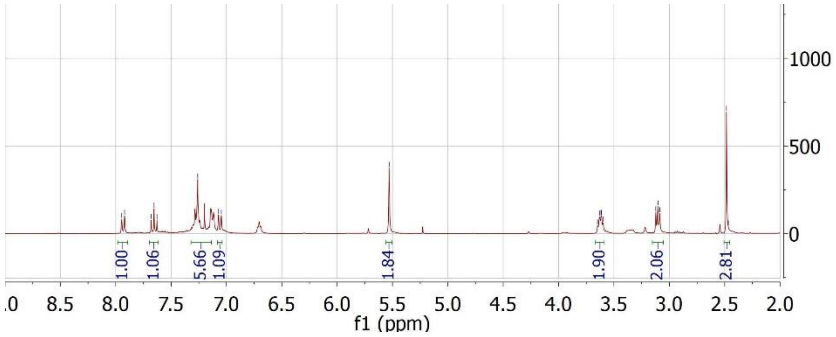

Figure 23 ^{1}H NMR spectrum of the purified ***T7*** *in CDCl3 (300 MHz).*

3.3 Synthesis of esters

After obtaining the ligands and complex **C2**, a polymerisable double bond needed to be introduced into the structure in order to render the molecule polymerisable by radical processes. In this section, five esters were synthesised. In all cases, the acrylate derivative of the ligand was targeted as acrylates are readily reactive (Scheme 19).

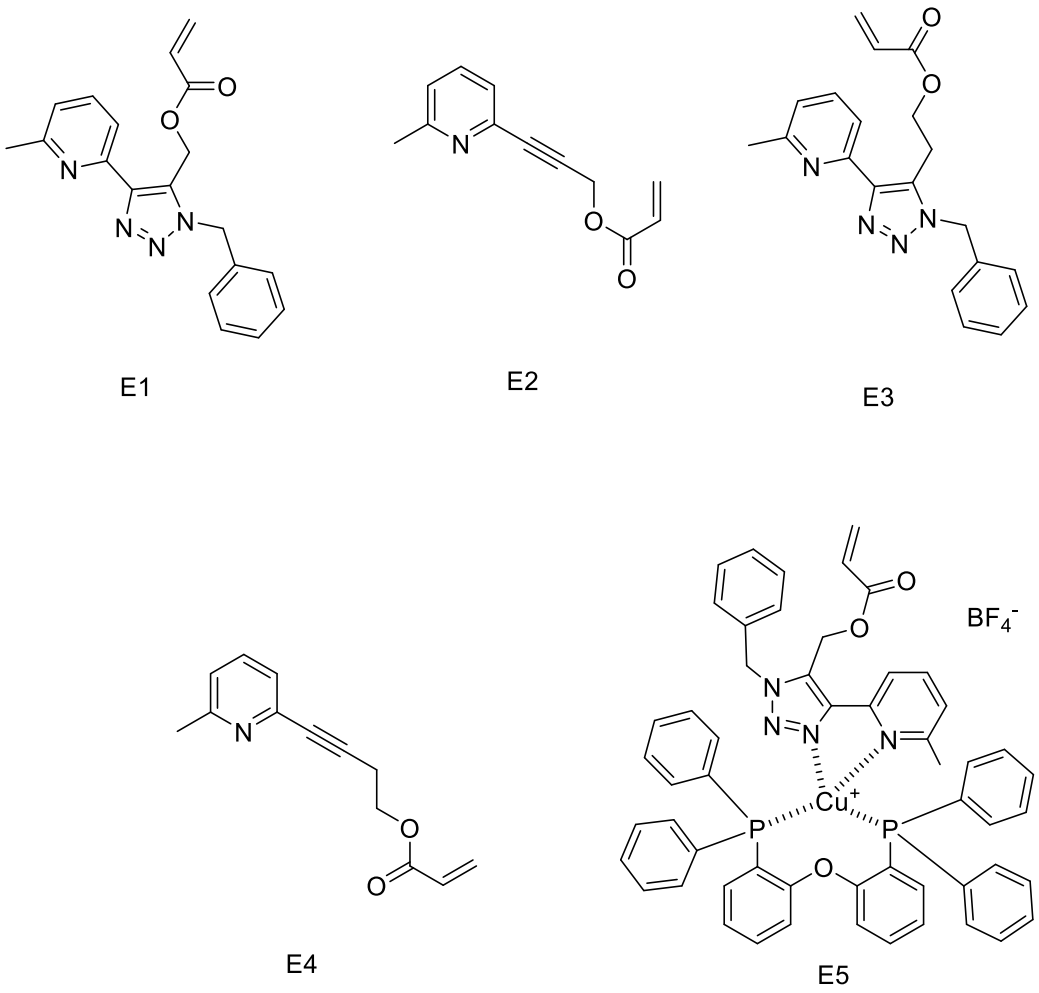

Scheme 19 Scheme of designed esters

*3.3.1 Ester (1-benzyl-4-(6-methylpyridin-2-yl)-1H-1,2,3-triazol-5-yl)methyl acrylate **E1***

Starting with the triazole T3, we screened the conditions needed to obtain the acrylate derivative employing either acrylic acid or acryloyl chloride.

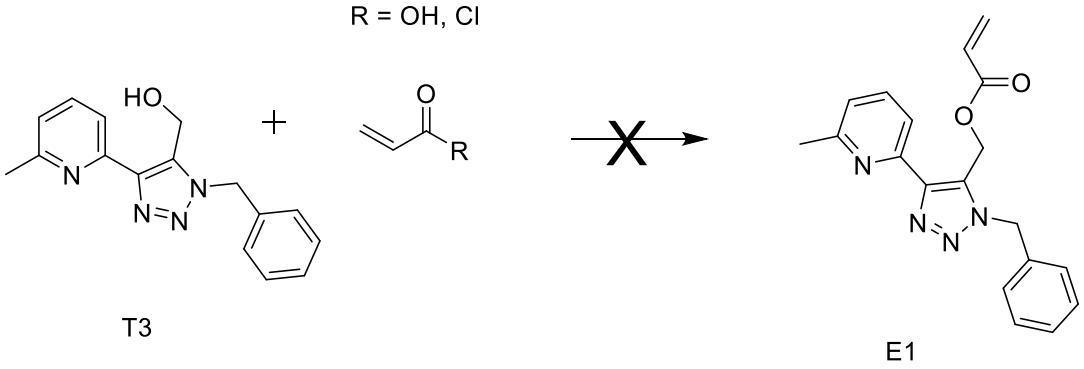

*Scheme 20 **E1** reaction*

Reagent	Catalyst	Yield
Acryloyl chloride	TEA	-
Acrylic acid	DMAP/DCC	-
Acrylic acid	DMAP/EDCI	-

Table 2 Screening of esterification condition

Despite trying various common reagents for esterification, ^{1}H NMR data showed no conversion as the same peaks were observed for the starting materials and the product. This suggested that the reaction did not take place which was attributed to the sterically hindered alcohol. The marked peaks indicate the hydroxyl peak and the methylene next to the hydroxyl group, in case of formation of the desired product one peak should be gone (the -OH) and one should be shifted (the methylene).

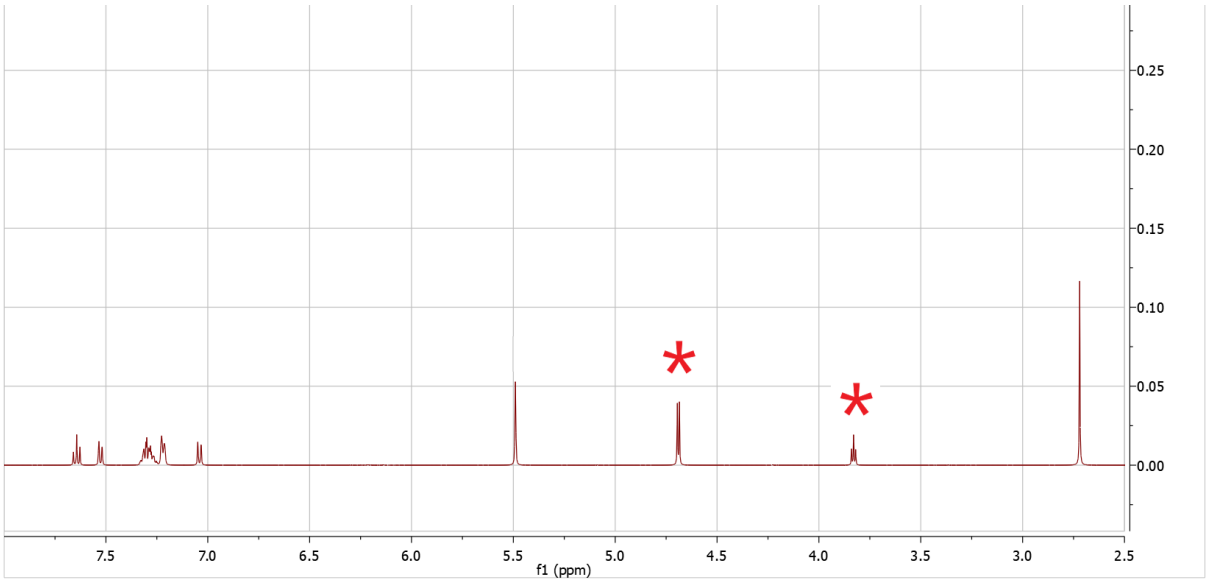

*Figure 24 ^{1}H NMR spectrum of **E1** product in CDCl3 (300 MHz).*

*3.3.2 Ester 3-(6-methylpyridin-2-yl)prop-2-yn-1-yl acrylate **E2***

Since the triazole was too sterically demanding, the same esterification reaction was attempted with PA2.

*Scheme 21 **E2** reaction*

This time, the isolation of a product was possible and further characterisation was pursued to determine the purity of the desired product.

Reagent	Catalyst	Yield
Acryloyl chloride	TEA	73.6%
Acrylic acid	DMAP/DCC	61.8%
Acrylic acid	DMAP/EDCI	66.3%

*Table 3 Screening for esterification condition **E2***

IR spectroscopy was used to confirm the presence of the product. The presence of a band at 1725 cm^{-1} was attributed to the C=O stretching of the newly formed ester while the disappearance of the band at 3202 cm^{-1} corresponding to the -OH stretching of the starting material suggested the successful esterification.

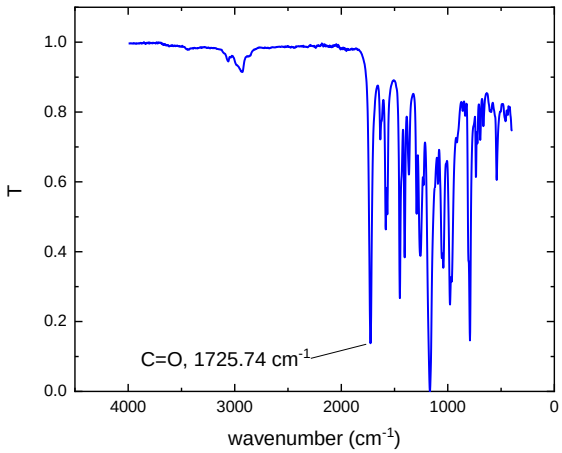

*Figure 25 IR spectra of **E2***

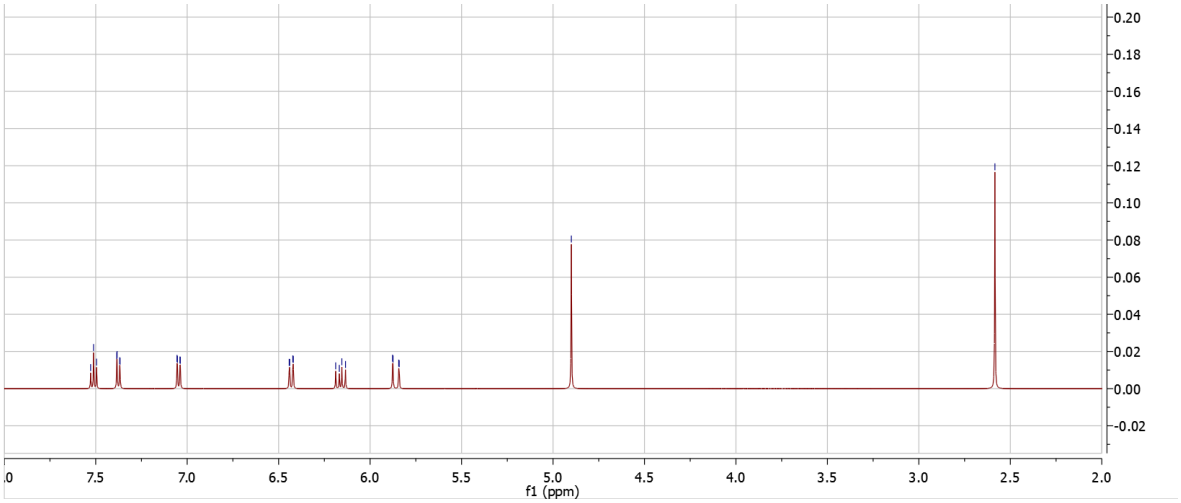

Figure 26 ^{1}H NMR spectrum of the purified E2 in CDCl3 (300 MHz).

^{1}H NMR (300 MHz, Chloroform-*d*) δ 7.50 (1H, t, ^{3}J = 7.7 Hz, -CH=CH-, *para*), 7.23 (1H, d, ^{3}J = 7.7 Hz, -CH=CH-, *meta*), 7.07 (1H, d, ^{3}J = 7.7 Hz, -CH=CH-, *meta*), 6.44 (1H, dd, ^{3}J = 17.3, 1.5 Hz, -CH=C**H**$_2$), 6.04 (m, 1H, -C**H**=CH$_2$), 5.85 (1H, dd, ^{3}J = 17.3, 1.5 Hz, 1H, -CH=C**H**$_2$), 4.96 (s, 2H, =C-CH$_2$-O-), 2.50 (3H, s, Ar-CH$_3$).

3.3.3 Ester 2-(1-benzyl-4-(6-methylpyridin-2-yl)-1H-1,2,3-triazol-5-yl)ethyl acrylate **E3**

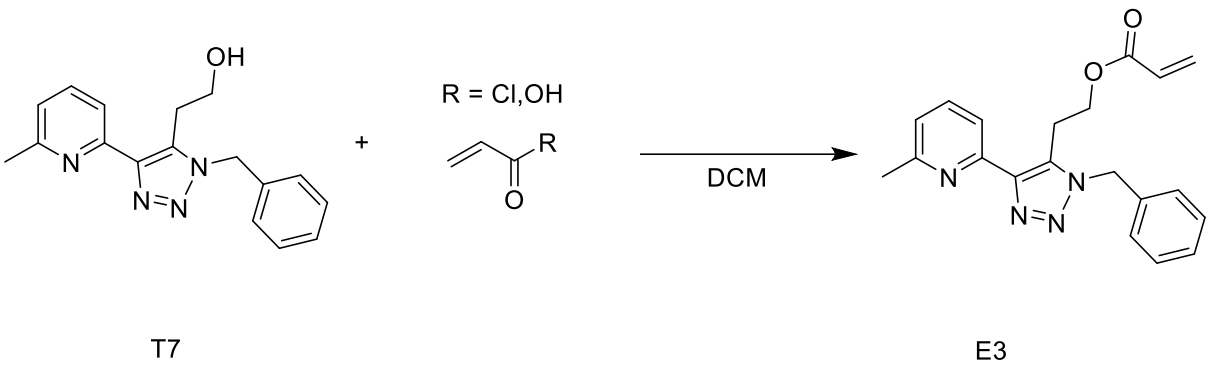

T7 E3

*Scheme 22 Reaction **E3***

Since T3 was found to not undergo esterification, T7 was employed instead, as T7 has one more methylene bridge between the alcohol and the triazole.

This reaction indeed was found to proceed with all the conditions attempted.

Acyl derivative	Catalyst	Yield
Acryloyl chloride	TEA	73.6%
Acrylic acid	DMAP/DCC	61.8%
Acrylic acid	DMAP/EDCI	66.3%

*Table 4 Screening for esterification condition **E3***

IR spectroscopy was used to confirm the presence of the product. The presence of a band at 1727 cm^{-1} was attributed to the C=O stretching of the newly formed ester while the disappearance of the band at 3212 cm^{-1} corresponding to the -OH stretching of the starting material suggested the successful esterification.

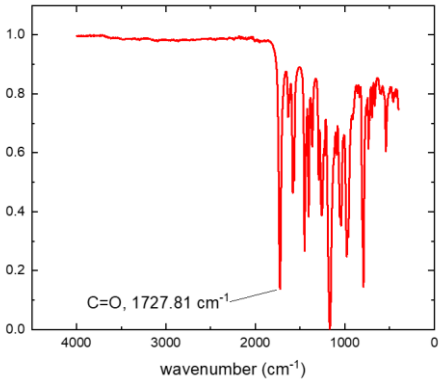

*Figure 27 IR spectra of **E3**.*

IR ν (cm^{-1}) 1727 (C=O stretch).

^{1}H NMR (300 MHz, Chloroform-*d*) δ 7.63 (1H, t, ^{3}J = 7.9 Hz, 1H, -CH=CH-, *para* pyridine), 7.47 (1H, d, ^{3}J = 7.9 Hz,-CH=CH-, *meta* pyridine), 7.26 (m, 6H, -CH=CH-, benzyl), 6.98 (d, ^{3}J = 7.9 Hz, 1H, -CH=CH-, *meta* pyridine), 6.45 (1H, dd, ^{3}J = 17.3, 1.5 Hz, -CH=C**H**$_2$), 6.17 (1H, m, -C**H**=CH$_2$), 5.80 (1H, dd, ^{3}J = 17.3, 1.5 Hz, -CH=C**H**$_2$), 4.48 (2H, t, ^{3}J = 6.7 Hz, -CH$_2$-), 2.85 (2H, t, ^{3}J = 6.7 Hz, -CH$_2$-), 2.75 (3H,s, -CH$_3$).

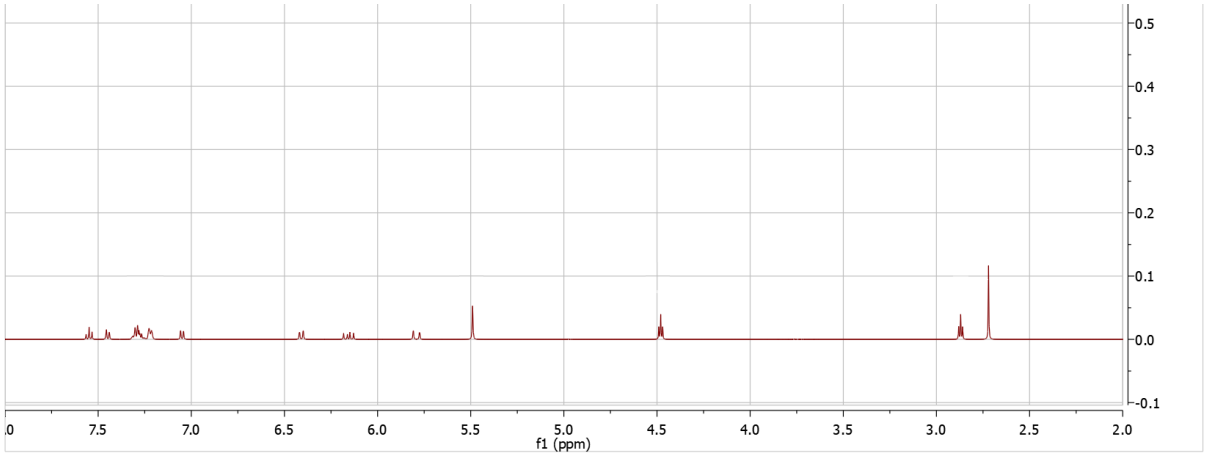

Figure 28 ^{1}H NMR spectrum of the purified E3 in CDCl3 (300 MHz).

*3.3.3 Ester 4-(6-methylpyridin2-yl)but-3-yn-1-yl acrylate **E4***

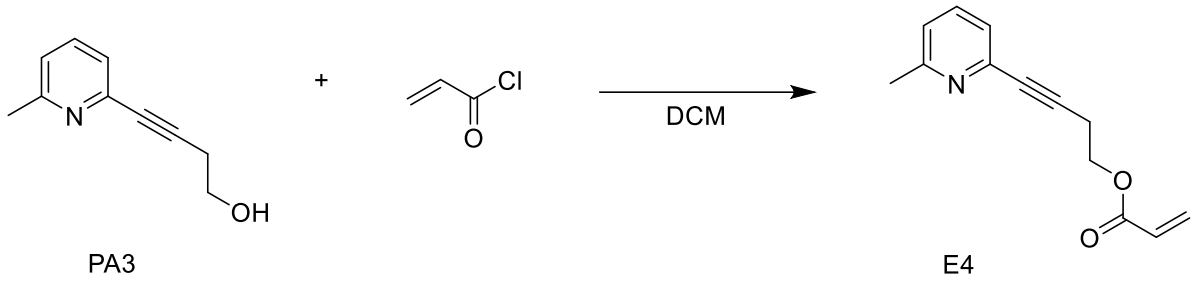

*Scheme 23 Reaction **E4***

The highest yielding conditions for the preparation of E3 were also employed to prepare E4, namely using acryloyl chloride and TEA.

IR spectroscopy was used to confirm the presence of the product. The presence of a band at 1723 cm^{-1} was attributed to the C=O stretching of the newly formed ester while the disappearance of the band at 3202 cm^{-1} corresponding to the -OH stretching of the starting material suggested the successful esterification.

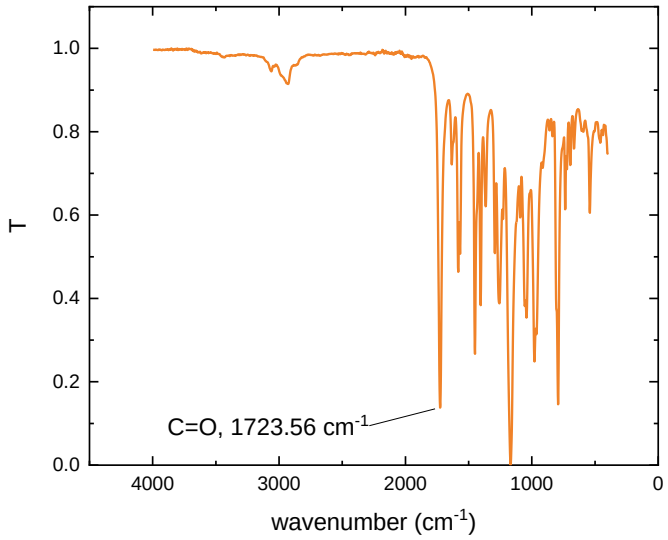

*Figure 29 IR spectra of **E4**.*

IR ν (cm^{-1}) 1723 (C=O stretch).

^{1}H NMR (300 MHz, Chloroform-*d*) δ 7.97 (1H, d, ^{3}J = 7.8 Hz, -CH=CH-, *meta*), 7.58 (1H, t, ^{3}J = 7.8 Hz, -CH=CH-, *para*), 6.98 (1H, d, ^{3}J = 7.8 Hz, -CH=CH-, *meta*), 6.28 (1H, dd, ^{3}J = 17.3, 1.5 Hz, -CH=C**H**$_2$), 5.95 (1H, dd, ^{3}J = 17.3, 1.5 Hz, -CH=C**H**$_2$), 5.74 (1H, m, -C**H**=CH$_2$), 4.33 (2H, t, ^{3}J = 6.6 Hz, -CH$_2$-C**H**$_2$-OH), 3.42 (2H, t, ^{3}J = 6.6 Hz, C-C**H**$_2$-CH$_2$), 2.45 (3H, s, Ar-CH$_3$).

*3.3.4 Ester **E5***

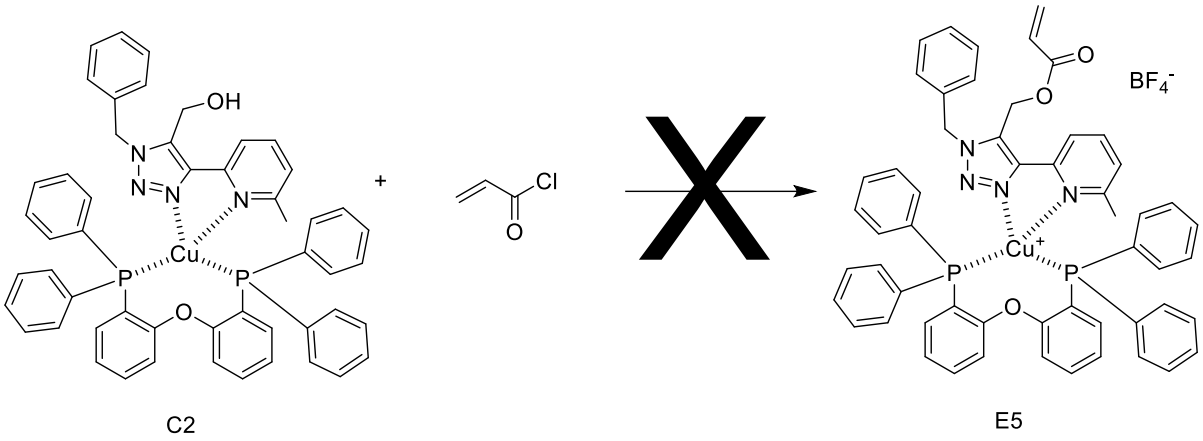

C2 E5

*Scheme 24 Reaction **E5***

Similarly to the reactions above, we sought to obtain the ester of the copper complex by reaction with acryloyl chloride. Unfortunately, the mass spectra showed no conversion, which was attributed to the steric hindrance of the complex.

HRMS m/z ($C_{56}H_{46}CuN_4O_3P_2$): 947.23 (calculated), 877.22 (found, starting material).

3.4 Complexation

After the synthesis of the ligands, the focus was shifted to the synthesis of the copper complex, starting from the previously obtained ligands.

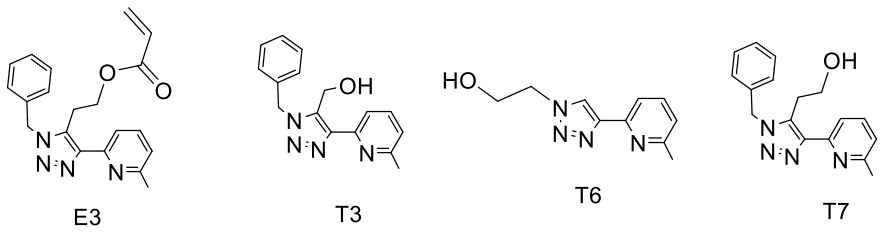

Scheme 25 Starting materials for complexation

All the designed complexes are heteroleptic complexes with bis[(2-diphenylphosphino)phenyl] ether (also called POP) as the second ligand. The copper was provided by a tetracetonitrile copper (I) salt which was synthesised by the Bizzarri group.

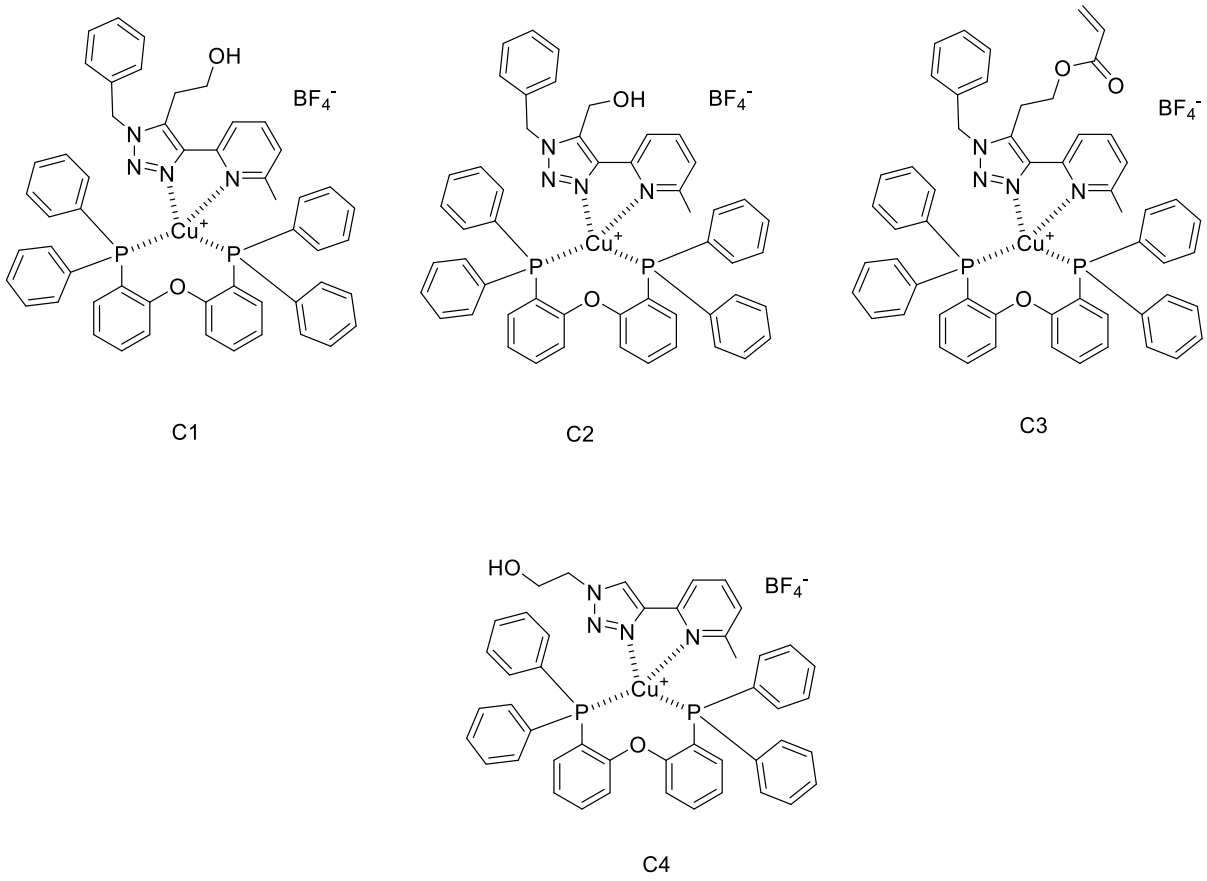

Scheme 26 Designed complexes

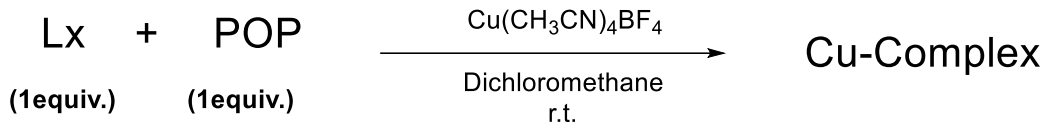

Scheme 27 General reaction scheme of complexation

All the copper (I) complexes designed are charged (+1) and use as counterion BF_4^-. It is noted that only one complex (**C3**) is suitable for direct polymerisation. All other complexes are suitable for polymer blends or nanoprecipitation.

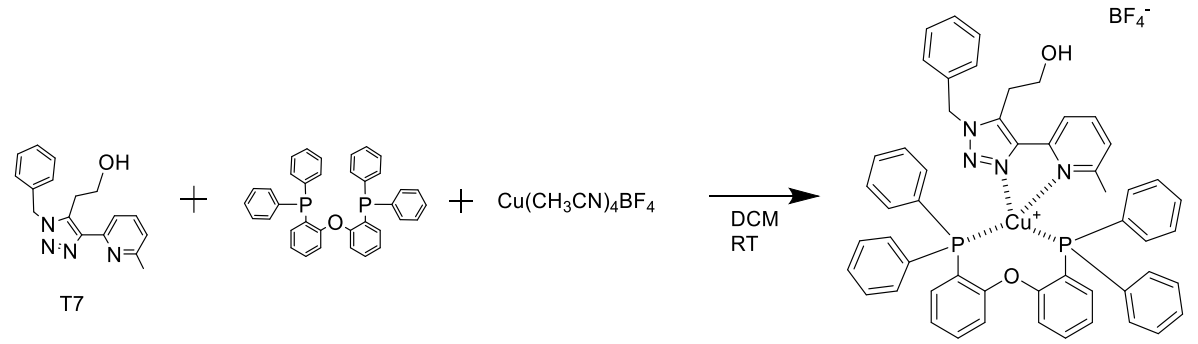

*Scheme 28 Complexation **C1***

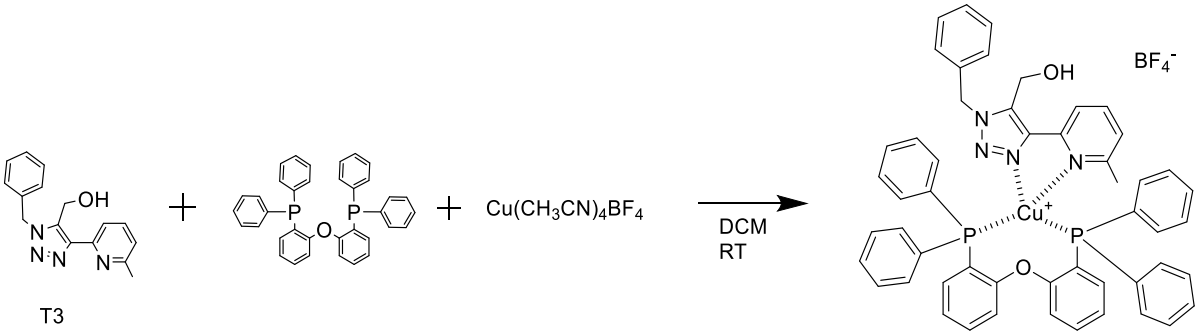

*Scheme 29 Complexation **C2***

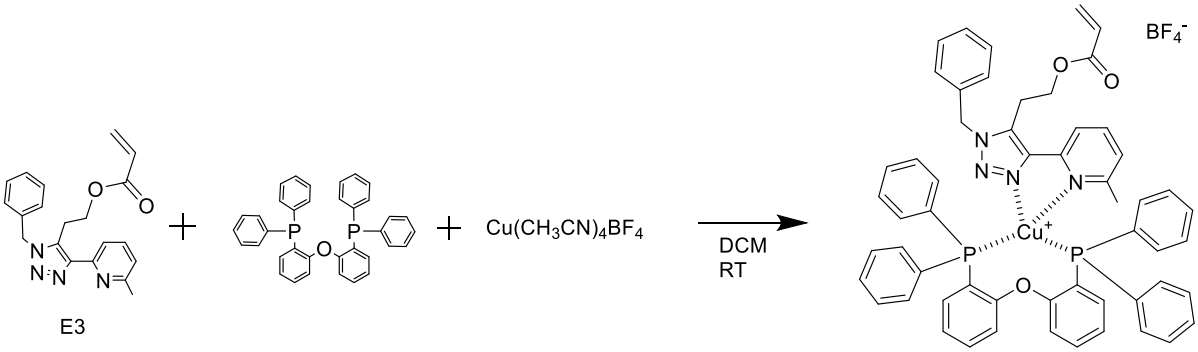

*Scheme 30 Complexation **C3***

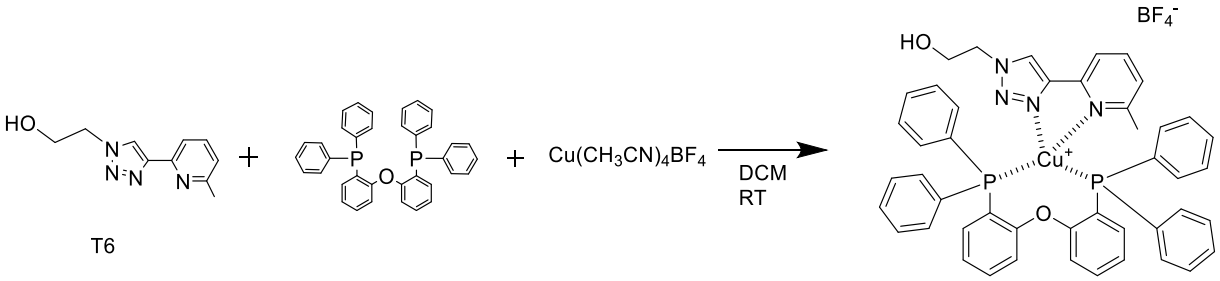

*Scheme 31 Complexation **C4***

All the complexes are pale yellow crystals and they all exhibit luminescence.

Figure 30 Complex 1 exhibits luminescence under irradiation with a UV lamp (λ =264 nm).

Figure 31 Complex 2 exhibits luminescence under irradiation with a UV lamp (λ =264 nm).

Figure 32 Complex 4 exhibits luminescence under irradiation with a UV lamp (λ =264 nm).

For checking the presence of the pure products, a mass spectrum for each complex was recorded. The spectra confirmed the presence of the complexes plus their counter ion (BF_4^-). Furthermore, a ^{1}H NMR spectrum for each complex was collected. The shifting of the pyridine signals (two *meta* hydrogens and one *para*) confirms the successful complexation reaction.

C1

^{1}H NMR (300 MHz, Chloroform-*d*) δ 7.87 (1H, t, ^3J = 7.8 Hz, -CH=CH-, *para* pyridine), 7.70 (1H, d, ^3J = 7.8 Hz, -CH=CH-, *meta*), 7.28 (m, 28H, -CH=CH-), 7.06 (1H, d, ^3J = 7.8 Hz, -CH=CH-, *meta*), 6.73 (6H, m, -CH=CH-, benzyl), 5.53 (2H, s, -CH_2-C**H**$_2$-OH), 3.59 (2H, t, ^3J = 8.8 Hz, -CH_2-C**H**$_2$-OH), 3.08 (2H, t, ^3J = 8.8 Hz, -C**H**$_2$-CH_2-OH), 1.94 (3H, s, Ar-CH_3),

HRMS m/z ($C_{53}H_{43}CuN_4O_2P_2BF_4$): 979.22 (calculated), 979.22 (found).

C2

^{1}H NMR (300 MHz, Chloroform-*d*) δ 7.99 (1H, d, ^3J = 7.8 Hz, -CH=CH-, *meta* pyridine), 7.87 (1H, t, ^3J = 7.8 Hz, -CH=CH-, *para* pyridine), 7.47 (1H, d, ^3J = 7.8 Hz, -CH=CH- *meta* pyridine), 7.26 (m, 28H, -CH=CH-, -phenyl), 6.67 (6H, m, -CH=CH-, -benzyl), 5.75 (2H, s, Ar-CH_2-), 2.00 (3H, s, Ar-CH_3).

HRMS m/z ($C_{52}H_{41}CuN_4O_2P_2BF_4$): 965.20 (calculated), 965.20 (found).

C3

^{1}H NMR (300 MHz, Chloroform-*d*) δ 7.99 (1H, t, ^3J = 7.8 Hz, 1H, -CH=CH-, *para* pyridine), 7.83 (1H, d, ^3J = 7.8 Hz, -CH=CH-, *meta* pyridine), 7.48 (6H, m, -CH=CH-, -benzyl), 7.08 (1H, d, ^3J = 7.8 Hz, -CH=CH-, *meta* pyridine) 6.92 (28H, m, -CH=CH-, -phenyl), 6.27 (1H, dd, ^3J = 17.3, 10.4 Hz, -CH=C**H**$_2$), 5.87 (1H, dd, ^3J = 17.3, 10.4 Hz, -CH=C**H**$_2$), 5.74 (1H, m, -C**H**=CH_2), 4.06 (2H, t, ^3J = 6.9 Hz, -CH_2-C**H**$_2$-OH), 3.40 (t, ^3J = 6.9 Hz, 2H, -C**H$_2$**-CH_2-OH), 2.04 (3H, s, Ar-CH_3).

IR ν (cm^{-1}) 1726 (C=O stretch)

HRMS m/z ($C_{56}H_{46}CuN_4O_3P_2BF_4$): 1034.24 (calculated), 1034.24 (found).

C4

HRMS m/z ($C_{46}H_{38}CuN_4O_2P_2BF_4$): 890.18 (calculated), 890.18 (found).

3.5 Synthesis of azides

Three azides were synthesised and used *in situ* in this work.

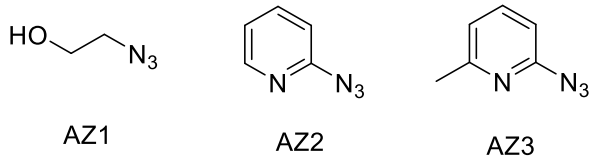

Scheme 32 AZs synthesised

As starting materials, we used commercially available pyridines and 2-bromoethanol. Owing to the intrinsic dangers of azides (they are explosive), all azides were used directly for the next reaction, without further purification.

*3.5.1 2-azidoethanol **AZ1***

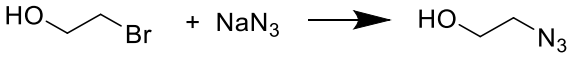

*Scheme 33 **AZ1** reaction*

Since the formation of A1 is an S_N2 reaction, we attempted to optimise the reaction by screening solvents.

Solvent	Solvent ratio	Time to complete conversion (h)
$EtOH/H_2O$	7:3	72
$EtOH/H_2O$	9:1	74
CH_3CN	-	32

Table 5 Screening conditions S_N2

The fastest reaction was obtained using acetonitrile as solvent.

*3.5.2 Azides 2- azidopyridine **AZ2** and 2-azido-6-methylpyridine **AZ3***

For the preparation of the desired triazoles we sought to synthesise two azides (AZ2, AZ3) that can be used in CuAAC with pyridine alkynes.

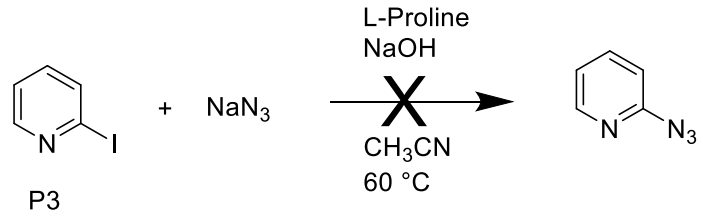

*Scheme 34 **AZ2** reaction*

Unfortunately, the TLC showed no conversion for either reaction. Only one spot corresponding to the starting halide (P3 r_f=0.25, P1 r_f=0.31 in MeOH/DCM 1:9) was observed. The lack of reactivity was attributed to the 2 position of pyridine being unsuitable for this type of aromatic S_N.

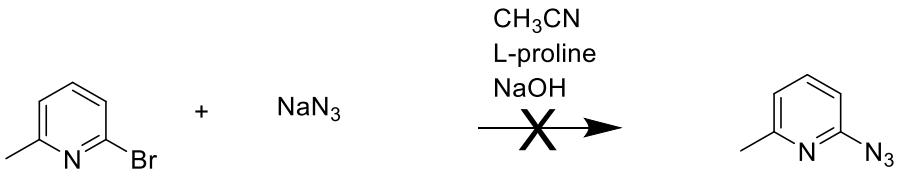

*Scheme 35 **AZ3** reaction*

3.6 Copolymer and polymer synthesis

After the synthesis of the complex and the ligands, we moved on to the synthesis of copolymers. In this section, radical polymerisation conditions were employed in order to assess the ability of the complex/ligands to copolymerise.

First, the homopolymerisation conditions for MA were assessed.

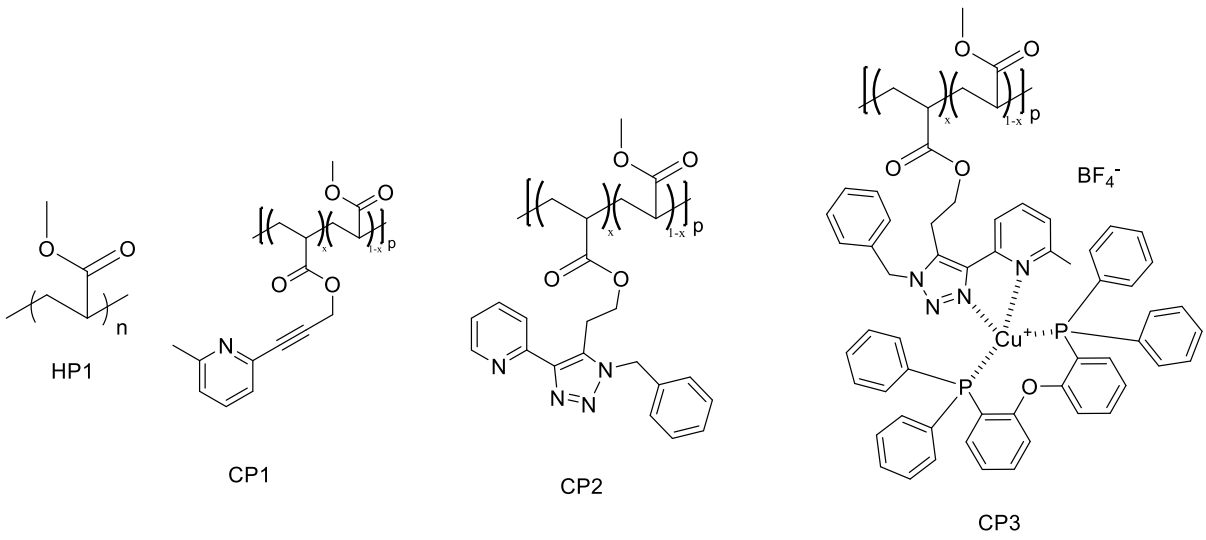

Scheme 36 Designed homopolymer and copolymers

*3.6.1 Homopolymer **HP1***

In order to establish the reaction conditions for the copolymerisation, we first sought the best conditions for the homopolymerisation of MA, taking into account the resulting M_w/M_n as an indication of the control of the polymerisation (with a M_w/M_n ideally < 2).

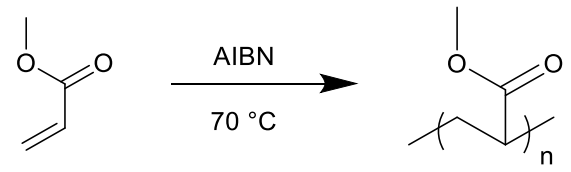

*Scheme 37 Reaction **HP1***

Solvent	Ratio between the monomer and the solvent (v/v)	M_w/M_n	M_w (g/mol)
DMSO	1:4	3.9	3,600
DMSO	1:8	2.8	3,300
DMSO	1:10	2.3	3,500
1,4-dioxane	1:4	2.4	3,500
1,4-dioxane	1:8	1.6	3,700

Table 6 Screening of polymerization condition

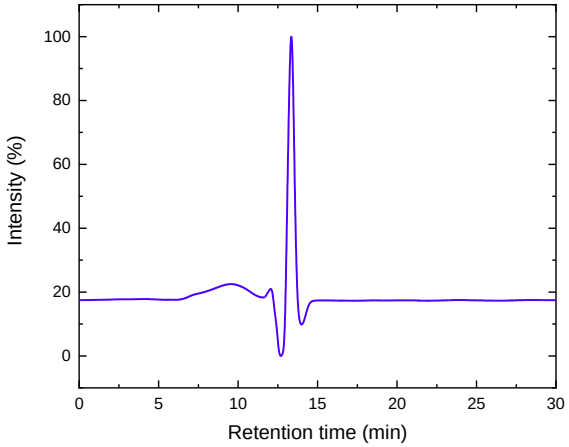

Figure 33 Chromatogram of HP1 in DMSO 1:4

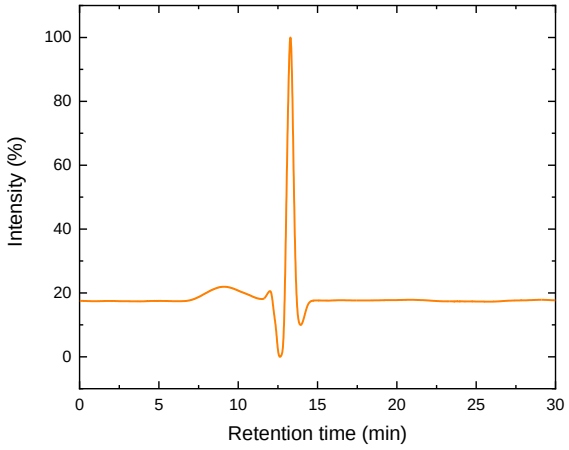

Figure 34 Chromatogram of HP1 in DMSO 1:8

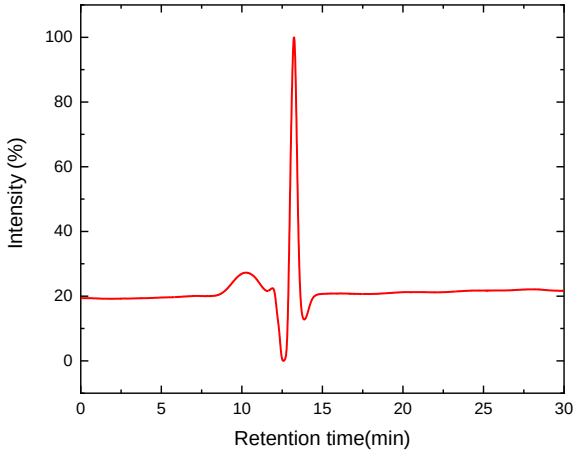

Figure 35 Chromatogram of HP1 in DMSO 1:10

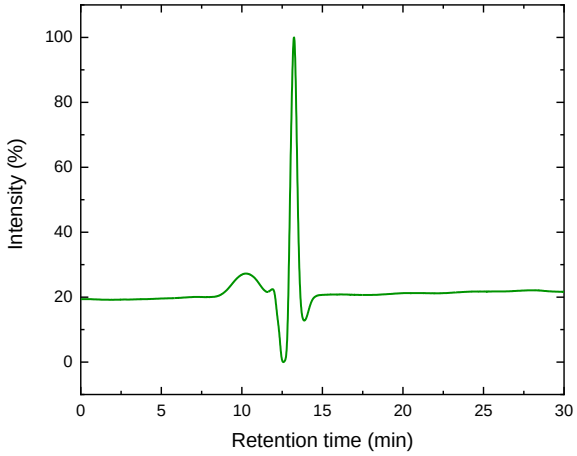

Figure 36 Chromatogram of HP1 in 1,4-dioxane 1:4

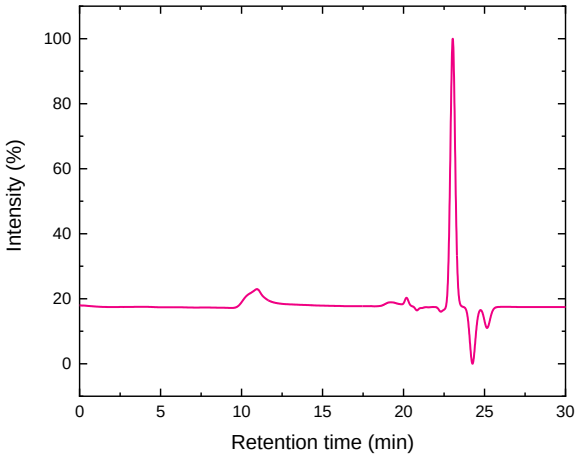

Figure 37 Chromatogram of HP1 in 1,4-dioxane 1:8

*3.6.2 Copolymers **CP1**, **CP2** and **CP3***

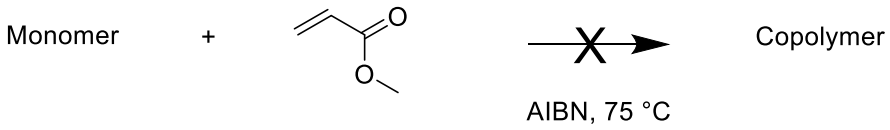

Table 7 Copolymerisation general scheme

Several conditions were tried to obtain the copolymers but unfortunately none worked. Indeed ^{1}H-NMR spectrum showed no conversion. The ratio of solvents was changed (as in reaction **HP1),** but no polymer was obtained. This was attributed to the vinyl group being inaccessible due to the bulky nature of the monomer. In future work, it will be necessary to synthesise a monomer with greater distance between the double bond and the copper/functional part.

Solvent	Ratio between the monomer and the solvent (v/v)	Yield (%)
DMSO	1:4	-
DMSO	1:8	-
DMSO	1:10	-
1.4-dioxane	1:4	-
1,4-dioxane	1:8	-
1,4-dioxane	-	-

Table 8 Screening of copolymerization condition

3.7 Nanoparticles

In order to prepare complex-containing nanoparticles, the complexes were encapsulated in the polymer *via* nanoprecipitation. Different complex contents were targeted by varying the weight ratio of the complex with respect to the polymer. The obtained nanoparticles were kept in solution and dynamic light scattering (DLS) analyses were carried out. The solutions containing the nanoparticles were opalescent and stable after 4 days.

NPs	Complex	Complex quantity (w/w)	Diameter (nm)	Polydispersity
NP1.1	Complex 1	1%	142.60	0.16
NP1.10	Complex 1	10%	126.90	0.07
NP2.1	Complex 2	1%	115.50	0.06
NP2.10	Complex 2	10%	95.50	0.11
NP3.1	Complex 3	1%	132.80	0.05
NP3.10	Complex 3	10%	109.00	0.10

Table 9 NPs synthetized

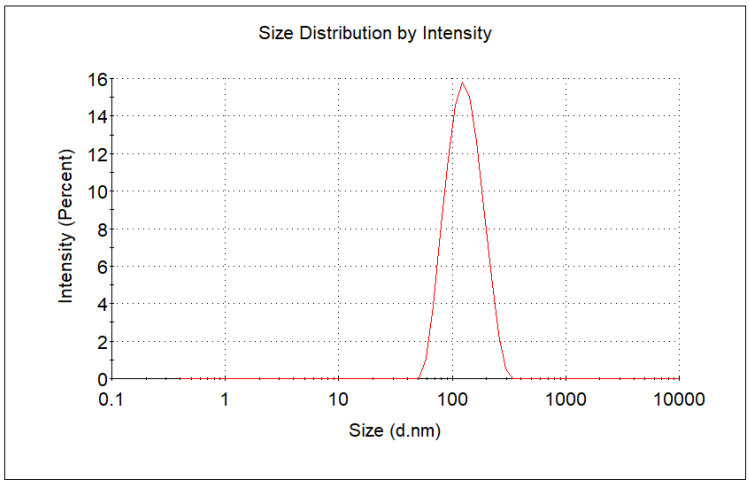

Figure 38 Size distribution graph of NP1.1

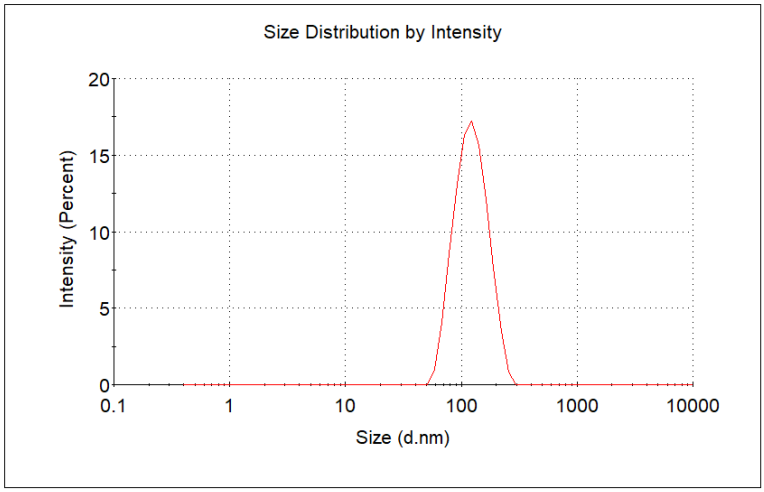

Figure 39 Size distribution graph of NP1.10

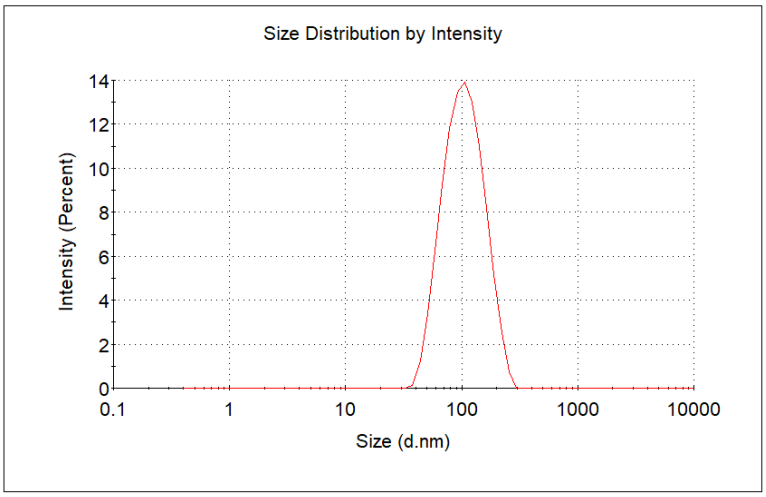

Figure 40 Size distribution graph of NP2.1

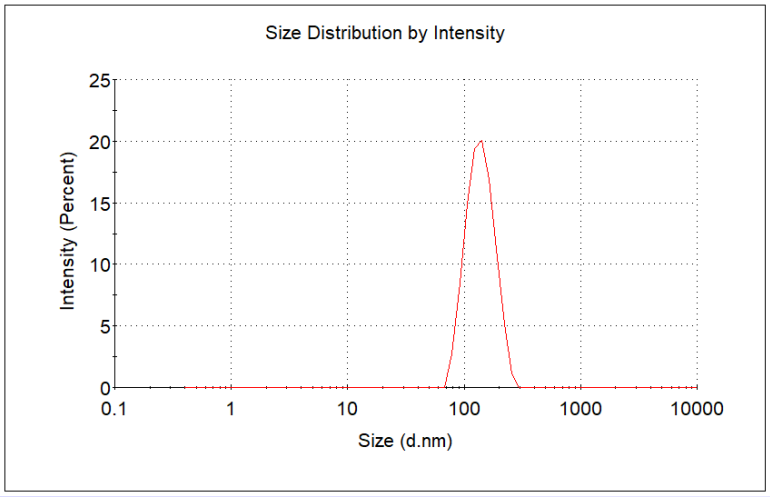

Figure 41 Size distribution graph of NP2.10

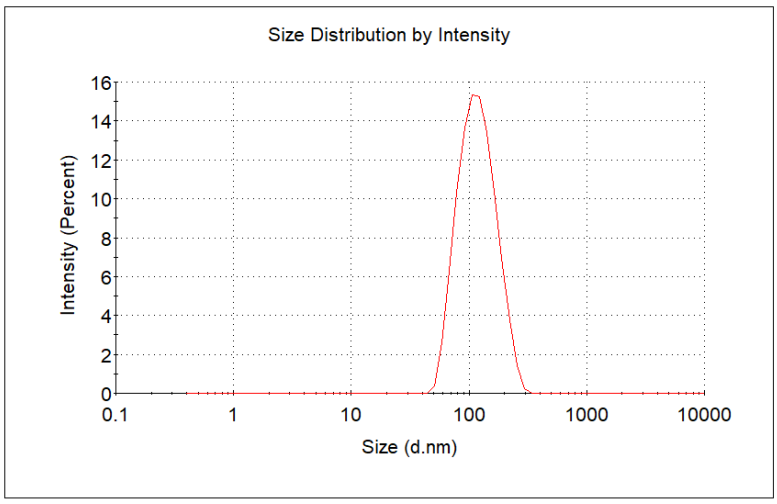

Figure 42 Size distribution graph of NP3.1

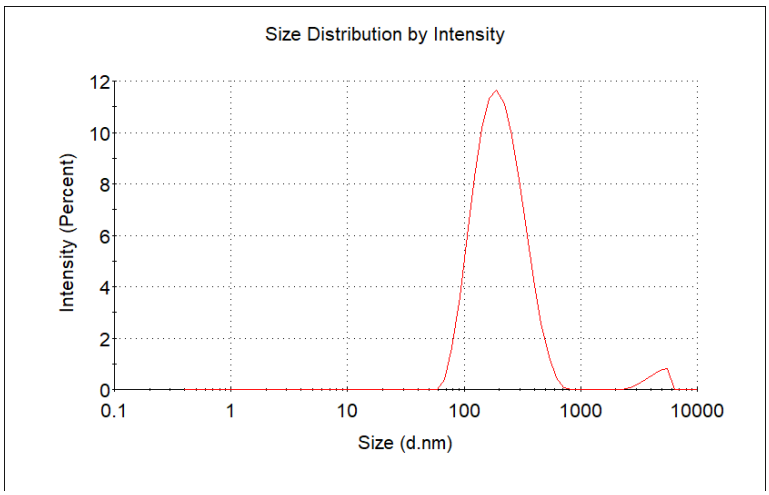

Figure 43 Size distribution graph of NP3.10

All the nano particles show a nano diameter and an acceptable polydispersity.

However, is interesting how when adding more complex the particles tend to be smaller and the distribution to be wider.

Furthermore, when investigating under UV lights luminescence was observed, suggesting the presence of the complex. Fluorescence spectra were collected at an excitation wavelength of 295 nm.

NPs	Maximum emission peak (nm)
NP1.1	399
NP1.10	401
NP2.1	404
NP2.10	405
NP3.1	410
NP3.10	411

Table 10 NPs maximum emission peak

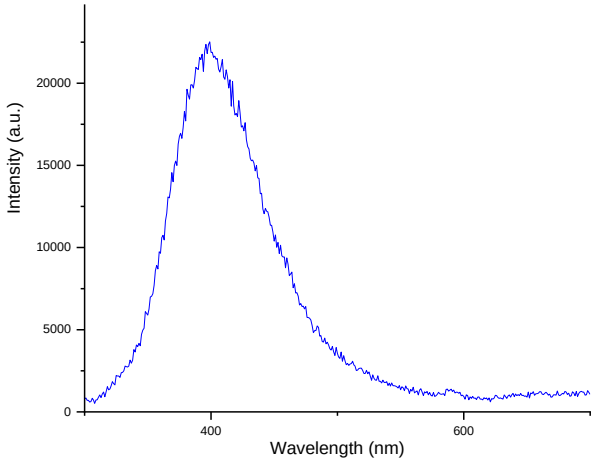

Figure 44 NP1.1 emission spectrum

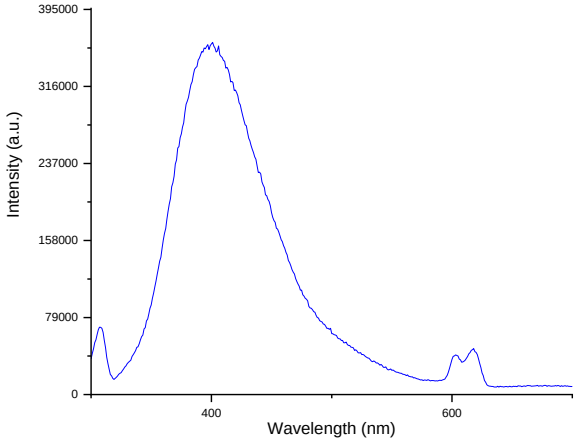

Figure 45 NP1.10 emission spectra

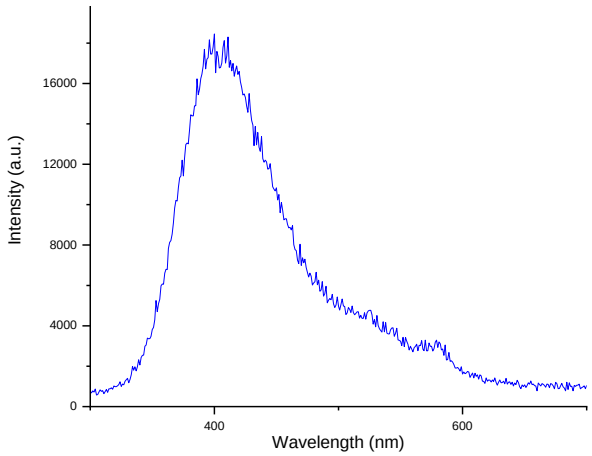

Figure 46 NP2.1 emission spectrum

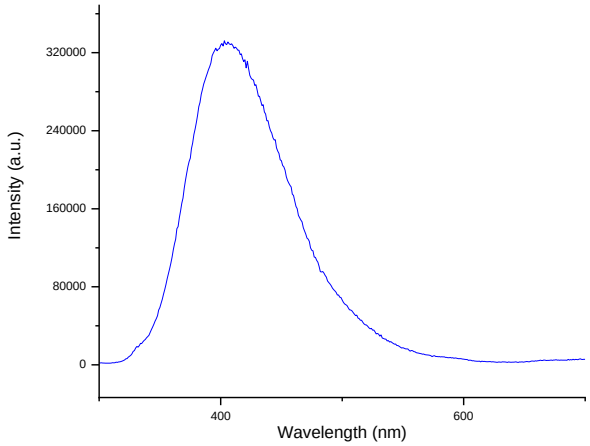

Figure 47 NP2.10 emission spectra

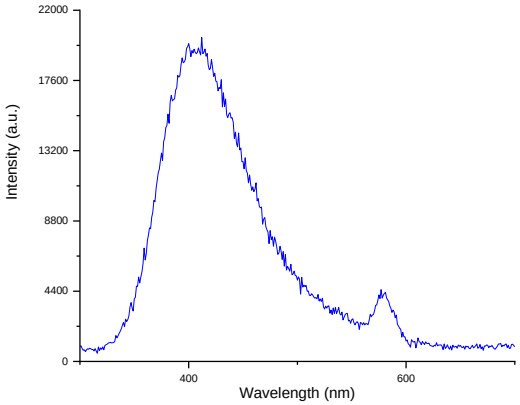

Figure 48 NP3.1 emission spectrum

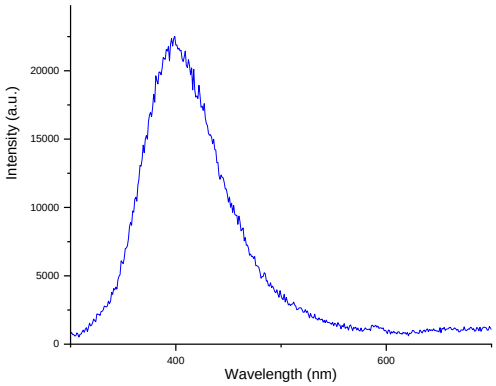

Figure 49 NP3.10 emission spectra

All the particles were found to emit with a maximum around 400 nm, with a slight red shifting observed for complexes 2 and 3. However, all the nanoparticles were found to be fluorescent in water suggesting that the encapsulation in PMA can prevent the solvent quenching of the luminescence.

3.8 Blends

After the synthesis of the NPs we decided to move forward and realise the blends between the complexes and the PMA previously synthesised (HP1). We prepared six different blends, each with a different quantity and type of complex (as shown in Table 11)

Blends	Complex	Quantity of complex (w/w)
B1.1	Complex 1	1%
B1.10	Complex 1	10%
B2.1	Complex 2	1%
B2.10	Complex 2	10%
B3.1	Complex 3	1%
B3.10	Complex 3	10%

Table 11 Blends made

The blends obtained have a thickness of about 1 mm, with a homogeneous appearance and were found to exhibit luminescence under UV light.

No further analysis of the blend was run (such as DSC, DMA) because of the lack of time.

Figure 50 Luminescence of blend B2.1 under irradiation with a UV lamp (λ =264 nm).

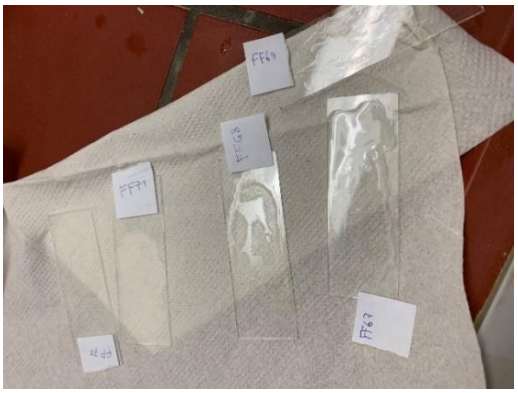

Figure 51 Blends obtained

4 Conclusion

The main goal of this thesis was to prepare a copper complex that exhibits luminescence and can be polymerised (both requisites to make the monomer suitable for photoinduced ATRP), in order to prevent its quenching by embedding it in a polymer matrix. At the end of this work, three copper complexes were prepared, one of which bearing a polymerisable moiety, while polymeric nanoparticles, as well as blends, were also prepared. In order to form the complexes, four pyridyl-triazoles were synthesised and different esterification and radical polymerisation conditions were screened. Unfortunately, it was not possible to obtain a copolymer of the monomer nor to perform a one-pot cycloaddition to get to the triazole.

All the complexes obtained in the course of this master thesis work showed good stability in air and exhibited luminescence. The nanoparticles showed luminescence in solution that confirms the idea that the nanoencapsulation can be a solution that helps to prevent the quenching of the luminescence in solution. Further investigations need to be carried out to determine the exact quantity of complexes encapsulated. For instance, transmission electron microscopy (TEM) imaging could be used to image the encapsulation as the metal complex would appear darker than the plain polymer, on account of its greater absorption of the electron beam. Another way to determine if the copper is encapsulated into the polymer matrix is to perform thermogravimetric analysis (TGA). With TGA, the degradation of the polymeric component is observed and thus the amount of copper can be determined. Furthermore, UV spectroscopy would be beneficial since PMA does not absorb in the UV region but the complex does, therefore recording UV spectra (of the synthesised nanoparticles) and using a series of nanoparticles with a known quantity of copper inside (as standards), would allow to quantify the amount of complex taken up by the nanoparticles (e.g. *via* the Beer-Lambert law). Lastly, bottom-up nanoparticle preparation techniques may be found better suited, such as to prepare microgels (colloidal polymer network that can sequester the desired compound)[70] or micelles (nanoscopic core-shell structures formed by the assembly of amphiphilic block copolymers).[71] Further work will investigate also the quantum yield of the nanoparticles.

The complex-polymer blends also were found to show luminescence, which was qualitatively valuable even at low complex contents (1% w/w). Further work utilising these materials will investigate the quantum yield of the blends and their mechanical properties.

With regards to the monomer copper complex derivative, it was found unable to polymerise, even in the presence of a comonomer This was attributed to the fact that the double bond of the monomer was too close to the triazole and was thus too sterically hindered to polymerise. In

future work, a longer spacer will be incorporated between the double bond and the triazole, using, for example, a longer alcohol in the Sonogashira step of the synthesis.

In conclusion, the prepared copper(I) complexes are bright luminescent in solid state, both as neat and as in blend with PMA polymers or encapsulated into nanoparticles, albeit all systems need further optimisation. The most promising are, as mentioned before, the blends and the nanoparticles. In the future it would be interesting to investigate and understand how the complexes modify the mechanical proprieties of the blends matrix, it would also be intriguing to understand how the blends and the nanoparticles can be used in photocatalysis and if switching the metal can influence the luminescence.

5 Materials and Methods

5.1 Analytical Resources and Apparatus

Nuclear Magnetic Resonance Spectroscopy (NMR)

The NMR spectra of compounds were recorded on a Bruker Avance 300 NMR instrument at 300 MHz for ^{1}H NMR and 75 MHz for ^{13}C NMR, or a Bruker Avance HD 500 NMR instrument at 500 MHz for ^{1}H NMR, 125 MHz for ^{13}C NMR. All NMR spectra were obtained at room temperature. The chemical shift is displayed in parts per million (ppm) using the residual solvent peak for reference: in deuterated chloroform 7.26 ppm for ^{1}H and 77.0 ppm for ^{13}C. When reporting couplings, the following abbreviations were used: s = singlet, d = doublet, t = triplet, m = multiplet, dd = doublet of doublet, ddd = doublet of doublet of doublet. Coupling constants "*J*" are given in Hertz (Hz) with the largest value first. Couplings are given with their respective number of bindings and binding partners, as far as they could be determined, written as index of the coupling constants.

Mass Spectrometry (MS)

Mass spectra (ESI) were recorded on Q-Tof Premier TM spectrometer from Waters-Micromass. For characterisation, the mass to charge ratio (*m/z*) is plotted against the relative intensity, with the base peak set to 100%.

Solvents and Chemicals

Solvents of p.a. quality (per analysis) were commercially acquired from Sigma Aldrich, Carl Roth, or Acros Fisher Scientific and, unless otherwise stated, used without further purification. Anhydrous solvents were purchased from Carl Roth, Acros, or Sigma Aldrich (less than 50 ppm of H_2O, kept over molecular sieves). All other reagents were commercially purchased (from ABCR, Acros, Alfa Aesar, or Sigma Aldrich) and, unless otherwise stated, used without further purification.

Pyridines: 2-ethynylpyridine (98%) (PA6) was bought from Sigma-Aldrich, 2-bromo-6-methylpyridine (98%) (P1) was bought from Alfa Aesar, 2-bromopyridine (99%) (P2) and 2-iodopyridine (98%) (P3) were bought by Sigma-Aldrich.

Alkynes: Propargyl bromide (80% w/w in toluene) (A1) was bought from Acros Organic, propargyl alcohol (98%) (A2), butynyl alcohol (97%) (A3) and trimethylsilane acetylene (98%) (A4) were bought from Sigma Aldrich
Azides: Azidotrimethylsilane (95%) (AZ4) and sodium azide (99.5%) (AZ5) were bought from Sigma Aldrich, benzyl azide (94%) (AZ6) was bought from Alfa Aesar.
Catalysts: Bis(triphenylphosphine)palladium(II) dichloride (98%) (CAT1) and chloro(pentamethylcyclopentadienyl)(cyclooctadiene)ruthenium(II) (99.5%) (CAT2) were bought from Sigma Aldrich**.**

Preparative Work

Air- and moisture-sensitive reactions were carried out under argon atmosphere in previously baked out apparatuses with standard Schlenk techniques. Liquid reagents and solvents were injected with syringes and stainless-steel cannulas of different sizes.

Product Purification

Reaction mixtures were purified by flash chromatography. For the stationary phase of the column, silica gel, produced by Merck (silica gel 60, 0.040 × 0.063 mm, 260 – 400 mesh ASTM) and sea sand by Riedel de Haën (baked out and washed with hydrochloric acid) were used. Solvents used were commercially acquired in HPLC grade and individually measured volumetrically before mixing.

5.2 Pyridine synthesis

*5.2.1 Synthesis of 2-(2-propyn-1-bromo)-6-methylpyridine (**PA1**)*

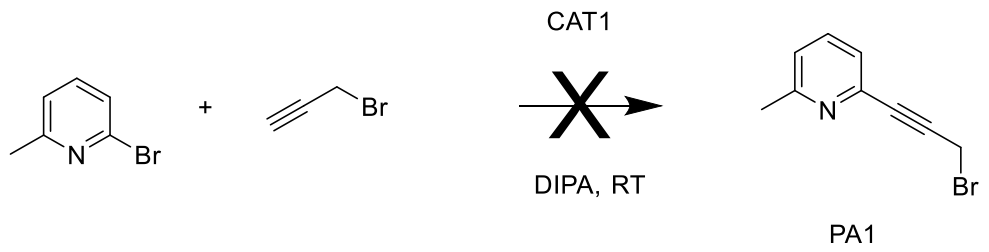

In a flame-dried 100 mL two-neck round bottom flask, 55 mL of diisopropylamine (DIPA) (391.4 mmol, 39.6 g, 225 eq) were added under argon, followed by the addition of P1 (960 µL, 1.74 mmol, 0.30 g, 1 eq), A1 (101 µL, 1.74 mmol, 0.098 g, 1 eq), and CAT1 (0.087 mmol, 0.061 g, 0.005 eq). The reaction mixture was allowed to stir at room temperature for 48 hours. The reaction conversion was monitored *via* TLC, however only spots corresponding to the starting materials were observed, therefore no purification was attempted.

*5.2.2 Synthesis of 2-(2-propyn-1-ol)-6-methylpyridine (**PA2**)*

In a typical procedure, into a flame-dried 50 mL two-neck round bottom flask, 25 mL of diisopropylamine (177.9 mmol, 18.0 g, 102.3 eq) were added under argon, followed by the addition of P1 (330 µL, 2.90 mmol, 0.499 g, 1 eq), A2 (170 µL, 2.90 mmol, 0.164 g, 1 eq), copper (I) iodide (0.578 mmol, 0.11 g, 0.10 eq) and CAT1 (0.284 mmol, 0.20 g, 0.05 eq). The reaction mixture was allowed to stir at room temperature for 48 hours. After removal of the solvent under reduced pressure, the residue was purified by column chromatography on silica gel using a mixture of dichloromethane and methanol (r_f = 0.43 in 3% v/v of methanol). The pure product was isolated as a brown solid at a yield of 71.3%. Slightly lower yields were

obtained when scaling up the reaction (Table 12 Quantities of reagents used for the synthesis of **PA2**..

^{1}H NMR ($CDCl_3$, 300 MHz) δ (ppm):), 7.47 (1H, d, ^3J = 1.0 Hz, -CH=CH-, *meta* pyridine), 7.12 (1H, t, ^3J = 1.0 Hz, -CH=CH-, *para* pyridine), 7.04 (1H, d, ^3J = 1.0 Hz, -CH=CH-, *meta* pyridine*)*, 4.54 (2H, s, C-C**H**$_2$-OH), 3.88 (1H, s, -OH), 2.52 (3H, s, Ar-CH_3).

IR *v* (cm^{-1}) 3202 (OH stretch), 1567 (C=C stretch).

P1	A2	CAT1	Yield (%)
0.499 g	0.164 g	0.20 g	71.3
1.0 g	0.328 g	0.40 g	68.6
10.0 g	3.28 g	4.00 g	65.3

*Table 12 Quantities of reagents used for the synthesis of **PA2**.*

*5.2.3 Synthesis of 2-(3-butynyl-1-ol)-6-methylpyridine (**PA3**)*

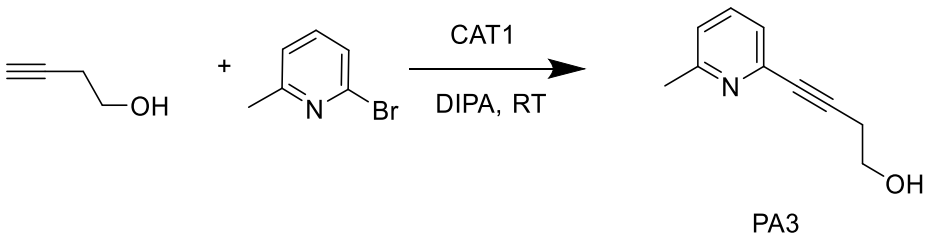

PA3

In a flame-dried 250 mL two-neck round bottom flask, 100 mL of diisopropylamine (708.53 mmol, 72.2 g, 12.5 eq) were added under argon, followed by the addition of P1 (2.11 mL, 18.55 mmol, 3.19 g, 1 eq), A3 (1.08 mL, 14.30 mmol, 1.00 g, 0.7 eq), copper (I) iodide (0.840 mmol, 0.16 g, 0.10 eq) and CAT1 (0.43 mmol, 0.300 g, 0.05 eq). The reaction mixture was allowed to stir at room temperature for 48 hours. After removal of the solvent under reduced pressure, the residue was purified by column chromatography on silica gel using

a mixture of dichloromethane and methanol (r_f = 0.37 in 3% v/v of methanol). The product was isolated as a brown solid at a yield of 72.5%.

^{1}H NMR (300 MHz, Chloroform-*d*) δ 7.57 (1H, t, ^3J = 7.7 Hz, -CH=CH-, *para* pyridine), 7.28 (1H, d, ^3J = 7.7 Hz, -CH=CH-, *meta* pyridine), 7.12 (1H, d, ^3J = 7.7 Hz, -CH=CH-, *meta* pyridine), 3.95 (2H, t, ^3J = 6.6 Hz, -CH_2-C**H**$_2$-OH), 2.78 (2H, t, ^3J = 6.6 Hz, -C**H**$_2$-CH_2-OH), 2.58 (3H, s, Ar-CH_3).

IR ν (cm^{-1}) 3213 (OH stretch), 1557 (C=C stretch).

*5.2.4 Synthesis of 2-(ethynyltrimethylsilane)-6-methylpyridine (**PA4**)*

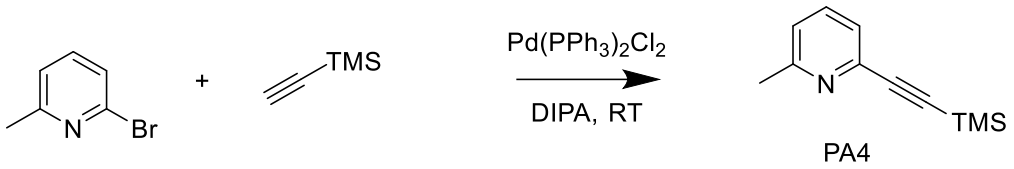

In a flame-dried 250 mL two-neck round bottom flask, 100 mL of diisopropylamine (708.53 mmol, 72.2 g, 12.5 eq) were added under argon, followed by the addition of P1 (2.11 mL, 18.55 mmol, 3.19 g, 1 eq), A4 (1.08 mL, 14.30 mmol, 1.00 g, 0.7 eq), copper (I) iodide (0.840 mmol, 0.16 g, 0.10 eq) and CAT1 (0.43 mmol, 0.300 g, 0.05 eq). The reaction mixture was allowed to stir at room temperature for 48 hours. After removal of the solvent under reduced pressure, the residue was purified by column chromatography on silica gel using a mixture of dichloromethane and methanol (r_f = 0.54 in 3% v/v of methanol). The product was isolated as a dark black solid at a yield of 81.3%

^{1}H NMR (300 MHz, Chloroform-*d*) δ 7.49 (1H, t, ^3J = 7.8 Hz, -CH=CH-, *para*), 7.26 (1H, d, ^3J = 7.8 Hz, -CH=CH-, *meta*), 7.05 (1H, d, ^3J = 7.8 Hz, -CH=CH-, *meta*), 2.52 (s, 3H, Ar-CH_3), 0.25 (9H, s, -CH_3).

*5.2.5 Synthesis of 2-ethynyl-6-methylpyridine (**PA5**)*

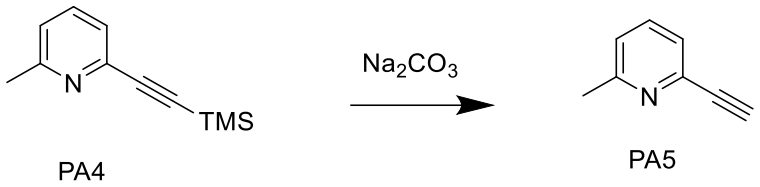

PA4 PA5

In a flame-dried 25 mL two-neck round bottom flask, 9 mL of acetonitrile (172.5 mmol, 7.1 g, 110.3 eq) were added under argon, followed by the addition of P4 (9.25 mmol, 1.74 g, 1 eq), and sodium carbonate (18.5 mmol, 1.96 g, 2 eq). The reaction mixture was allowed to stir at 65 °C for 72 hours. Then the reaction mixture was used directly for the synthesis of **T6**

5.3 Synthesis of triazoles

*5.3.1 Synthesis of (5-(6-methylpyridin-2-yl)-1-(trimethylsilyl)-1H-1,2,3-triazol-4-yl)methanol (**T1**)*

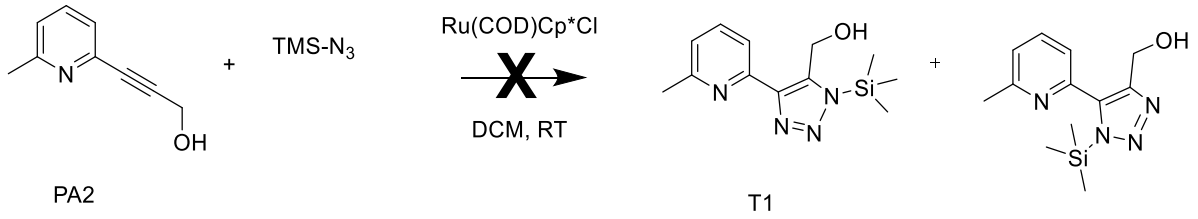

In a flame-dried 50 mL two-neck round bottom flask, 25 mL of dichloromethane (391.2 mmol, 33.3 g, 113.3 eq) were added under argon, followed by the addition of PA2 (3.46 mmol, 0.51 g, 1 eq), AZ4 (1.30 mL, 9.84 mmol, 1.31 g, 3 eq), and CAT2 (0.068 mmol, 0.026 g, 0.02 eq). The reaction mixture was allowed to stir at room temperature for 48 hours. After removal of the solvent under reduced pressure, the residue was dissolved in 20 mL of DCM and washed twice with 15 mL of Na_2CO_3 solution (1.0 M) and twice with brine. After the work-up a ^{1}H NMR spectrum was collected , however only starting materials signals were observed.

*5.3.2 Synthesis of (5-(6-methylpyridin-2-yl)-1H-1,2,3-triazol-4-yl)methanol (**T2**)*

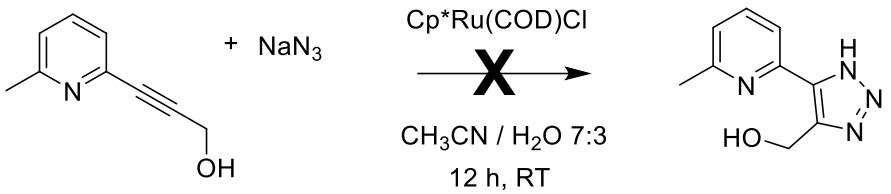

In a flame-dried 50 mL two-neck round bottom flask, 21 mL of acetonitrile (399.2 mmol, 16.4 g, 113.3 eq) and 9 mL of water (9 g, 500 mmol) were added under argon, followed by the addition of PA2 (2.38 mmol, 0.35 g, 1 eq), AZ5 (0.46 g, 7.01 mmol, 3 eq), and CAT2 (0.047 mmol, 0.018 g, 0.02 eq). The reaction mixture was allowed to stir at room temperature for 48 hours. After removal of the solvent under reduced pressure, the residue was dissolved in 20 mL of DCM and washed twice with 15 mL of Na_2CO_3 solution (1.0 M) and twice with brine. After the work-up a ^{1}H NMR spectrum was collected, however only starting materials signals were observed.

*5.3.3 Synthesis of (1-benzyl-4-(6-methylpyridin-2-yl)-1H-1,2,3-triazol-5yl)methanol (**T3**)*

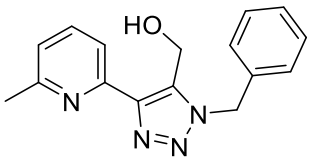

T3 main isomer

In a typical procedure, in a flame-dried 50 mL two-neck round bottom flask, 25 mL of dichloromethane (391.2 mmol, 33.3 g, 113.3 eq) were added under argon, followed by the addition of PA2 (0.67 mmol, 0.10 g, 1 eq), AZ6 (0.30 mL, 2.33 mmol, 0.31 g, 3.4 eq), and CAT2 (0.014 mmol, 0.005 g, 0.02 eq). The reaction mixture was allowed to stir at room temperature for 48 hours. After removal of the solvent under reduced pressure, the residue was purified by column chromatography on silica gel using a mixture of dichloromethane and methanol (r_f = 0.35 in 4.5% v/v of methanol). The product was isolated as a light brown solid at a yield of 52.1% (main isomer). Similar yields were obtained when scaling up the reaction (Table 13).

^{1}H NMR ($CDCl_3$, 300 MHz) δ (ppm): 8.24 (1H, d, ^3J = 1.0Hz, -CH=CH-,*meta* pyridine), 7.74 (2H, d, ^3J = 1.0Hz, -CH=CH-, *meta* benzyl), 7.70 (1H, t, ^3J = 1.0 Hz, -CH=CH-, *para* pyridine), 7.35 (2H, t, ^3J = 1.0Hz, -CH=CH-,), 7.26 (2H, t, ^3J = 1.0 Hz, -CH=CH-), 7.12 (1H, d, ^3J = 1.0 Hz, -CH=CH-), 4.69 (2H, s, -CH_2-) 5.62 (2H, s, -CH_2-), 3.88 (1H, s, -OH), 2.52 (3H, s, CH_3).
IR ν (cm^{-1}) 3202 (OH stretch), 1567 (C=C stretch).

PA2	A4	CAT2	Yield (%)
0.10 g	0.31 g	0.0050 g	52.10
0.50 g	0.50 g	0.0025 g	50.60
0.85 g	0.85 g	0.0038 g	50.30
1.00 g	1.10 g	0.050 g	46.80

Table 13 Quantities of reagents used for the synthesis of T3.

*5.3.4 Synthesis of 2-(4-(pyridine-2-yl)-1H-1,2,3-triazol-1-yl)ethan-1-ol (**T4**)*

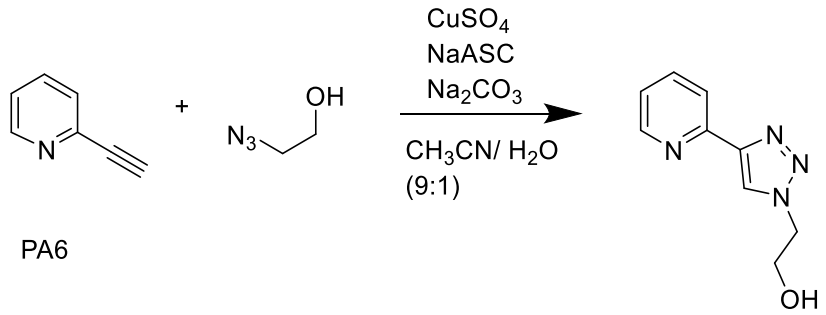

In a typical procedure, in a flame-dried 100 mL two-neck round bottom flask, 28 mL of ethanol (480.9 mmol, 22.1 g, 113.3 eq) and 12 mL of water (666.6 mmol, 12 g, 83 eq) were added under argon, followed by the addition of PA6 (0.50 mL, 4.95 mmol, 0.51 g, 1 eq), 2-bromoethanol (0.36 mL, 4.95 mmol, 0.634 g, 1eq), AZ5 (5.81 mmol, 0.378 g, 1.3 eq), copper sulfate pentahydrate (0.24 mmol, 0.060 g, 0.05 eq), sodium ascorbate (0.096 g, 0.484 mmol, 0.1 eq), sodium carbonate (0.051 g, 0.49 mmol, 0.20 eq). The reaction mixture was allowed to stir at room temperature for 48 hours. After removal of the solvent under reduced pressure, the residue was dissolved in 20 mL of DCM and washed twice with 15 mL of Na_2CO_3 solution (1.0 M) and twice with brine. The yield is 64.5%, the product is a solid light brown. Different yields were obtained changing the solvent mixture and ratio (Table 15)

^{1}H NMR (300 MHz, Chloroform-*d*) δ 8.04 (1H, d, ^3J = 7.7 Hz 1H, -CH=CH-, *ortho*), 7.66 (1H, d, ^3J = 7.7 Hz 1H, -CH=CH-, *meta*), 7.37 (1H, t, ^3J = 7.7 Hz, -CH=CH-, *para*), 7.12 (1H, d, ^3J = 7.7 Hz, -CH=CH-, *meta*), 7.59 (1H, s, =CH-), 3.92 (2H, t, ^3J = 6.6 Hz, -CH_2-), 3.66 (2H, t, ^3J = 6.6 Hz, -CH_2-).

Solvent	Solvent ratio	Yield
EtOH/H_2O	7:3	64.5%
DMSO/H_2O	9:1	68.3%
CH_3CN/ H_2O	9:1	74.2%

*Table 14 Solvent ratio used for reaction **T4.***

*5.3.5 Synthesis of 2-(1-(pyridine-2-yl)-1H-1,2,3-triazol-4-yl)ethan-1-ol (**T5**)*

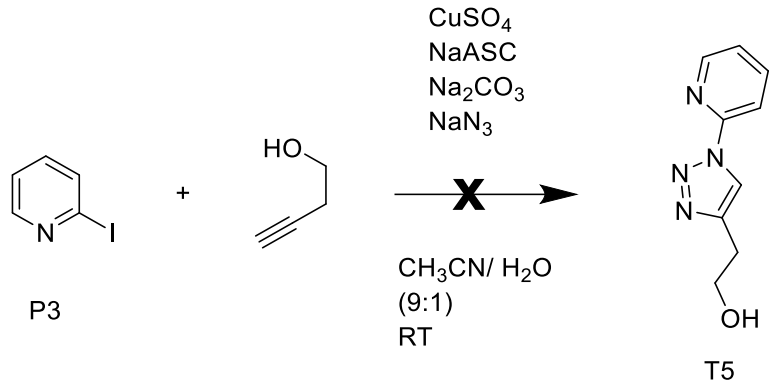

In a flame-dried 25 mL two-neck round bottom flask, 4.5 mL of dimethyl sulfoxide (63.4 mmol, 4.95 g, 12.8 eq) and 0.5 mL of water (27.8 mmol, 0.5 g, 16.7 eq) were added under argon, followed by the addition of P3 (0.52 mL, 4.95 mmol, 1.01 g, 1 eq), A3 (0.36 mL, 4.95 mmol, 0.35 g, 1eq), AZ5 (5.81 mmol, 0.378 g, 1.3 eq), copper sulfate pentahydrate (0.24 mmol, 0.060 g, 0.05 eq), sodium ascorbate (0.096 g, 0.484 mmol, 0.1 eq), sodium carbonate (0.051 g, 0.49 mmol, 0.20 eq). The reaction mixture was allowed to stir at 60 °C for 48 hours. After removal of the solvent under reduced pressure, the residue was dissolved in 20 mL of DCM. A ^{1}H NMR spectrum of the residue was collected , however only starting materials signals were observed.

*5.3.6 Synthesis of 2-(4-(6-methylpyridin-2-yl)-1H-1,2,3-triazol-1-yl)ethan-1-ol (**T6**)*

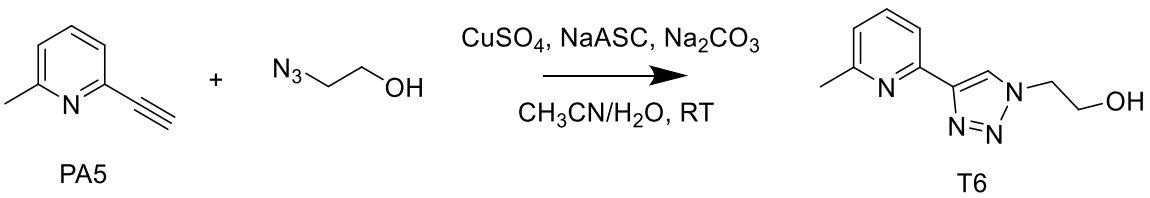

In a typical procedure, in a flame-dried 25 mL two-neck round bottom flask, previously charged with 9 mL of acetonitrile (172.5 mmol, 7.1 g, 110.3 eq) and PA5 (9.25 mmol, 1.74 g, 1 eq) were added AZ1 (9.25 mmol, 0.80 g, 1 eq), copper sulfate pentahydrate (0.9 mmol, 0.16 g, 0.10 eq), sodium ascorbate (0.384 g, 1.8 mmol, 0.2 eq), sodium carbonate (0.20 g, 1.9 mmol, 0.20 eq). The reaction mixture was allowed to stir at room temperature for 16 hours. After removal of the solvent under reduced pressure, the residue was dissolved in 20 mL of DCM and washed twice with 15 mL of ammonia solution (pH= 8) and twice with brine.

The yield is 70.5%, the product is a solid light brown. Different yields were obtained changing the solvent mixture and ratio (Table 15)

Solvent	Solvent ratio	Yield
EtOH/H_2O	7:3	70.5%
DMSO/H_2O	9:1	71.3%
CH_3CN/ H_2O	9:1	76.2%

*Table 15 Solvent ratios used for reaction **T6***

^{1}H NMR (300 MHz, Chloroform-*d*) δ 7.81 (1H, d, ^3J = 7.8 Hz, 1H, -CH=CH-, *meta*), 7.41 (1H, t, ^3J = 7.8 Hz, -CH=CH-, *para*), 7.00 (1H, d, ^3J = 7.8 Hz, -CH=CH-, *meta*), 4.51 (2H, t, ^3J = 5.0 Hz, -CH_2-), 4.03 (2H, t, ^3J = 5.0 Hz, -CH_2-), 2.47 (3H, s, -CH_3).

*5.3.7 Synthesis of 2-(1-benzyl-5-(6-methylpyridin-2-yl)-1H-1,2,3-triazol-4-yl)ethan-1-ol (**T7**)*

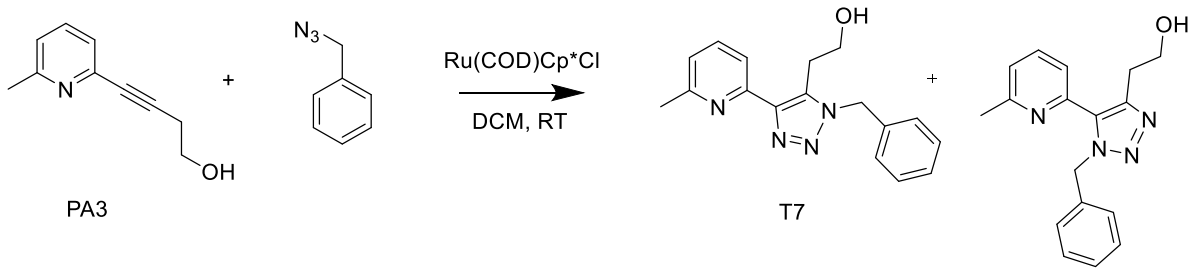

In a flame-dried 50 mL two-neck round bottom flask, 25 mL of dichloromethane (391.2 mmol, 33.3 g, 113.3 eq) were added under argon, followed by the addition of PA3 (5.25 mmol, 0.840 g, 1 eq), AZ6 (0.80 mL, 6.20 mmol, 0.82 g, 1.2 eq), and CAT2 (0.14 mmol, 0.05 g, 0.03 eq). The reaction mixture was allowed to stir at room temperature for 48 hours. After removal of the solvent under reduced pressure, the residue was purified by column chromatography on silica gel using a mixture of dichloromethane and methanol (r_f = 0.35 in 4.5% v/v of methanol). The product was isolated as a light brown solid at a yield of 64.3% (main isomer).

^{1}H NMR (300 MHz, Chloroform-*d*) δ 7.93 (1H, d, ^3J = 7.8 Hz, -CH=CH-, *meta pyridine*), 7.65 (1H, t, ^3J = 7.8 Hz, -CH=CH-, *para pyridine*), 7.26 (m, 6H, -CH=CH-, benzyl), 7.06 (1H, d, ^3J = 7.8 Hz, -CH=CH-, *meta*), 5.53 (2H, s, -CH_2), 3.68 (2H, t, ^3J = 8.8 Hz, -CH_2-), 3.16 (2H, t, ^3J = 8.8 Hz, -CH_2-), 2.48 (3H, s, -CH_3).

5.4 Synthesis of Esters

*5.4.1 Synthesis of ester 1-benzyl-4-(6-methylpyridin-2-yl)-1H-1,2,3-triazol-5-yl)methyl acrylate **E1***

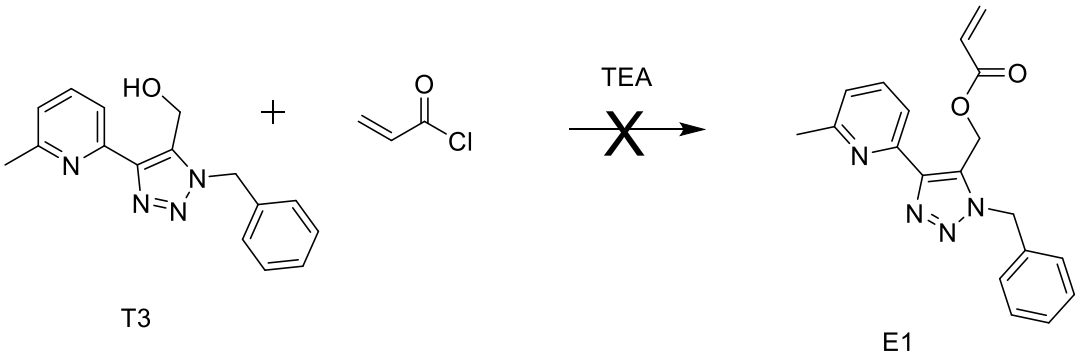

T3 E1

In a flame-dried 50 mL two-neck round bottom flask, 25 mL of dichloromethane (391.2 mmol, 33.3 g, 113.3 eq) were added under argon, followed by the addition of T3 (0.67 mmol, 0.28 g, 1 eq), acryloyl chloride (0.17 mL, 2.10 mmol, 0.19 g, 2 eq), and triethylamine (2.52 mmol, 0.3 mL, 0.18 g, 3 eq). The reaction mixture was allowed to stir at 0 °C for 48 hours. After removal of the solvent under reduced pressure, the residue was dissolved in 20 mL of DCM and washed twice with 15 mL of Na_2CO_3 solution (1.0 M) and twice with brine After the work-up a ^1H NMR spectrum was collected , however only starting materials signals were observed.

*5.4.2 Synthesis of ester 1-benzyl-4-(6-methylpyridin-2-yl)-1H-1,2,3-triazol-5-yl)methyl acrylate **E1***

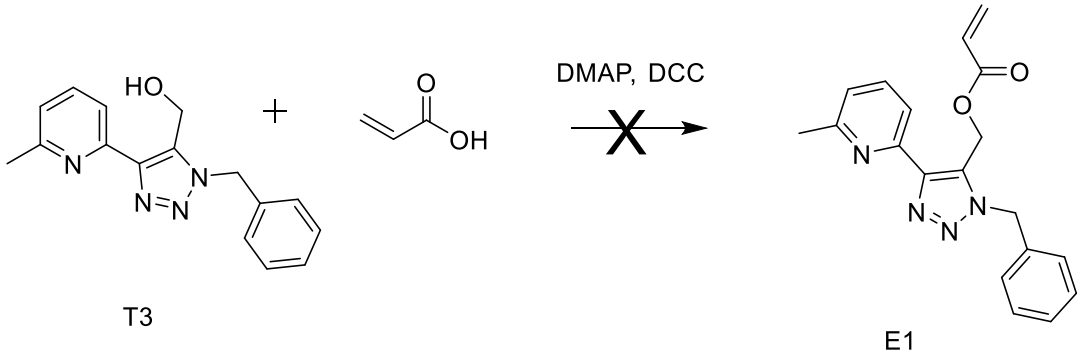

T3 E1

In a flame-dried 50 mL two-neck round bottom flask, 25 mL of dichloromethane (391.2 mmol, 33.3 g, 113.3 eq) were added under argon, followed by the addition of T3 (1.34 mmol, 0.6 g, 1 eq), acrylic acid (1.05 mL, 13.87 mmol, 1.0 g, 10 eq), *N,N′*-dicyclohexylcarbodiimide (15.51 mmol, 3.20 g, 10 eq) and 4-(dimethylamino)pyridine (0.90 mmol, 0.1 g, 0.7 eq). The reaction mixture was allowed to stir at room temperature for 48 hours. After removal of the solvent under reduced pressure, the residue was dissolved in 20 mL of DCM and washed twice with 15 mL of Na_2CO_3 solution (1.0 M) and twice with brine. After the work-up a ^1H NMR spectrum was collected , however only starting materials signals were observed.

*5.4.3 Synthesis of ester 3-(6-methylpyridin-2-yl)prop-2-yn-1-yl acrylate **E2***

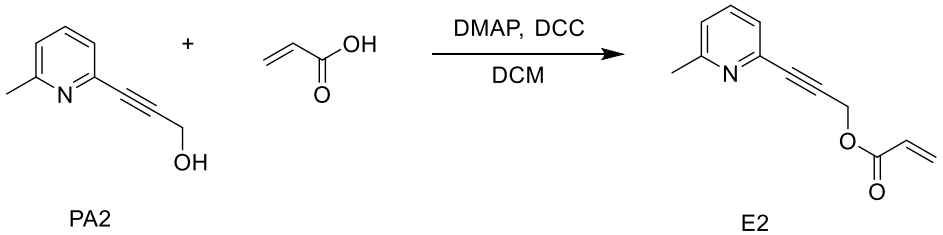

PA2 E2

In a flame-dried 50 mL two-neck round bottom flask, 25 mL of dichloromethane (391.2 mmol, 33.3 g, 113.3 eq) were added under argon, followed by the addition of PA2 (0.58 mmol, 0.1 g, 1 eq), acrylic acid (0.15 mL, 1.87 mmol, 0.15 g, 3 eq), *N,N′*-dicyclohexylcarbodiimide (4.1 mmol, 0.50 g, 2 eq) and 4-(dimethylamino)pyridine (0.16 mmol, 0.02 g, 0.3 eq). The reaction mixture was allowed to stir at room temperature for 48 hours. After removal of the solvent

under reduced pressure, the residue was dissolved in 20 mL of DCM and washed twice with 15 mL of Na_2CO_3 solution (1.0 M) and twice with brine. The yield is 73.4%, the product is a yellow oil.

^{1}H NMR (300 MHz, Chloroform-*d*) δ 7.50 (1H, t, ^3J = 7.7 Hz, -CH=CH-, *para*), 7.23 (1H, d, ^3J = 7.7 Hz, -CH=CH-, *meta*), 7.07 (1H, d, ^3J = 7.7 Hz, -CH=CH-, *meta*), 6.44 (1H, dd, ^3J = 17.3, 1.5 Hz, -CH=C**H**$_2$), 6.04 (m, 1H, -C**H**=CH$_2$), 5.85 (1H, dd, ^3J = 17.3, 1.5 Hz, 1H, -CH=C**H**$_2$), 4.96 (s, 2H, =C-CH$_2$-O-), 2.50 (3H, s, Ar-CH$_3$).

*5.4.4 Synthesis of ester 2-(1-benzyl-4-(6-methylpyridin-2-yl)-1H-1,2,3-triazol-5-yl)ethyl acrylate **E3***

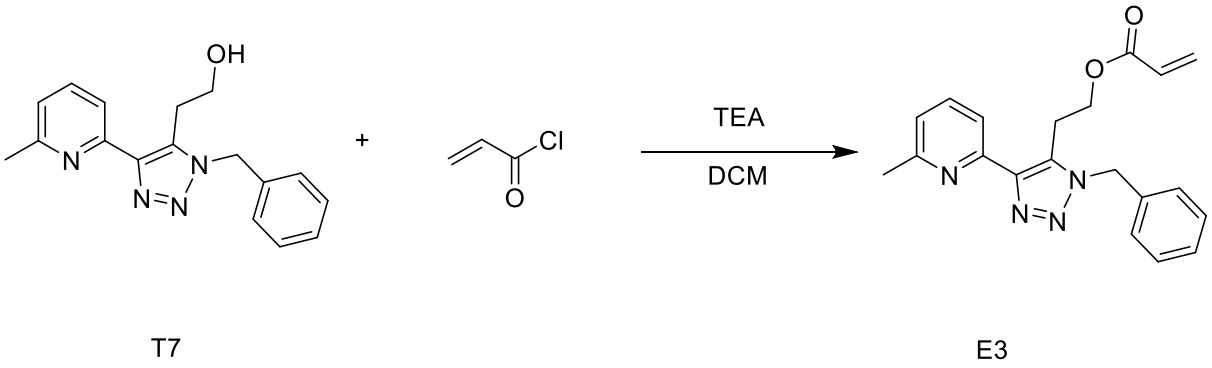

T7 E3

In a flame-dried 50 mL two-neck round bottom flask, 25 mL of dichloromethane (391.2 mmol, 33.3 g, 113.3 eq) were added under argon, followed by the addition of T7 (0.12 mmol, 0.035 g, 1 eq), acryloyl chloride (15 µL, 0.17 mmol, 0.015 g, 1.5 eq), and triethylamine (0.25 mmol, 33 µL, 0.017 g, 2 eq). The reaction mixture was allowed to stir at room temperature for 48 hours. After removal of the solvent under reduced pressure, the residue was dissolved in 20 mL of DCM and washed twice with 15 mL of Na_2CO_3 solution (1.0 M) and twice with brine, the organic phase was then dried over magnesium sulfate and the solvent removed under reduced pressure. The yield was 71.6% and the product was isolated as a yellow oil.

^{1}H NMR (300 MHz, Chloroform-*d*) δ 7.63 (1H, t, ^3J = 7.9 Hz, 1H, -CH=CH-, *para* pyridine), 7.47 (1H, d, ^3J = 7.9 Hz,-CH=CH-, *meta* pyridine), 7.26 (m, 6H, -CH=CH-, benzyl), 6.98 (d,

^3J = 7.9 Hz, 1H, -CH=CH-, *meta* pyridine), 6.45 (1H, dd, ^3J = 17.3, 1.5 Hz, -CH=C**H**$_2$), 6.17 (1H, m, -C**H**=CH$_2$), 5.80 (1H, dd, ^3J = 17.3, 1.5 Hz, -CH=C**H**$_2$), 4.48 (2H, t, ^3J = 6.7 Hz, -CH$_2$-), 2.85 (2H, t, ^3J = 6.7 Hz, -CH$_2$-), 2.75 (3H,s, -CH$_3$).

5.4.5 Synthesis of 4-(6-methylpyridin2-yl)but-3-yn-1-yl acrylate ***E4***

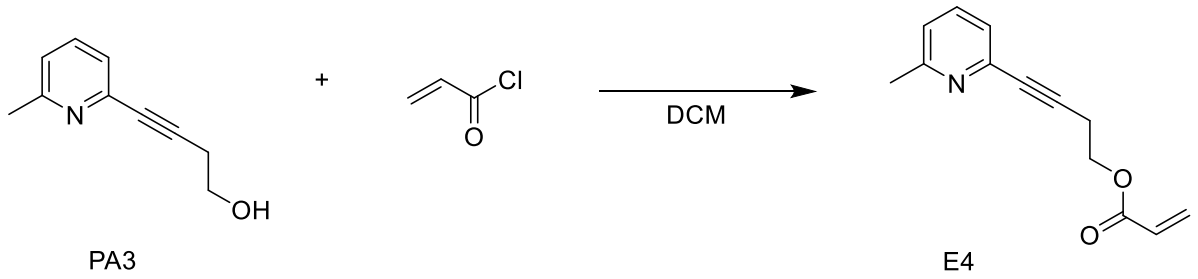

PA3 E4

In a flame-dried 50 mL two-neck round bottom flask, 25 mL of dichloromethane (391.2 mmol, 33.3 g, 113.3 eq) were added under argon, followed by the addition of PA3 (0.10 mmol, 0.03 g, 1 eq), acryloyl chloride (124 µL, 0.03 mmol, 125 mg, 1.5 eq), and triethylamine (180 µL, 0.13 mmol, 134 mg, 2 eq). The reaction mixture was allowed to stir at 0 °C for 48 hours. After removal of the solvent under reduced pressure, the residue was dissolved in 20 mL of DCM and passed through a plug of silica using as eluent a mixture of DCM/MeOH (4% v/v of alcohol).

The yield is 74.5%, the product is a yellow oil.

^{1}H NMR (300 MHz, Chloroform-*d*) δ 7.97 (1H, d, ^3J = 7.8 Hz, -CH=CH-, *meta*), 7.58 (1H, t, ^3J = 7.8 Hz, -CH=CH-, *para*), 6.98 (1H, d, ^3J = 7.8 Hz, -CH=CH-, *meta*), 6.28 (1H, dd, ^3J = 17.3, 1.5 Hz, -CH=C**H**$_2$), 5.95 (1H, dd, ^3J = 17.3, 1.5 Hz, -CH=C**H**$_2$), 5.74 (1H, m, -C**H**=CH$_2$), 4.33 (2H, t, ^3J = 6.6 Hz, -CH$_2$-C**H**$_2$-OH), 3.42 (2H, t, ^3J = 6.6 Hz, C-C**H**$_2$-CH$_2$), 2.45 (3H, s, Ar-CH$_3$).

IR ν (cm^{-1}) 1723 (C=O stretch).

5.4.6 Synthesis of ester E5

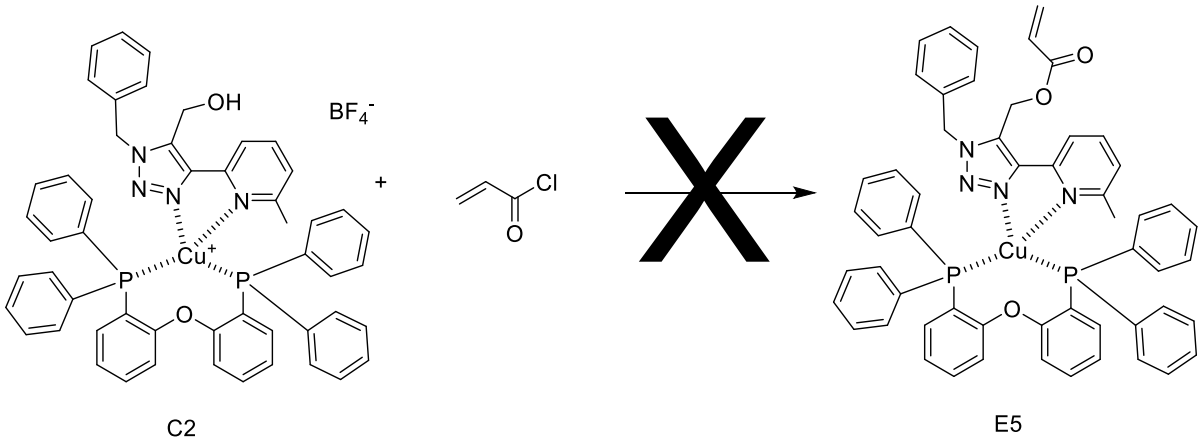

In a flame-dried 50 mL two-neck round bottom flask, 25 mL of dichloromethane (391.2 mmol, 33.3 g, 113.3 eq) were added under argon, followed by the addition of C2 (0.02 mmol, 1.0 g, 1 eq), acryloyl chloride (2.76 µL, 0.03 mmol, 2.77 mg, 1.5 eq), and triethylamine (9.49 µL, 0.07 mmol, 6.89 mg, 3 eq). The reaction mixture was allowed to stir at room temperature for 48 hours. After removal of the solvent under reduced pressure, the residue was dissolved in 20 mL of DCM and passed through a plug of silica using as eluent a mixture of DCM/MeOH (4% v/v of alcohol). The residue was checked *via* ^{1}H-NMR spectroscopy, and the spectra showed no conversion of the starting materials.

5.5 Complexation

*5.5.1 Synthesis of heteroleptic Cu(I) complex **C1***

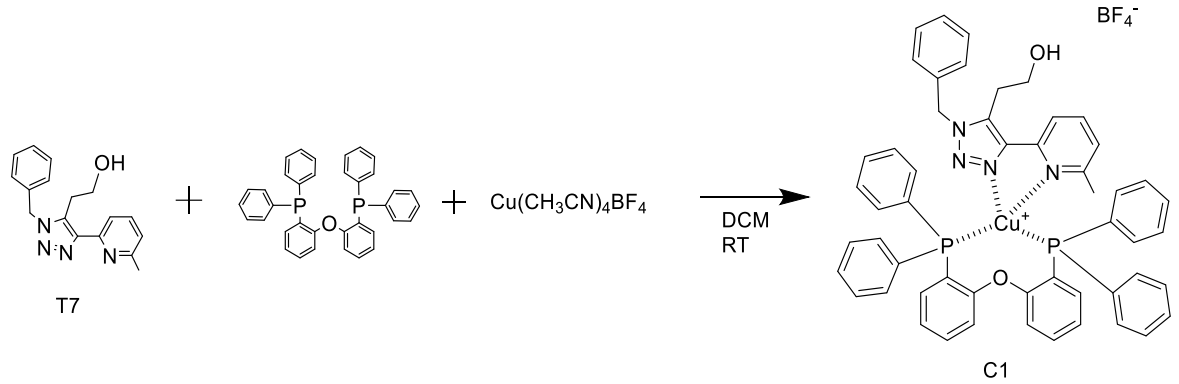

In a flame-dried 50 mL two-neck round bottom flask, 25 mL of dichloromethane (391.2 mmol, 33.3 g, 113.3 eq) were added under argon, followed by the addition of copper tetraacetonitrile salt (0.14 mmol, 0.043 g, 1 eq) and diphenylphosphine ether (0.14 mmol, 0.073 g, 1 eq). After 30 minutes under stirring, T7 (0.14 mmol, 0.040 g, 1 eq) was added. The reaction mixture was allowed to stir at room temperature for 48 hours. After removal of the solvent under reduced pressure, the residue was dissolved in 10 mL of DCM and cyclohexane was added dropwise. The biphasic solution obtained was then left in the fridge 48 hours to obtain a yellow precipitate. The yield is 68.3%, the product is a solid yellow.

^{1}H NMR (300 MHz, Chloroform-*d*) δ 7.87 (1H, t, ^3J = 7.8 Hz, -CH=CH-, *para* pyridine), 7.70 (1H, d, ^3J = 7.8 Hz, -CH=CH-, *meta*), 7.28 (m, 28H, -CH=CH-), 7.06 (1H, d, ^3J = 7.8 Hz, -CH=CH-, *meta*), 6.73 (6H, m, -CH=CH-, benzyl), 5.53 (2H, s, -CH_2-C**H**$_2$-OH), 3.59 (2H, t, ^3J = 8.8 Hz, -CH_2-C**H**$_2$-OH), 3.08 (2H, t, ^3J = 8.8 Hz, -C**H**$_2$-CH_2-OH), 1.94 (3H, s, Ar-CH_3),

IR ν (cm^{-1}) 3554 (OH stretch)

HRMS m/z ($C_{53}H_{43}CuN_4O_2P_2BF_4$): 979.22 (calculated), 979.22 (found).

*5.5.2 Synthesis of heteroleptic Cu(I) complex **C2***

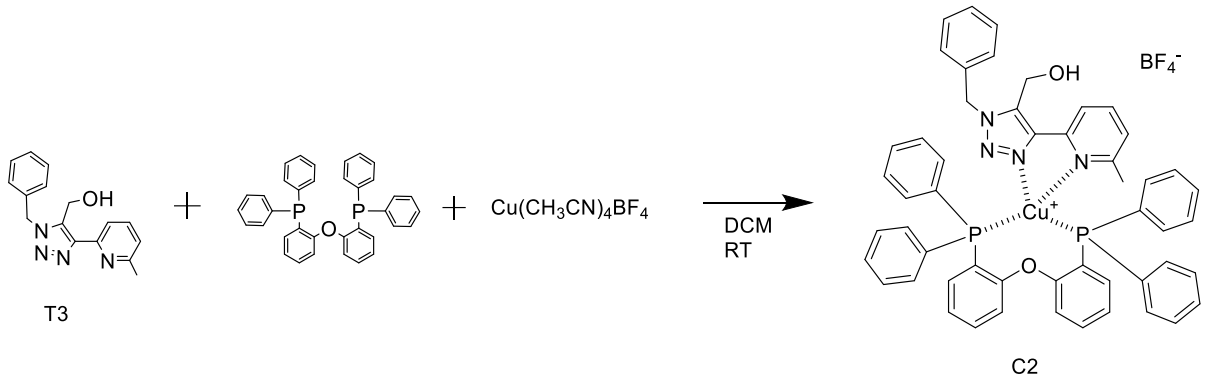

In a flame-dried 50 mL two-neck round bottom flask, 25 mL of dichloromethane (391.2 mmol, 33.3 g, 113.3 eq) were added under argon, followed by the addition of copper tetra acetonitrile salt (0.14 mmol, 0.043 g, 1 eq) and diphenylphosphine ether (0.14 mmol, 0.073 g, 1 eq), and after 30 minutes under stirring was added T3 (0.14 mmol, 0.040 g, 1 eq). The reaction mixture was allowed to stir at room temperature for 48 hours.

After removal of the solvent under reduced pressure, the residue was dissolved in 10 mL of DCM and cyclohexane was added dropwise, the biphasic solution obtained was then left in the fridge 48 hours to obtain a yellow precipitate. The yield is 63.6%, the product is a solid yellow.

^{1}H NMR (300 MHz, Chloroform-*d*) δ 7.99 (1H, d, ^3J = 7.8 Hz, -CH=CH-, *meta* pyridine), 7.87 (1H, t, ^3J = 7.8 Hz, -CH=CH-, *para* pyridine), 7.47 (1H, d, ^3J = 7.8 Hz, -CH=CH- *meta* pyridine), 7.26 (m, 28H, -CH=CH-, -phenyl), 6.67 (6H, m, -CH=CH-, -benzyl), 5.75 (2H, s, Ar-CH_2-), 2.00 (3H, s, Ar-CH_3).

HRMS m/z ($C_{52}H_{41}CuN_4O_2P_2BF_4$): 965.20 (calculated), 965.20 (found).

*5.5.3 Synthesis of heteroleptic Cu(I) complex **C3***

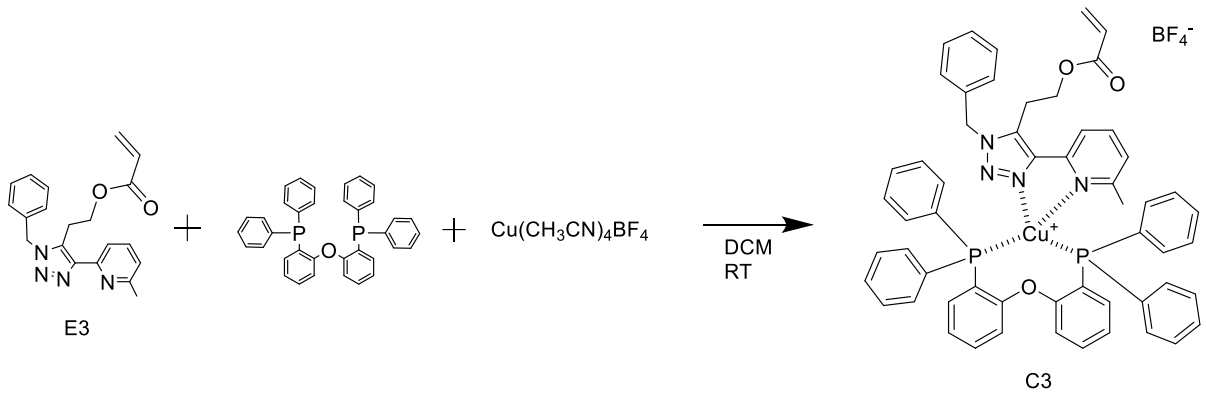

In a flame-dried 50 mL two-neck round bottom flask, 12.5 mL of dichloromethane (195.6 mmol, 16.7 g) were added under argon, followed by the addition of copper tetraacetonitrile salt (0.073 mmol, 0.023 g, 1 eq) and diphenylphosphine ether (0.073 mmol, 0.039 g, 1 eq), and after 30 minutes under stirring was added E3 (0.073 mmol, 0.025 g, 1 eq). The reaction mixture was allowed to stir at room temperature for 48 hours. After removal of the solvent under reduced pressure, the residue was dissolved in 10 mL of DCM and cyclohexane was added dropwise. The biphasic solution obtained was then left in the fridge 48 hours to obtain a yellow precipitate.
The yield is 74.2%, the product is a solid yellow.

^{1}H NMR (300 MHz, Chloroform-*d*) δ 7.99 (1H, t, ^3J = 7.8 Hz, 1H, -CH=CH-, *para* pyridine), 7.83 (1H, d, ^3J = 7.8 Hz, -CH=CH-, *meta* pyridine), 7.48 (6H, m, -CH=CH-, -benzyl), 7.08 (1H, d, ^3J = 7.8 Hz, -CH=CH-, *meta* pyridine) 6.92 (28H, m, -CH=CH-, -phenyl), 6.27 (1H, dd, ^3J = 17.3, 10.4 Hz, -CH=C**H**$_2$), 5.87 (1H, dd, ^3J = 17.3, 10.4 Hz, -CH=C**H**$_2$), 5.74 (1H, m, -C**H**=CH$_2$), 4.06 (2H, t, ^3J = 6.9 Hz, -CH$_2$-C**H**$_2$-OH), 3.40 (t, ^3J = 6.9 Hz, 2H, -C**H$_2$**-CH$_2$-OH), 2.04 (3H, s, Ar-CH$_3$).

IR ν (cm^{-1}) 1726 (C=O stretch)
HRMS m/z ($C_{56}H_{46}CuN_4O_3P_2BF_4$): 1034.24 (calculated), 1034.24 (found).

*5.5.4 Synthesis of heteroleptic Cu (I) complex **C4***

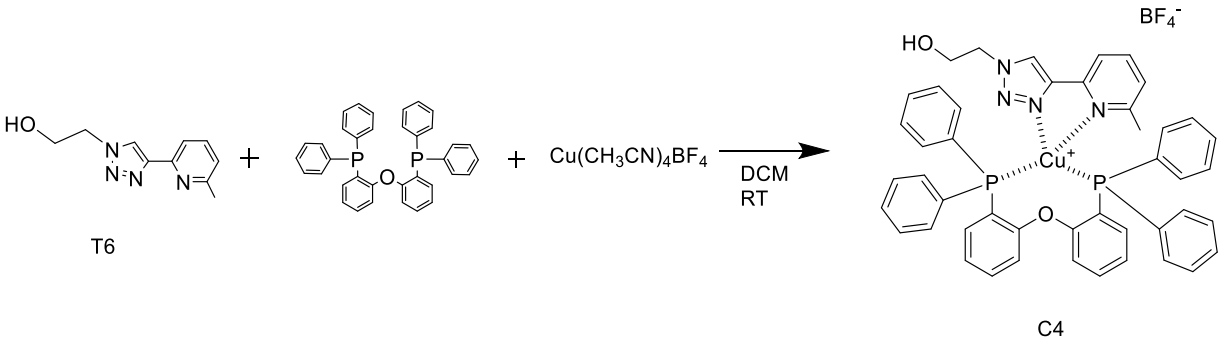

In a flame-dried 50 mL two-neck round bottom flask, 25 mL of dichloromethane (391.2 mmol, 33.3 g, 113.3 eq) were added under argon, followed by the addition of copper tetra acetonitrile salt (0.14 mmol, 0.043 g, 1 eq) and diphenylphosphine ether (0.14 mmol, 0.073 g, 1 eq), and after 30 minutes under stirring was added T6 (0.14 mmol, 0.040 g, 1 eq). The reaction mixture was allowed to stir at room temperature for 48 hours. After removal of the solvent under reduced pressure, the residue was dissolved in 10 mL of DCM and cyclohexane was added dropwise, the biphasic solution obtained was then left in the fridge 48 hours to obtain a white precipitate.

The yield is 63.8%, the product is a solid white.

IR ν (cm^{-1}) 3551 (OH stretch)

HRMS m/z ($C_{46}H_{38}CuN_4O_2P_2BF_4$): 890.18 (calculated), 890.18 (found).

5.6 Synthesis of Azides

*5.6.1 Synthesis 2-azidoethanol **AZ1***

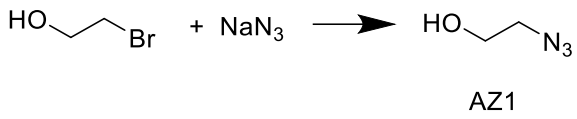

In a flame-dried 25 mL two-neck round bottom flask, 7 mL of ethanol (121.7 mmol, 5.6 g, 111.3 eq) and 2 mL of H_2O (111.1 mmol, 2.0 g, 110.3 eq) were added under argon, followed by the addition of 2-bromoethanol (0.12 mL, 1.60 mmol, 0.20 g, 1 eq), sodium azide (1.90 mmol, 0.124 g, 1.3 eq), copper iodide (I) (0.05 mmol, 0.091 g, 0.03 eq). The reaction mixture was allowed to stir at 65 °C for 48 hours. The reaction mixture was used directly, without any further purification for the preparation of **T4** and **T6**

*5.6.2 Synthesis 2-azidopyridine **AZ2***

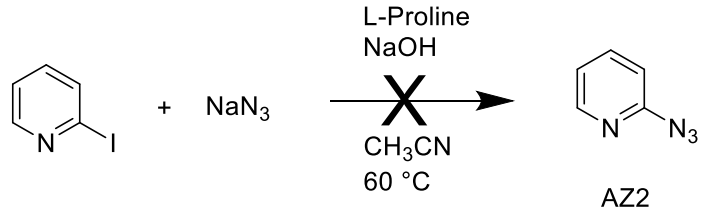

In a flame-dried 25 mL two-neck round bottom flask, 9 mL of acetonitrile (172.5 mmol,7.1 g, 110.3 eq) were added under argon, followed by the addition of 2-iodopyrdine(0.05 mL, 0.47 mmol, 0.10 g, 1 eq), sodium azide (0.80 mmol, 0.063 g, 1.7 eq), L-proline (0.095 mmol, 0.011 g, 0.1 eq) and sodium hydroxide (0.095 mmol, 40 mg, 0.1 eq). The reaction mixture was allowed to stir at 60 °C for 48 hours. The reaction conversion was monitored *via* TLC, however only spots corresponding to the starting materials were observed, therefore no purification was attempted.

5.6.3 Synthesis of azido 2-azido-6-methylpyridine ***AZ3***

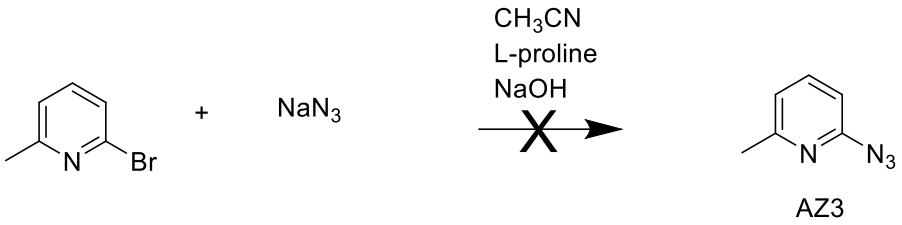

In a flame-dried 25 mL two-neck round bottom flask, 9 mL of acetonitrile (172.5 mmol, 7.1 g, 110.3 eq) were added under argon, followed by the addition of 2-bromo-6-methylpyrdine(0.34 mL, 3.02 mmol, 0.52 g, 1 eq), sodium azide (5.84 mmol, 0.38 g, 2 eq), L-proline (0.87 mmol, 0.1 g, 0.1 eq) and sodium hydroxide (0.87 mmol, 34 mg, 0.1 eq). The reaction mixture was allowed to stir at 65 °C for 48 hours. The reaction conversion was monitored *via* TLC, however only spots corresponding to the starting materials were observed, therefore no purification was attempted.

5.7 Copolymer and polymer synthesis

*5.7.1 Synthesis of copolymer **CP1***

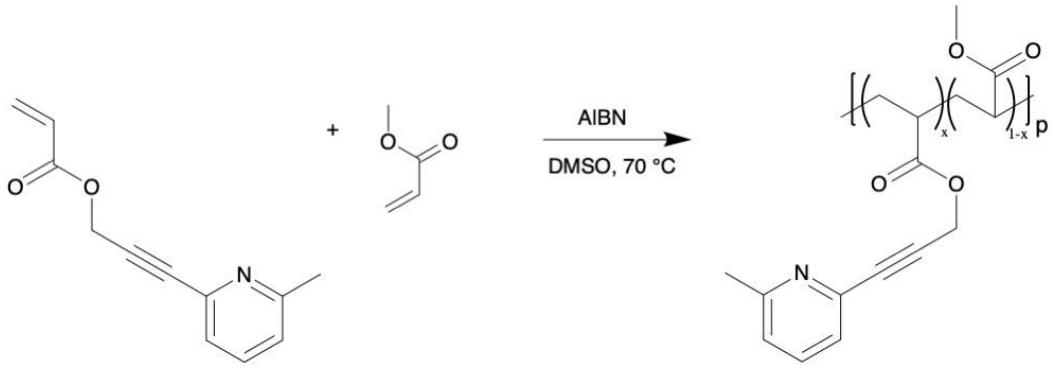

In a flame-dried 1 mL two-neck round bottom flask, 60 µL of dioxane (0.68 mmol, 0.06 g, 113.3 eq) were added, followed by the addition of E2 (0.07 mmol, 0.015 g, 1 eq), methyl acrylate (60 µL, 0.66 mmol, 0.06 g, 10 eq), and 2,2′-azobis(2-methylpropionitrile) (AIBN) (0.037 mmol, 0.0062 g, 0.5 eq). Argon was bubbled through the solution for 5 minutes and then the reaction mixture was allowed to stir at 65 °C for 4 hours. The residue was checked *via* ^{1}H-NMR, and the spectra showed no conversion of the starting materials.

*5.7.2 Synthesis of copolymer **CP2***

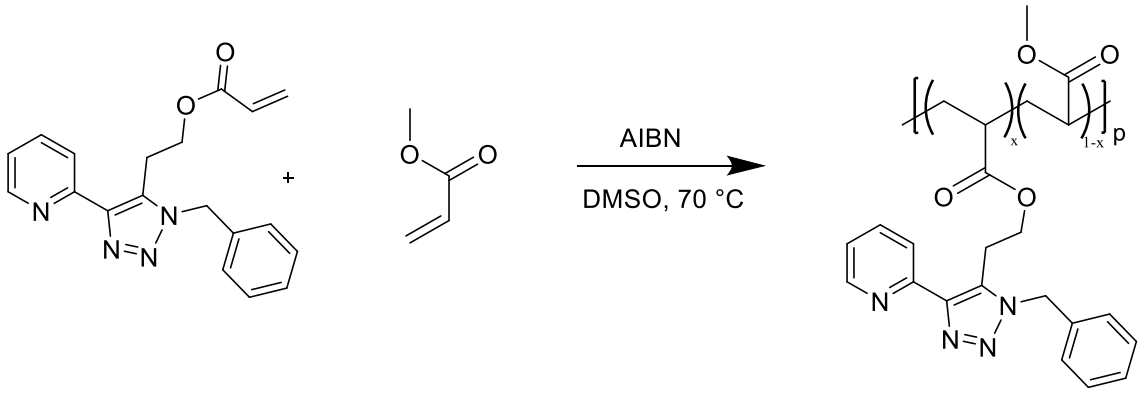

CP2

In a flame-dried 100 mL two-neck round bottom flask, 683 µL of DMSO (279.04 mmol, 22 g, 4.8 eq) were added, followed by the addition of methyl acrylate (85 µL, 0.98 mmol, 85.0 mg, 9 eq), E3 (36.7 mg, 0.10 mmol) and 2,2′-azobis(2-methylpropionitrile) (0.01 mmol, 0.0017 g, 0.01 eq). Argon was bubbled through the solution for 5 minutes and then the reaction mixture was allowed to stir at 70 °C for 4 hours. The residue was checked *via* ^{1}H-NMR, and the spectra showed no conversion of the starting materials.

5.7.3 Synthesis of copolymer ***CP3***

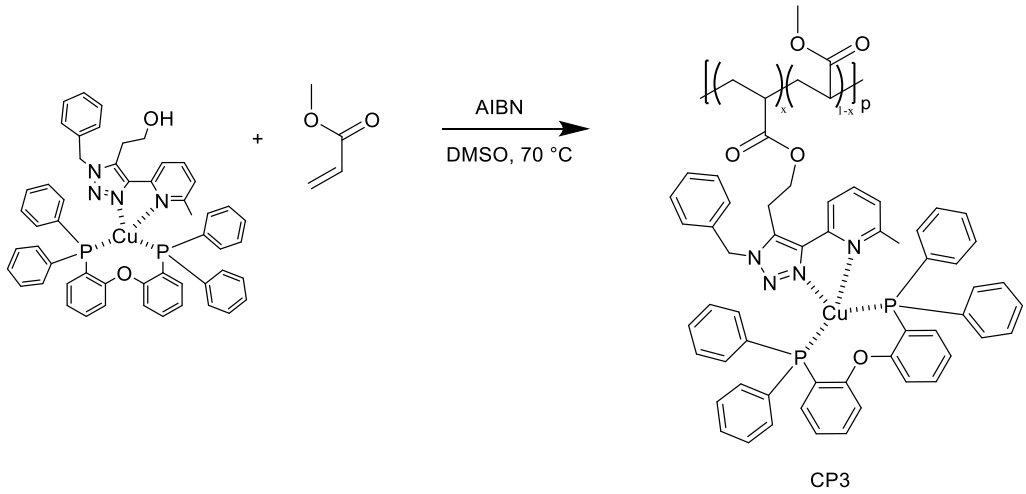

CP3

In a flame-dried 100 mL two-neck round bottom flask, 130 µL of dioxane (1.48 mmol, 130 mg, 90 eq) were added, followed by the addition of methyl acrylate (16.2 µL, 0.19 mmol, 16.50 mg, 9 eq), C3 (20.0 mg, 0.020 mmol) and 2,2′-azobis(2-methylpropionitrile) (0.0018 mmol, 0.0003 g, 0.01 eq). Argon was bubbled through the solution for 5 minutes and then the reaction mixture was allowed to stir at 70 °C for 4 hours. The residue was checked *via* ^{1}H-NMR, and the spectra showed no conversion of the starting materials.

5.7.4 Synthesis of homopolymer ***HP1***

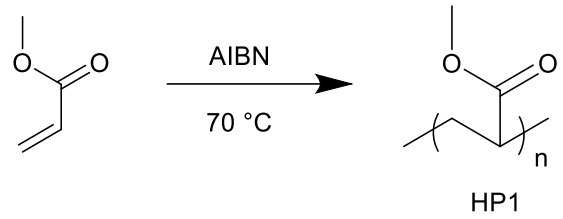

In a typical procedure (Table 16), in a flame-dried 10 mL two-neck round bottom flask, 1 mL of dioxane (0.68 mmol, 0.06 g, 113.3 eq) were added, followed by the addition of methyl acrylate (951 µL, 10.52 mmol, 0.90 g, 10 eq), and 2,2′-azobis(2-methylpropionitrile) (0.29 mmol, 0.048 g, 0.3 eq). Argon was bubbled through the solution for 5 minutes and then the reaction mixture was allowed to stir at 70 °C for 4 hours. The polymer was then precipitated in 10 mL of cold methanol. The product was isolated as a transparent solid at a yield of 83.4%.

Solvent	Ratio between the monomer and the solvent (v/v)	M_w/M_n	M_w (g/mol)
DMSO	1:4	3.9	3,600
DMSO	1:8	2.8	3,300
DMSO	1:10	2.3	3,500
1,4-dioxane	1:4	2.4	3,500
1,4-dioxane	1:8	1.6	3,700

Table 16 Different solvents used for reaction ***HP1***

5.8 Nanoparticles

5.8.1 Nanoprecipitation procedure

In a typical procedure, in a 5 mL beaker, 1 mL of acetone was added, followed by the addition of PMA (0.0033 mmol, 0.10 g, 1 eq) and complex 4 (0.013 mmol, 0.010 g, 0.02 eq). The solution was stirred until complete dissolution of the solids. In a 10 mL beaker, 3 mL of distilled water was put under stirring (200 rpm) and the previously prepared solution of acetone was added dropwise. The dispersion was left under stirring for 10 hours until the complete evaporation of acetone. Different complexes and weight ratios were used to obtain different nanoparticles (Table 16).

NPs	Complex	Complex quantity (w/w)
NP1.1	Complex 1	1%
NP1.10	Complex 1	10%
NP2.1	Complex 2	1%
NP2.10	Complex 2	10%
NP3.1	Complex 3	1%
NP3.10	Complex 3	10%

Table 17 Weight ratios of complexes used in nanoprecipitation

5.9 Blends

5.9.1 Blends procedure

In a typical procedure, in a 5 mL beaker, 1 mL of acetone was added, followed by the addition of PMA (0.033 mmol, 0.10 g, 1 eq) and complex 4 (0.013 mmol, 0.010 g, 0.02 eq), the solution was stirred until complete dissolution of the solids. With a Pasteur pipette, the solution was deposited on a thin glass layer. The film was allowed to dry in air. Different complexes and weight ratio were used to obtain different blends (Table 18).

Blends	Complex	Quantity of complex (w/w)
B1.1	Complex 1	1%
B1.10	Complex 1	10%
B2.1	Complex 2	1%
B2.10	Complex 2	10%
B3.1	Complex 3	1%
B3.10	Complex 3	10%

Table 18 Weight ratio of complexes used in blends formation

Bibliography

1. Saunders, B. R.; Laajam, N.; Daly, E.; Teow, S.; Hu, X.; Stepto, R., Microgels: From responsive polymer colloids to biomaterials. *Advances in Colloid and Interface Science* **2009,** *147-148*, 251-262.

2. Croy, S. R.; Kwon, G. S., Polymeric Micelles for Drug Delivery. *Current Pharmaceutical Design* **2006,** *12* (36), 4669-4684.

1. Michelet, B.; Deldaele, C.; Kajouj, S.; Moucheron, C.; Evano, G., A General Copper Catalyst for Photoredox Transformations of Organic Halides. *Organic Letters* **2017,** *19* (13), 3576-3579.

2. Gamage, J.; Zhang, Z., Applications of Photocatalytic Disinfection. *International Journal of Photoenergy* **2010,** *2010*.

3. Wang, K.; Li, Q.; Liu, B.; Cheng, B.; Ho, W.; Yu, J., Sulfur-doped g-C3N4 with enhanced photocatalytic CO2-reduction performance. *Applied Catalysis B: Environmental* **2015,** *176-177*, 44-52.

4. Teegardin, K.; Day, J. I.; Chan, J.; Weaver, J., Advances in Photocatalysis: A Microreview of Visible Light Mediated Ruthenium and Iridium Catalyzed Organic Transformations. *Organic Process Research & Development* **2016,** *20* (7), 1156-1163.

5. Paria, S.; Reiser, O., Copper in Photocatalysis. *ChemCatChem* **2014,** *6* (9), 2477-2483.

6. Hernandez-Perez, A. C.; Vlassova, A.; Collins, S. K., Toward a Visible Light Mediated Photocyclization: Cu-Based Sensitizers for the Synthesis of [5]Helicene. *Organic Letters* **2012,** *14* (12), 2988-2991.

7. Demmer, C. S.; Benoit, E.; Evano, G., Synthesis of Allenamides by Copper-Catalyzed Coupling of Propargylic Bromides and Nitrogen Nucleophiles. *Organic Letters* **2016,** *18* (6), 1438-1441.

8. Lipshutz, B. H.; Taft, B. R., Heterogeneous Copper-in-Charcoal-Catalyzed Click Chemistry. *Angewandte Chemie International Edition* **2006,** *45* (48), 8235-8238.

9. Graciani, J.; Mudiyanselage, K.; Xu, F.; Baber, A. E.; Evans, J.; Senanayake, S. D.; Stacchiola, D. J.; Liu, P.; Hrbek, J.; Sanz, J. F.; Rodriguez, J. A., Highly active copper-ceria and copper-ceria-titania catalysts for methanol synthesis from CO₂. *Science* **2014,** *345* (6196), 546-550.

10. Yashima, T.; Sato, K.; Hayasaka, T.; Hara, N., Alkylation on synthetic zeolites: III. Alkylation of toluene with methanol and formaldehyde on alkali cation exchanged zeolites. *Journal of Catalysis* **1972,** *26* (3), 303-312.

11. Kozell, V.; McLaughlin, M.; Strappaveccia, G.; Santoro, S.; Bivona, L. A.; Aprile, C.; Gruttadauria, M.; Vaccaro, L., Sustainable Approach to Waste-Minimized Sonogashira Cross-Coupling Reaction Based on Recoverable/Reusable Heterogeneous Catalytic/Base System and Acetonitrile Azeotrope. *ACS Sustainable Chemistry & Engineering* **2016,** *4* (12), 7209-7216.

12. Ponce, A. A.; Klabunde, K. J., Chemical and catalytic activity of copper nanoparticles prepared via metal vapor synthesis. *Journal of Molecular Catalysis A: Chemical* **2005,** *225* (1), 1-6.

13. Feynman, R. P., There's Plenty of Room at the Bottom. *Engineering and Science* **1960,** *23* (5), 22-36.

14. Laurent, S.; Forge, D.; Port, M.; Roch, A.; Robic, C.; Vander Elst, L.; Muller, R. N., Magnetic Iron Oxide Nanoparticles: Synthesis, Stabilization, Vectorization, Physicochemical Characterizations, and Biological Applications. *Chemical Reviews* **2010,** *110* (4), 2574-2574.

15. Tiwari, J. N.; Tiwari, R. N.; Kim, K. S., Zero-dimensional, one-dimensional, two-dimensional and three-dimensional nanostructured materials for advanced electrochemical energy devices. *Progress in Materials Science* **2012,** *57* (4), 724-803.

16. Khan, I.; Saeed, K.; Khan, I., Nanoparticles: Properties, applications and toxicities. *Arabian Journal of Chemistry* **2017**.

17. Wang, Y.; Xia, Y., Bottom-Up and Top-Down Approaches to the Synthesis of Monodispersed Spherical Colloids of Low Melting-Point Metals. *Nano Letters* **2004,** *4* (10), 2047-2050.

18. Iravani, S., Green synthesis of metal nanoparticles using plants. *Green Chemistry* **2011,** *13* (10), 2638-2650.

19. Nasir, A.; Kausar, A.; Younus, A., A Review on Preparation, Properties and Applications of Polymeric Nanoparticle-Based Materials. *Polymer-Plastics Technology and Engineering* **2015,** *54* (4), 325-341.

20. Allouche, J., Synthesis of Organic and Bioorganic Nanoparticles: An Overview of the Preparation Methods. In *Nanomaterials: A Danger or a Promise? A Chemical and Biological Perspective*, Brayner, R.; Fiévet, F.; Coradin, T., Eds. Springer London: London, 2013; pp 27-74.

21. Crucho, C. I. C.; Barros, M. T., Polymeric nanoparticles: A study on the preparation variables and characterization methods. *Materials Science and Engineering: C* **2017,** *80*, 771-784.

22. Fessi, H.; Puisieux, F.; Devissaguet, J. P.; Ammoury, N.; Benita, S., Nanocapsule formation by interfacial polymer deposition following solvent displacement. *International Journal of Pharmaceutics* **1989,** *55* (1), R1-R4.

23. Mora-Huertas, C. E.; Fessi, H.; Elaissari, A., Influence of process and formulation parameters on the formation of submicron particles by solvent displacement and emulsification–diffusion methods: Critical comparison. *Advances in Colloid and Interface Science* **2011,** *163* (2), 90-122.

24. Sternling, C. V.; Scriven, L. E., Interfacial turbulence: Hydrodynamic instability and the marangoni effect. *AIChE Journal* **1959,** *5* (4), 514-523.

25. Swinehart, D. F., The Beer-Lambert Law. *Journal of Chemical Education* **1962,** *39* (7), 333.

26. Hawkins, S.; Wolf, M.; Guyard, G.; Greenberg, S.; Dayan, N., 9 - Microcapsules as a Delivery System. In *Delivery System Handbook for Personal Care and Cosmetic Products*, Rosen, M. R., Ed. William Andrew Publishing: Norwich, NY, 2005; pp 191-213.

27. Free Radical Polymerization. In *Handbook of Polymer Synthesis, Characterization, and Processing*, pp 65-83.

28. Halasa, A. F., Recent Advances in Anionic Polymerization. *Rubber Chemistry and Technology* **1981,** *54* (3), 627-640.

29. Moad, G., A Critical Assessment of the Kinetics and Mechanism of Initiation of Radical Polymerization with Commercially Available Dialkyldiazene Initiators. *Progress in Polymer Science* **2019,** *88*, 130-188.

30. https://sites.google.com/a/iastate.edu/mate453-lab1-synthesis/home/synthesis-theory.

31. Sciannamea, V.; Jérôme, R.; Detrembleur, C., In-Situ Nitroxide-Mediated Radical Polymerization (NMP) Processes: Their Understanding and Optimization. *Chemical reviews* **2008,** *108*, 1104-26.

32. Nicolas, J.; Guillaneuf, Y., Living Radical Polymerization: Nitroxide-Mediated Polymerization. In *Encyclopedia of Polymeric Nanomaterials*, Kobayashi, S.; Müllen, K., Eds. Springer Berlin Heidelberg: Berlin, Heidelberg, 2014; pp 1-16.

33. Klumperman, B.; McLeary, J. B.; van den Dungen, E. T. A.; Pound, G., NMR Spectroscopy in the Optimization and Evaluation of RAFT Agents. *Macromolecular Symposia* **2007,** *248* (1), 141-149.

34. Kato, M.; Kamigaito, M.; Sawamoto, M.; Higashimura, T., Polymerization of Methyl Methacrylate with the Carbon Tetrachloride/Dichlorotris-(triphenylphosphine)ruthenium(II)/Methylaluminum Bis(2,6-di-tert-butylphenoxide) Initiating System: Possibility of Living Radical Polymerization. *Macromolecules* **1995,** *28* (5), 1721-1723.
35. Wang, J.-S.; Matyjaszewski, K., Controlled/"living" radical polymerization. atom transfer radical polymerization in the presence of transition-metal complexes. *Journal of the American Chemical Society* **1995,** *117* (20), 5614-5615.
36. Yamahiro, M. F., M.; Oikawa, T.; Okuma, Y.; Watanabe, K.; Ono, K.; Tsujii, T.; Fukuda, T. , *Jpn. Kokai Tokkyo Koho; (Chisso Corp., Japan)* **2005**, 75

37. Matyjaszewski, K.; Coca, S.; Gaynor, S. G.; Wei, M.; Woodworth, B. E., Controlled Radical Polymerization in the Presence of Oxygen. *Macromolecules* **1998,** *31* (17), 5967-5969.
38. Braunecker, W. A.; Matyjaszewski, K., Controlled/living radical polymerization: Features, developments, and perspectives. *Progress in Polymer Science* **2007,** *32* (1), 93-146.
39. Seeliger, F.; Matyjaszewski, K., Temperature Effect on Activation Rate Constants in ATRP: New Mechanistic Insights into the Activation Process. *Macromolecules* **2009,** *42* (16), 6050-6055.
40. Tang, W.; Kwak, Y.; Braunecker, W.; Tsarevsky, N. V.; Coote, M. L.; Matyjaszewski, K., Understanding Atom Transfer Radical Polymerization: Effect of Ligand and Initiator Structures on the Equilibrium Constants. *Journal of the American Chemical Society* **2008,** *130* (32), 10702-10713.
41. Tang, W.; Matyjaszewski, K., Effects of Initiator Structure on Activation Rate Constants in ATRP. *Macromolecules* **2007,** *40* (6), 1858-1863.
42. Pintauer, T.; Matyjaszewski, K., Atom transfer radical addition and polymerization reactions catalyzed by ppm amounts of copper complexes. *Chemical Society Reviews* **2008,** *37* (6), 1087-1097.
43. Kabachii, Y. A.; Kochev, S. Y.; Bronstein, L. M.; Blagodatskikh, I. B.; Valetsky, P. M., Atom Transfer Radical Polymerization with Ti(III) Halides and Alkoxides. *Polymer Bulletin* **2003,** *50* (4), 271-278.
44. Matyjaszewski, K., Atom Transfer Radical Polymerization (ATRP): Current Status and Future Perspectives. *Macromolecules* **2012,** *45* (10), 4015-4039.

45. Kotani, Y.; Kamigaito, M.; Sawamoto, M., Re(V)-Mediated Living Radical Polymerization of Styrene: ReO2I(PPh3)2/R−I Initiating Systems. *Macromolecules* **1999,** *32* (8), 2420-2424.

46. Wang, G.-X.; Lu, M.; Hou, Z.-H.; Gao, Y.; Liu, L.-C.; Wu, H., Photoirradiated Fe-Mediated AGET ATRP of Methyl Methacrylate in the Presence of Alcohol. *Journal of Macromolecular Science, Part A* **2014,** *51* (7), 565-571.

47. Simal, F.; Demonceau, A.; Noels, A. F., Highly Efficient Ruthenium-Based Catalytic Systems for the Controlled Free-Radical Polymerization of Vinyl Monomers. *Angewandte Chemie International Edition* **1999,** *38* (4), 538-540.

48. Percec, V.; Barboiu, B.; Neumann, A.; Ronda, J. C.; Zhao, M., Metal-Catalyzed "Living" Radical Polymerization of Styrene Initiated with Arenesulfonyl Chlorides. From Heterogeneous to Homogeneous Catalysis. *Macromolecules* **1996,** *29* (10), 3665-3668.

49. Patten, T. E.; Xia, J.; Abernathy, T.; Matyjaszewski, K., Polymers with Very Low Polydispersities from Atom Transfer Radical Polymerization. *Science* **1996,** *272* (5263), 866-868.

50. Konkolewicz, D.; Magenau, A. J. D.; Averick, S. E.; Simakova, A.; He, H.; Matyjaszewski, K., ICAR ATRP with ppm Cu Catalyst in Water. *Macromolecules* **2012,** *45* (11), 4461-4468.

51. Coca, S.; Jasieczek, C. B.; Beers, K. L.; Matyjaszewski, K., Polymerization of acrylates by atom transfer radical polymerization. Homopolymerization of 2-hydroxyethyl acrylate. *Journal of Polymer Science Part A: Polymer Chemistry* **1998,** *36* (9), 1417-1424.

52. Dong, H.; Matyjaszewski, K., ARGET ATRP of 2-(Dimethylamino)ethyl Methacrylate as an Intrinsic Reducing Agent. *Macromolecules* **2008,** *41* (19), 6868-6870.

53. Tasdelen, M. A.; Çiftci, M.; Uygun, M.; Yagci, Y., Possibilities for Photoinduced Controlled Radical Polymerizations. In *Progress in Controlled Radical Polymerization: Mechanisms and Techniques*, American Chemical Society: 2012; Vol. 1100, pp 59-72.

54. Mosnáček, J.; Ilčíková, M., Photochemically Mediated Atom Transfer Radical Polymerization of Methyl Methacrylate Using ppm Amounts of Catalyst. *Macromolecules* **2012,** *45* (15), 5859-5865.

55. https://www.cmu.edu/maty/atrp-how/procedures-for-initiation-of-ATRP/photoinitiated-atrp.html.

56. Runt, J.; Huang, J., Chapter 8 - Polymer blends and copolymers. In *Handbook of Thermal Analysis and Calorimetry*, Cheng, S. Z. D., Ed. Elsevier Science B.V.: 2002; Vol. 3, pp 273-294.

57. Sumita, M.; Sakata, K.; Asai, S.; Miyasaka, K.; Nakagawa, H., Dispersion of fillers and the electrical conductivity of polymer blends filled with carbon black. *Polymer Bulletin* **1991,** *25* (2), 265-271.
58. Yeoh, O. H., Characterization of Elastic Properties of Carbon-Black-Filled Rubber Vulcanizates. *Rubber Chemistry and Technology* **1990,** *63* (5), 792-805.
59. Huang, J.-C., Carbon black filled conducting polymers and polymer blends. *Advances in Polymer Technology* **2002,** *21* (4), 299-313.
60. McGehee, M. D.; Bergstedt, T.; Zhang, C.; Saab, A. P.; O'Regan, M. B.; Bazan, G. C.; Srdanov, V. I.; Heeger, A. J., Narrow Bandwidth Luminescence from Blends with Energy Transfer from Semiconducting Conjugated Polymers to Europium Complexes. *Advanced Materials* **1999,** *11* (16), 1349-1354.
61. Cassar, L., Synthesis of aryl- and vinyl-substituted acetylene derivatives by the use of nickel and palladium complexes. *Journal of Organometallic Chemistry* **1975,** *93* (2), 253-257.
62. Dieck, H. A.; Heck, F. R., Palladium catalyzed synthesis of aryl, heterocyclic and vinylic acetylene derivatives. *Journal of Organometallic Chemistry* **1975,** *93* (2), 259-263.
63. Sonogashira, K.; Tohda, Y.; Hagihara, N., A convenient synthesis of acetylenes: catalytic substitutions of acetylenic hydrogen with bromoalkenes, iodoarenes and bromopyridines. *Tetrahedron Letters* **1975,** *16* (50), 4467-4470.
64. R., H., Proceedings of the Chemical Society. October 1961. *Proceedings of the Chemical Society* **1961,** (October), 357-396.
65. Kolb, H. C.; Sharpless, K. B., The growing impact of click chemistry on drug discovery. *Drug Discovery Today* **2003,** *8* (24), 1128-1137.
66. Hein, J. E.; Fokin, V. V., Copper-catalyzed azide–alkyne cycloaddition (CuAAC) and beyond: new reactivity of copper(i) acetylides. *Chemical Society Reviews* **2010,** *39* (4), 1302-1315.
67. Johansson, J. R.; Beke-Somfai, T.; Said Stålsmeden, A.; Kann, N., Ruthenium-Catalyzed Azide Alkyne Cycloaddition Reaction: Scope, Mechanism, and Applications. *Chemical Reviews* **2016,** *116* (23), 14726-14768.
68. Iwamura, M.; Takeuchi, S.; Tahara, T., Real-Time Observation of the Photoinduced Structural Change of Bis(2,9-dimethyl-1,10-phenanthroline)copper(I) by Femtosecond Fluorescence Spectroscopy: A Realistic Potential Curve of the Jahn−Teller Distortion. *Journal of the American Chemical Society* **2007,** *129* (16), 5248-5256.

69. Kalsani, V.; Schmittel, M.; Listorti, A.; Accorsi, G.; Armaroli, N., Novel Phenanthroline Ligands and Their Kinetically Locked Copper(I) Complexes with Unexpected Photophysical Properties. *Inorganic Chemistry* **2006,** *45* (5), 2061-2067.
70. Saunders, B. R.; Laajam, N.; Daly, E.; Teow, S.; Hu, X.; Stepto, R., Microgels: From responsive polymer colloids to biomaterials. *Advances in Colloid and Interface Science* **2009,** *147-148*, 251-262.
71. Croy, S. R.; Kwon, G. S., Polymeric Micelles for Drug Delivery. *Current Pharmaceutical Design* **2006,** *12* (36), 4669-4684.

Abbreviations

DMSO	dimethyl sulfoxide
DCC	*N*,*N*′-dicyclohexylcarbodiimide
EDCI	1-ethyl-3-(3-dimethylaminopropyl)carbodiimide
DMAP	4-dimethylaminopyridine
DCM	dichloromethane
DLS	dynamic light scattering
PDI	polydispersity
TLC	thin layer chromatography
TEA	triethylamine
POP	bis[(2-diphenylphosphino)phenyl] ether
UV	ultraviolet